THE ULTRASTRUCTURE OF TREPONEMA REFRINGENS AND THE ISOLATION AND CHARACTERIZATION OF CYTOPLASMIC FIBRILS

A Dissertation
for the Degree of Ph. D.
MICHIGAN STATE UNIVERSITY
Susan Radtke Eipert
1976

THESIS

LIBRARY
Michigan State
University

This is to certify that the

thesis entitled

THE ULTRASTRUCTURE OF *TREPONEMA REFRINGENS*
AND THE ISOLATION AND CHARACTERIZATION
OF CYTOPLASMIC FIBRILS

presented by

Susan Radtke Eipert

has been accepted towards fulfillment
of the requirements for

Ph.D. degree in Microbiology

J. H. Black
Major professor

Date 1976

O-7639

t
a
t
T
T
e
o
e
c
C
o
l
l
Ex
t
ce

G99364

ABSTRACT

THE ULTRASTRUCTURE OF *TREPONEMA REFRINGENS* AND THE ISOLATION AND CHARACTERIZATION OF CYTOPLASMIC FIBRILS

By

Susan Radtke Eipert

The structural relationship of treponemal cytoplasmic fibrils to other cell components was determined and the fibrils were isolated and characterized ultrastructurally and chemically. Scanning and transmission electron microscopy of whole and disrupted cells of *Treponema refringens* (formerly the Nichols nonpathogenic strain of *T. pallidum*) confirmed that the cells were spiral and had a cell envelope resembling that of gram negative cells. Axial filaments, originating subterminally near each end of the cell, remained enclosed in the outer envelope through their entire length. A band of parallel fibrils extended along the cell on the inside of the cytoplasmic membrane. The band was oriented along the inner curve of the cell's helix. The nuclear area of the cell was always located adjacent to the fibrils. In micrographs of spheroplast-like forms an actual connection between fibrils and DNA was evident. Experiments to demonstrate further this connection by cell fractionation or electron microscopy of the DNA from partially lysed cells were inconclusive.

After various lytic agents were tested, a procedure was developed to lyse completely the cells and release the cytoplasmic fibrils. Cells were treated with guinea pig serum, lysozyme and Brij 58 overnight and then sonicated until the suspension cleared. A fibril-containing fraction was isolated by equilibrium ultracentrifugation of the lysate on a 0 to 57% or 0 to 76% linear Renografin gradient. A band which contained most of the fibrils, along with some membrane and axial filament hooks and basal bodies, was found on the gradient. After treatment with DNAse and/or Triton X-100, the fibril fraction was further purified by two or more Renografin gradients. A protein with a molecular weight of 97,000 was shown to be the major component of the partially purified fibril preparation by SDS polyacrylamide gel electrophoresis. Cross sectioned fibrils were polygonal, with visible substructure. Electron micrographs of negatively stained isolated fibrils showed two views or types of fibrils: wide and narrow. Each wide fibril had a 3.0 nm periodicity. A model of fibril structure is proposed to account for the ultrastructural observations. Each fibril is definitely a complex arrangement of several strands rather than a simple tubule. Much of the electron microscopic evidence can be accounted for by a model in which four strands are arranged so that each is at a corner of a rectangular cross section. Fibrils in situ are viewed from the narrow side, whereas both the wide and the narrow sides are viewed in preparations of isolated fibrils.

Treponemal fibrils bear little ultrastructural or chemical similarity to other prokaryotic or eukaryotic intracytoplasmic structures. The function of the fibrils is unknown, but speculations

can be made based on their location within the cell. Their position on the insides of the curves of the cell suggests that they may, along with the peptidoglycan, play a role in maintaining the shape of the organism. A likely possibility is that fibrils play a role in DNA replication, segregation or transcription since the DNA of these treponemes was always located next to the fibrils.

The ultrastructure of *Treponema hyodysenteriae* was also studied. The morphology of these cells was similar to that of *T. refringens* with the most obvious difference being the presence of 9 to 11 axial filaments on each end of the cell as opposed to one to 3. Attempts to demonstrate intracytoplasmic fibrils by electron microscopy of negatively stained whole cells and cell fractions were inconclusive. The axial filaments displayed a polarity sometimes seen in bacterial flagella--the distal end of each fragment of a broken filament was indented while the other end was pointed.

THE ULTRASTRUCTURE OF *TREPONEMA REFRINGENS* AND THE ISOLATION AND CHARACTERIZATION OF CYTOPLASMIC FIBRILS

By

Susan Radtke Eipert

A DISSERTATION

Submitted to
Michigan State University
in partial fulfillment of the requirements
for the degree of

DOCTOR OF PHILOSOPHY

Department of Microbiology and Public Health

1976

ACKNOWLEDGEMENTS

I would like to express my sincere appreciation to Dr. Sam Black for his interest, guidance and encouragement through the years. Stuart Pankratz has provided invaluable instruction and advice. I would like to thank Dr. Tom Corner for acting as substitute major professor and for his helpful comments on this manuscript.

Appreciation is also extended to my committee members, Dr. L. Snyder and Dr. E. Kuntz, and to those whose equipment I used: Dr. L. Snyder, Dr. R. Patterson, Dr. T. Beaman, Dr. L. Velicer, Dr. R. Costilow and Dr. G. Hooper.

Cultures were provided by Dr. S. Jackson (*T. refringens*) and J. Kinyon (*T. hyodysenteriae*). Special thanks to Leigh Martin, who cultured *T. hyodysenteriae* and provided comments and discussion.

These investigations were supported by the Department of Microbiology and Public Health and by a National Institutes of Health training grant through this department.

R

M

RE

TABLE OF CONTENTS

Page

INTRODUCTION. 1

REVIEW OF THE LITERATURE. 3

Historical Perspective on Spirochetes and Treponemes 3
Shape and Morphology of Spirochetes. 5
Treponemal Cytoplasmic Fibrils 7
Spirochetal Cell Envelope Fibrils. 11
Isolation of Structural Components from Treponemes . . . 11

MATERIALS AND METHODS 13

Organism and Cultivation 13
Nephelometry 13
CLBS Lysis Procedure 14
Fibril Isolation Procedure 14
Chemical Characterization of Fibrils 15
Light Microscopy 15
Phase Microscopy. 15
Darkfield Microscopy. 16
Fluorescence Microscopy 16
Electron Microscopy. 17
Scanning Electron Microscopy. 17
Negative Stains 17
DNA Spreading 17
Thin Sections 18
Shadowing 18

RESULTS 19

Growth Curves. 19
General Ultrastructure 21
Determination of Optimal Microscopy Techniques. . . 21
Shape and Size of Typical Cells 24
Cell Envelope 30
Spherical Atypical Cells. 37
Axial Filaments 43
Cytoplasmic Fibrils 52
DNA and Cytoplasm 56
Induction of Spherical Forms 62
Treatment with Penicillin 62
Treatment with Lysozyme 62

DI

AP

LI

Page

Cell Lysis . . . 63
Treatment with Guinea Pig Serum . . . 63
Treatment with Guinea Pig Serum, Detergents and Sonication . . . 75
Fibril Isolation . . . 79
Sucrose Gradients . . . 79
Renografin Gradients . . . 80
Chemical Characterization of Fibrils . . . 88
DNA-Fibril Connection . . . 91
Aqueous Spreading Technique for Electron Microscopy . . . 92
^{3}H-Thymidine Labeling . . . 92
Ultrastructure of Fibrils . . . 93
Thin Sectioned and Shadowed Fibrils . . . 95
Negatively Stained Fibrils . . . 100
Effect of Chemical, Physical or Enzymatic Treatment of Fibrils . . . 114

DISCUSSION . . . 118

Cell Envelope and Axial Filaments . . . 118
Fibril Purification . . . 120
Fibril Location in Cell . . . 122
Fibril Ultrastructure . . . 123
Comparison of Fibrils with Other Prokaryotic and Eukaryotic Structures . . . 129
Prokaryotic Structures . . . 129
Eukaryotic Structures . . . 131
Function of Fibrils . . . 132
Maintenance of Shape . . . 133
Cell Division . . . 134

APPENDIX . . . 137

LITERATURE CITED . . . 144

LIST OF TABLES

Table Page

1 Terminology used for treponemal cytoplasmic fibrils and axial filaments by various authors 9

2 Generation times of cultures inoculated with populations of varying ages. 19

3 Mean diameter of normal cells as measured from micrographs produced by transmission electron microscopy (TEM) and scanning electron microscopy (SEM). 30

4 Inductions of convoluted forms by suspension of treponemes in lysozyme solutions and buffers 64

5 Disruption of cells after treatment with guinea pig serum (GPS) plus detergent or sonication or both 78

6 Treatments which did not disaggregate clumps of fibrils, as determined by electron microscopy. 88

7 Means of various fibril dimensions measured from fibrils in thin sectioned cells. 98

8 Mean measurements of various dimensions of negatively stained fibrils 99

LIST OF FIGURES

Figure Page

1 Growth curve showing growth of cultures using inocula of various ages. 20

2 Growth curve showing slow growth of culture inoculated with 20-month-old culture and its recovery when transferred 22

3 Phase micrograph of *T. refringens*. 25

4 Darkfield micrograph of *T. refringens* from a 6-day culture. 25

5 Longitudinal section through cell from 3-day culture . . 26

6 Scanning electron micrograph of helical treponeme among straighter cells 27

7 Scanning electron micrograph of helical treponeme among straighter cells 28

8 PTA-stained cells which have recently divided. 29

9 Thin section of cells from a 5-day culture 31

10 PTA-stained divided cells (from a 3-day culture) still bridged with outer envelope (OE) 33

11 Thin sections of cells from a 5-day culture. 34

12 Outer envelope vesicles and striated tubules (ST) with knobbed ends (K) from population of cells disrupted with guinea pig serum in Tris 35

13 PTA-stained cell with a striated tubule (ST) extending from its outer envelope (OE) 36

14 Thin sectioned striated tubules. 38

15 Thin sectioned cells, from a 9-day culture, which have internal membrane structures (arrows) 38

16 PTA-stained cell, from a 4-day culture, with numerous membrane structures (arrows) 39

Figure Page

17 PTA-stained cells from a 4-day culture 40

18 Three PTA-stained cells, two wide and one narrow, bridged with outer envelope (OE) 41

19 Phase micrograph of convoluted cell. 42

20 Phase micrograph of a spheroplast-like cell. 42

21 Thin sectioned convoluted form 42

22 Thin sectioned spheroplast-like cell surrounded with OE 42

23 Two partially convoluted cells and a completely convoluted cell, stained with PTA. 44

24 Ammonium molybdate-stained cell which was disrupted with guinea pig serum and lysozyme 45

25 Negative stain of band A of Renografin gradient. 47

26 Uranyl oxalate-stained basal body (BB) and hook (H) with visible substructure. 48

27 Uranyl oxalate-stained basal body (BB) which has stain deposited around the point at which the axial filament hook was attached (arrow) 48

28 Thin sectioned cell with axial filament hook (H) and basal body (BB) apparently embedded in pocket of cytoplasmic membrane (CM) 48

29 Longitudinal sections of axial filaments in periplasmic space (AF) and within a tube of membrane (T) . . 49

30 Cross sections of cells with axial filaments (AF) in periplasmic space. 50

31 Thin sectioned axial filament (AF) in space between outer envelope and cytoplasm of spheroplast-like form 50

32 Thin sections of cells and tubes of membrane (T) containing axial filaments 51

33 Negative stain of cells from a 2-month culture 53

34 Distribution of the number of fibrils per cross section of cell. 54

35 Longitudinal section of cell with fibrils (F) adjacent to inner edge of cytoplasmic membrane (CM) 55

Figure Page

36 PTA-stained cell disrupted with guinea pig serum and lysozyme 57

37 Thin sectioned cell with fibrils (F) and nuclear area (N) visible 58

38 Thin sectioned spheroplast-like cell 59

39 Thin sectioned spheroplast-like cell 59

40 Two wet-mounted cells stained with euchrysine. 61

41 Wet-mounted cells stained with euchrysine. 61

42 Two recently divided cells vitally stained with euchrysine 61

43 Wet-mounted spheroplast-like cell stained with euchrysine 61

44 Phase micrograph of 5-day culture suspended in 0.067 M phosphate buffer, pH 7.8, with 2% n-butanol and 100 g/ml lysozyme. 65

45 Phase micrograph of a 5-day culture suspended in 0.067 M phosphate buffer, pH 7.8, guinea pig serum . . . 65

46 Cells disrupted with guinea pig serum and negatively stained with uranyl acetate. 67

47 Cell disrupted with guinea pig serum and negatively stained with ammonium molybdate. 68

48 Cells disrupted with guinea pig serum and lysozyme and negatively stained with PTA. 69

49 Cell disrupted with guinea pig serum and lysozyme and negatively stained with 0.5% PTA, pH 6.7 70

50 Cell disrupted with guinea pig serum and lysozyme and negatively stained with ammonium molybdate 71

51 Cell disrupted with guinea pig serum and lysozyme and negatively stained with PTA. 72

52 PTA-stained spiral band of fibrils from cell disrupted with guinea pig serum and lysozyme 73

53 Thin sections of disrupted cells and membrane vesicles from culture treated with guinea pig serum and lysozyme 74

Figure Page

54 Cells disrupted with guinea pig serum and Brij 58 and negatively stained with PTA. 76

55 Ammonium molybdate stain of cell sonicated after exposure to guinea pig serum and lysozyme. 77

56 Silicon tungstate-stained membrane from Renografin band A 77

57 Average position of bands A and C when cell lysate, with or without DNase, was centrifuged to equilibrium on 0 to 76% Renografin gradients 82

58 Ammonium molybdate-stained material from Renografin band A 83

59 PTA-stained material from Renografin band D. 84

60 PTA stain of large clump of fibrils from Renografin band C 86

61 Flow chart of procedure for isolation of fibrils from treponemes. 87

62 Uranyl oxalate-stained band C from third Renografin gradient 89

63 Absorbance readings of SDS polyacrylamide electrophoresis gels stained with Coomassie blue. 90

64 DNA from T_4 bacteriophage. 93

65 Cell disrupted with guinea pig serum, prepared for electron microscopy by the Kleinschmidt spreading technique and stained with PTA and uranyl acetate. . . . 93

66 Cells disrupted with CLBS, prepared for electron microscopy by the Kleinschmidt spreading technique, stained with uranyl acetate and rotary shadowed with platinum. 94

67 Cell disrupted with CLBS, prepared for electron microscopy by the Kleinschmidt technique and stained with uranyl acetate. 94

68 Direct cross sections of fibrils in normal cells (a,b,c), a convoluted cell (d) and disrupted cells (e,f). 96

69 Drawings of sectioned fibrils drawn approximately to scale and positioned on the cytoplasmic membrane. . . 97

Fi

Figure Page

70 Sectioned disrupted cell containing fibrils (F) which have been freed from the cytoplasmic membrane (CM) 101

71 Longitudinally sectioned fibrils (F) 101

72 Isolated fibrils which were shadowed with platinum-carbon in the direction of the arrow 102

73 PTA-stained narrow (N) and wide (W) two-stranded fibrils. 103

74 PTA-stained wide two-stranded fibrils (W) from preparation which had been kept frozen. 104

75 Silicon tungstate-stained wide fibrils with ribbon (R) of stained material lying on each side 104

76 Drawings of fibril types and substructure seen in preparations of isolated fibrils stained with PTA or UOx 106

77 UOx-stained wide fibrils with periodic cross striations (P). 107

78 UOx-stained wide fibrils with ribbons (R) alongside. . . 107

79 UOx-stained wide fibrils 108

80 UOx-stained wide (W) and narrow (N) fibrils. 109

81 UOx-stained wide and narrow fibrils. 109

82 Distribution of widths of narrow fibrils 111

83 Distribution of widths of wide fibrils 112

84 Each histogram shows the distribution of wide fibril widths from micrographs taken of one microscope grid . . 113

85 PTA-stained spiral band of narrow fibrils from fibril preparation which had been dried and resuspended 115

86 Negative stain of narrow fibrils in bands (arrows) . . . 116

87 PTA-stained fibrils (F) disrupted with exposure to 4 M urea overnight 116

88 Relationship between components of cross and longitudinally sectioned fibrils. 125

89 Model of ultrastructure of treponemal fibril as constructed from micrographs of negatively stained fibrils. 128

Figure Page

90 *T. hyodysenteriae* negatively stained with PTA. 139

91 Enlargement of Figure 90 140

92 PTA-stained bundles of fibers from CLBS-disrupted *T. hyodysenteriae*. 141

93 PTA-stained axial filament fragments from CLBS-disrupted *T. hyodysenteriae*. 141

94 PTA-stained axial filament fragments from CLBS-disrupted *T. hyodysenteriae*. 142

mor

suf

pre

res

all

str

fib

lis

ins

tion

ever

disp

cyto

clar

othe

ultr

the

Base

INTRODUCTION

Since the first observation of spirochetes, their unique morphology has fascinated many researchers. Light microscopy was sufficient to show the helical nature of the cells and even the presence of axial filaments, but the use of electron microscopy resolved many aspects of spirochetal ultrastructure. It also allowed the discovery in treponemes of a previously unknown structure--cytoplasmic fibrils. Although discovered in 1968, the fibrils have not been well characterized. The only clearly established fact is that several parallel fibrils are located on the inside of the cytoplasmic membrane of treponemes. Little information has been available on their chemistry or ultrastructure and even the question of whether there are one or more bands has been disputed.

This study was undertaken to determine the function of the cytoplasmic fibrils in treponemes. This objective was pursued by clarifying the structural relationship of treponemal fibrils to other cell components and by isolating the fibrils to examine their ultrastructural and chemical nature.

The fibrils were found to be adjacent to the nuclear area of the cell and to be located on the inner side of the cell's curves. Based on this evidence, two possible functions for fibrils were pro

of

a l

fro

bef

pig

whi

cor

ult

vid

arr

nat

oth

proposed--shape maintenance and association with DNA in the process of cell division.

Treponemal cytoplasmic fibrils had not been isolated, nor had a lysis procedure been developed which efficiently released fibrils from the cells. In the present study several methods were tried before a satisfactory procedure was developed. The use of guinea pig serum, Brij 58 and sonication disrupted the cells to a degree which permitted the isolation of the fibrils from all other cell components visible in the electron microscope. Examination of the ultrastructure of isolated fibrils and fibrils within cells provided evidence on which each fibril was proposed to be a complex arrangement of strands. Study of the chemical and ultrastructural nature of the fibrils demonstrated that they are not similar to any other known prokaryotic or eukaryotic structure.

had

eel

and

qui

obs

Oct

kin

fil

(17

spi

hel

tha

ges

the

spi

the

dis

a

REVIEW OF THE LITERATURE

Historical Perspective on Spirochetes and Treponemes

Antony van Leewenhoek reported to Robert Hooke in 1681 that he had seen "a sort of animalcules that had the figure of our river-eels" in fecal material. These animalcules had "a wavy nimble motion" and bent their bodies serpent-wise, and shot through the stuff as quick as a pike through the water" (27). Van Leewenhoek later observed similar spiral organisms in material from between teeth. Dobell believed the descriptions to be those of spirochetes.

In 1838 Ehrenberg classified the bacteria within the animal kingdom and defined the genus of large free-living flexible helical filaments as *Spirochaeta*. It has only one species, *S. plicatilis* (17). His drawings and terminology suggest that he considered the spirochetes to be helical chains of bacteria rather than single helical cells. Cohn classified the bacteria with the plants rather than the animals and in his 1875 classification system even suggested that *S. plicatilis* was nothing more than a colorless form of the alga *Spirulina*. The genus *Spirochaete* was described as long spiral flexuous filaments of cells without phycochrome (16).

Winter's 1881 classification system (112) is one example of the many classifications of that time. In it, *Spirochaeta* was distinguished from *Bacillus* and *Beggiatoa* only by being composed of a long flexible spiral filament of cells rather than a straight chain of cells. In an English translation of this classification, bacteria belonging to the genus *Spirochaeta* were described as

> ...cells united in long slender threads, mostly showing narrow spiral windings. The filaments have the liveliest of movements and clearly propel themselves forward and backward, but are also able to bend in various ways. (19)

The practice of describing spirochetes as spiral filaments of cells rather than single spiral cells was followed in most, but not all, classification systems in the 19th century. This practice changed near the turn of the century, so that by 1917, when the Committee of the Society of American Bacteriologists on Characterization and Classification of Bacterial Types made its preliminary report (111), spirochetes were clearly considered individual spiral organisms.

Spirocheta pallidum and other spirochetes were given the generic name of *Treponema* in 1905 by Schaudinn (93,94) shortly after he and Hoffmann (95) discovered spirochetes in syphilitic chancres. At the same time that they found spirochetes connected with syphilis, they found another type of spirochete, *T. refringens*, in condylomata of a patient without syphilis (93,95). Swellengrebel initiated the term Spirochaetaceae, which contained the genera *Spirochaeta* and *Treponema* as well as a new genus, *Borrelia* (16). Through the years, other genera have been included with the spirochetes or removed from that group. The most recent classification (99) lists 5 genera in the order Spirochaetales and the class Spirochaetaceae: *Spirocheta, Cristispira, Leptospira, Borrelia* and *Treponema*.

The

biotype N

T. pallid

from a ra

pallidum.

successfu

pathogenic

so-called

other spec

immunologi

pathogenic

saprophytic

Spiroc

organisms (

darkfield o

treponemes

For example

chancres an

is a right-

pallidum ce

cell.

Beside

spirochetes

twining wit

envelope (9

The treponeme used in the present studies is *Treponema refringens* biotype Nichols, formerly called the Nichols nonpathogenic strain of *T. pallidum*. It has been cultured since 1933, when it was isolated from a rabbit infected with the pathogenic Nichols strain of *T. pallidum*. At the time, Kast and Kolmer (61) considered it to be a successful cultivation of *T. pallidum*, even though it was no longer pathogenic for rabbits. Recently this organism, along with other so-called cultivable strains of *T. pallidum*, was reclassified in other species of treponemes (99). Since these organisms differ immunologically and morphologically from *T. pallidum* and are not pathogenic (108), they probably were originally cultured from saprophytic genital treponemes rather than *T. pallidum* (98).

Shape and Morphology of Spirochetes

Spirochetes have usually been described as spiral or helical organisms (or chains of organisms). Occasional reports based on darkfield observation of the cells disputed this, claiming that some treponemes are not helical, but rather are in planar wave forms. For example, Sequira (96) reported that *T. pallidum* from syphilitic chancres and *T. pertenue* are flat wave forms, whereas *T. refringens* is a right-handed spiral. More recently, Cox (22) found that *T. pallidum* cells are made up of flat wave forms, in 1 to 5 planes per cell.

Besides being helical, or perhaps planar wave forms, and flexible, spirochetes are defined by the presence of axial filaments intertwining with the protoplasmic cylinder and enclosed by the outer envelope (99). Bradfield and Cater (14) hypothesized that the axial

filaments a
filaments a
which pulls
(72) showe
from one e
subtermina
a variable
ends overla
responsible
(59) demons
ing cells w
the organis
Spirocheta
coiled conf
were mainta
glycan laye
Peptidoglyca
wavy shape.

The si
ultrastruct
for assumin
but that rol
demonstrate
axial filame
by nonlethal
or axial fi

filaments are the cause of the spiral shape of spirochetes. Axial filaments attached at each end of a cell would provide the tension which pulls the cell into a spiral shape. Listgarten and Socransky (72) showed, however, that the axial filaments are not continuous from one end of the cell to the other. Each filament is inserted subterminally at one end only and extends towards the other end for a variable distance. Usually filaments originating from opposite ends overlap. As further evidence that the axial filaments are not responsible for the shape of spirochetes, Joseph and Canale-Parole (59) demonstrated that the removal of the axial filaments by treating cells with hydrochloric acid did not alter the coiled shape of the organisms. Furthermore, the peptidoglycan layer purified from *Spirocheta stenostrepta* or *S. litoralis* frequently retained its coiled configuration (59,60). Thus, they concluded that spirochetes were maintained in a permanently coiled shape by the helical peptidoglycan layer, and not by tension on the cell by axial filaments. Peptidoglycan isolated from leptospires (102) also retained its wavy shape.

The similarity of axial filaments to bacterial flagella in ultrastructural and chemical characteristics (59) has been the basis for assuming that axial filaments play a role in spirochetal motility, but that role has not been proven. It has not been possible to demonstrate loss of motility after removal of axial filaments because axial filaments lie inside the outer envelope and cannot be removed by nonlethal treatments. Mutant spirochetes lacking axial filaments or axial filament components have not yet been obtained (59). The

use of ant
informatic

Surrc
plasmic me
(21). The
gram-negat
ference be
membrane (
glycan (53
of spiroch
in contras
gap betwee
transparen
cytoplasm
(48,62,88

In 1
cytoplasm
there we
body of
pattern
Society
cussion
structur
masses i
of *T. pa*

use of antisera against axial filaments yielded no conclusive information (9).

Surrounding the cytoplasm of gram-negative cells is the cytoplasmic membrane, the peptidoglycan layer and the outer membrane (21). The cell envelope of spirochetes is similar to that of gram-negative bacteria, with the most obvious morphological difference being the presence of the axial filaments between the outer membrane (termed outer envelope in spirochetes) and the peptidoglycan (53,70,87,88). In electron micrographs the peptidoglycan of spirochetes is located directly next to the cytoplasmic membrane, in contrast to most gram-negative organisms, in which there is a gap between the membrane and the peptidoglycan (70,75). An electron transparent area which contains tiny strands is present inside the cytoplasm of spirochetes and is regarded as the nuclear area (48,62,88,91,107).

Treponemal Cytoplasmic Fibrils

In 1968 Ovčinnikov and Delektorskij observed filaments in the cytoplasm of sectioned treponemes (83). They also mentioned that there were several thin, parallel bands which stretched along the body of negatively stained treponemes. These they regarded as the pattern of the treponeme surface. At a meeting of the Italian Society of Parasitology in 1968, two reports at a round table discussion on the fine morphology of spirochaetes mentioned unusual structures: Swain and Anderson (101) reported wedge- or comma-shaped masses in the cytoplasm next to the cytoplasmic membrane of sections of *T. pallidum*, and Babudieri (4) observed small bundles of slender

fibrils in
not realize
structures.
of "microtu
the cytopla

Since
one or more
negatively
cross secti
pathogenic
T. pertenue
nemes such
(4,48,51,58
(45) and *T.*
is no unive
confused wi

The di
in the rang
a diameter
since they
the axial f
nm (63). T
Hougen to b
and 5 to 20
the end of
ments (47,5
one band of

fibrils in negatively stained Reiter treponemes. It was apparently not realized that these were probably different views of the same structures. Also in 1968, Klingmüller *et al.* (68) reported a band of "microtubule filaments" lying next to the cytoplasmic membrane in the cytoplasm of *T. pallidum.*

Since that time, other researchers have repeatedly observed one or more bands of parallel fibrils situated along the length of negatively stained treponemes or under the cytoplasmic membrane of cross sectioned treponemes. These fibrils have been reported in pathogenic treponemes such as *T. pallidum* (47,68,80,82,83,101,107), *T. pertenue* (81), and *T. cuniculi* (49) and in nonpathogenic treponemes such as the Reiter, Kazan, Stavropol and Nichols strains (4,48,51,58,80,82,83), *T. microdentium, T. minutem,* and *T. calligyrum* (45) and *T. phagedenis, T. refringens* and *T. vincentii* (44). There is no universal name for these fibrils and often the terminology is confused with that for axial filaments (Table 1).

The diameters of the fibrils have usually been reported to be in the range of 6 nm (58) to 9 nm (51). Klingmüller *et al.* reported a diameter of 4 nm (68), but this measurement is open to question since they gave 10 nm as the diameter of axial filaments, whereas the axial filament diameter probably ranges from 12 nm (58) to 30 nm (63). The number of fibrils per band was reported by Hovind Hougen to be 6 to 8 (44,45,47,49), but wider ranges of 4 to 14 (58) and 5 to 20 (51) have also been noted. The fibrils originate near the end of the cell, close to the insertion points of the axial filaments (47,51). Most researchers apparently assumed that there is one band of fibrils running the length of the cell (51,58,68,107),

Table 1.

Authors
Klingmülle
Ovčinnikov
Jones et al
Jackson and
Hovind Houg Andersen
Hovind Houg
Wiegand et
Hovind Houg

but it has
rather than
the cell an
gators have
the cell as
81,101).

Fibril
(51) or fro
sonication
and homogen
parallel ar

Table 1. Terminology used for treponemal cytoplasmic fibrils and axial filaments by various authors

Authors	Date	Axial filaments	Cytoplasmic fibrils
Klingmüller *et al.*	1968	Fibrillen	Mikrotubuli-filamente
Ovčinnikov and Delektorskij	1969	superficial fibrils	deep fibrils
Jones *et al.*	1970	axial fibers	body fibrils
Jackson and Black	1971	axial filaments	fibrils
Hovind Hougen and Birch-Andersen	1971	endoflagella	microtubules
Hovind Hougen	1972	flagella	microtubules
Wiegand *et al.*	1972	axial filaments	deep filaments
Hovind Hougen	1974	flagella	tubules

but it has been reported that there are 2 or 3 bands of fibrils rather than one (4,66,79) or that bands originate at either end of the cell and interdigitate in the middle (44,45,57). Many investigators have stated that the fibrils are located on the same side of the cell as, and directly under, the axial filaments (44,47,48,49,68, 81,101).

Fibrils were at least partially released from autolyzed cells (51) or from cells treated with Myxobacter AL-1 protease (44,45,47,48), sonication and detergent (51), trypsin, or sodium dodecyl sulfate and homogenization (50). Fibrils released from cells often remained parallel and spiral (50,51) and were sometimes broken (44). The

fibrils of
T. phageder

The ul
tubular bec
(44,47,49,5
possibly st
outer stran
units. Crc
comma-shape
oblong (107
centers (49
fibrils has
probably ar

Hovind
could be us
Treponema s
have been f
microscopy
to find fib
been succes
in preparat
strepta (59
ultrastruct

Hypoth
have includ
and maintena
suggested tl

fibrils of *T. refringens* appeared to be less fragile than those of *T. phagedenis* or *T. vincentii* (44).

The ultrastructure of the fibrils has usually been described as tubular because negative stain appeared to penetrate the lumen (44,47,49,51). Jones (58) noted that the fibrils have a beaded or possibly striated appearance and Jackson (50) hypothesized that the outer strands of the fibrils are the outer edges of spherical subunits. Cross sectioned fibrils are not round, but wedge- or comma-shaped (101), slightly elongated (81), triangular (50), or oblong (107). Fibril cross sections have slightly electron dense centers (49) or a punctate structure (79). The chemical nature of fibrils has not been mentioned, with the sole exception that they probably are protein because they are sensitive to trypsin (51).

Hovind Hougen (47) has suggested that the presence of fibrils could be used as a criterion for classification of the genus *Treponema* since they appear to be unique to that genus. Fibrils have been found in every treponeme species observed by electron microscopy with the single exception of *T. genitalis* (46). Attempts to find fibrils in leptospires (26,47) or borreliae (75) have not been successful. Fibrils with a diameter of 5 to 8 nm were seen in preparations of intact and disrupted cells of *Spirocheta stenostrepta* (59), but no mention was made of their number, location or ultrastructure.

Hypotheses as to the function of treponemal cytoplasmic fibrils have included motility (58,80,81,83), skeletal support (48,81,82) and maintenance of the spiral shape (51,58,83). It has also been suggested that fibrils may be the site for enzymatic processes

(82,101), i
protein (48

Other
envelope of
the presenc
the protopl
treponemes
or hyaluron
found to be
had a molec
tion). Sim
spirochetes
icterohaemo
leptospires
(110), in d
of two out
and in the
vary somewh
associated
ultrastruct
mural fibri
cytoplasmic

I

Many a
extracted f

(82,101), intracytoplasmic transport (48), or synthesis of flagellar protein (48).

Spirochetal Cell Envelope Fibrils

Other types of fibrils have also been reported in the cell envelope of spirochetes. Yanigihara and Mifuchi (115,116) reported the presence of branched microfibers 3 to 5 nm in diameter between the protoplasmic cylinder and the outer envelope of Borreliae treponemes and leptospires that had been treated with dilute alkali or hyaluronidase. The leptospiral microfibrils were isolated and found to be carbohydrate and protein in a 1:1 ratio. The protein had a molecular weight of 72,000 (Yanigihara, personal communication). Similar fibrils have been observed in the envelope of large spirochetes (12,72), in sodium deoxycholate-treated *Leptospira icterohaemorrhagiae* (114), in the cell wall of thin sectioned leptospires (98), in sodium deoxycholate-treated sex-ratio organisms (110), in disrupted *Borrelia vincentii* (11), in the outer envelope of two out of seven species of treponemes observed by Hougen (44,46), and in the outer envelope of *T. refringens* (50). These descriptions vary somewhat and probably portray more than one type of fibril associated with the cell envelope of various species. The location, ultrastructure and generally smaller size of these spirochetal perimural fibrils indicate that they are clearly different from treponemal cytoplasmic fibrils.

Isolation of Structural Components from Treponemes

Many antigens and other cell components have been chemically extracted from treponemes (53,86), but isolation of intact structural component

outer env

was solub

dialysis

had been

axial fil

A cell wa

was isola

cell fract

cytoplasmi

been devel

components from spirochetes has been limited to axial filaments, outer envelope, and a cell wall preparation. The outer envelope was solubilized by sodium dodecyl sulfate and then reaggregated by dialysis against a $MgCl_2$ solution (36,57). After the outer envelope had been solubilized with sodium dodecyl sulfate or butanol, the axial filaments were sheared from the cells in a blender (8,34). A cell wall preparation including peptidoglycan and polysaccharide was isolated by centrifugation after cells were disrupted with a cell fractionator and proteolytic enzymes (3). No internal or cytoplasmic components have been isolated, nor has a lysis procedure been developed which would allow isolation of such components.

The c

Nichols no
S. Jackson
consisted
(BBL), 1.4
0.025; and
Laboratori
and added
vol). A 9
from 10 to
Incubation
vacuum jar
routinely
at 7000 to

To mo
Phosphate
Nepho-Colo
2×10^8 ce

MATERIALS AND METHODS

Organism and Cultivation

The culture of *Treponema refringens*, formerly called the Nichols nonpathogenic strain of *T. pallidum*, was obtained from Dr. S. Jackson, Baylor College of Medicine, Houston. The growth medium consisted of (g/100 ml glass distilled water):spirolate broth base (BBL), 1.45; brain heart infusion (BBL), 1.85; tryptone (DIFCO), 0.025; and asparagine (DIFCO), 0.05. Filtered rabbit serum (Flow Laboratories) was heated for 30 min at 56 C to inactivate complement and added to the autoclaved medium at a concentration of 9% (vol/vol). A 9% (vol/vol) inoculum was added and cultures were grown in from 10 to 400 ml lots in screw-capped tubes or prescription bottles. Incubation was at 35 C inside an anaerobic jar (Torbal) or glass vacuum jar under a nitrogen atmosphere. Cultures were transferred routinely every 4 to 7 days. Cells were harvested by centrifugation at 7000 to 10,000 x g for 10 min.

Nephelometry

To monitor growth, 1 ml of culture was diluted with 9 ml of phosphate buffer (pH 7.0) and read in a nephelometer (Coleman Nepho-Colorimeter). According to Jackson (50), a suspension of 2×10^8 cells per ml had a reading of about 40 nephelos units.

The
in 1 ml c
serum (re
Company o
approxima
solution
temperatur
watt Ultra
15 to 45 s
3.1.4.5 (S
35 C.

Linear
66% meglum
made with
were made
Gradients
L3-50 ultra
fibrils was
against wa
DNase, Tri
gradient.
repeated o

CLBS Lysis Procedure

The pellet from 200 ml of centrifuged culture was resuspended in 1 ml of Tris buffer (0.04 M Tris pH 7.6) and 1.5 ml guinea pig serum (reconstituted lyophilized serum from Grand Island Biological Company or fresh frozen serum from Suburban Serum Labs), after which approximately 5 mg of lysozyme (Sigma) and 0.6 ml of a 5% (wt/vol) solution of Brij 58 were added. The suspension was left at room temperature from 2 h to overnight and then sonicated on an MSE 100 watt Ultrasonic Disintegrator until the suspension cleared (usually 15 to 45 sec). Three milligrams deoxyribonuclease I, E.C. No. 3.1.4.5 (Sigma) was added and the lysate was shaken for an hour at 35 C.

Fibril Isolation Procedure

Linear 0 to 57% or 0 to 76% Renografin (Squibb Renografin-76; 66% meglumine diatrizoate and 10% sodium diatrizoate) gradients were made with 0.04 M Tris buffer (pH 7.4). Four milliliter gradients were made in 5 ml tubes and 1 ml of CLBS lysate was layered on top. Gradients were centrifuged in a SW 50.1 rotor in a Beckman Model L3-50 ultracentrifuge at 130,000 x g for 2 h. The band containing fibrils was collected with a Pasteur pipet and dialyzed overnight against water or buffer. The dialyzed fibrils were incubated with DNase, Triton X-100, or both and centrifuged again on a Renografin gradient. The incubation and centrifugation of the fibrils was repeated one more time.

Sodi
gels used
Fairbanks
glass tub
allowed t
and allowe
polyacryla
amperage o
protein we
on the gel
were scann
photometer.
by Weber a

Protei
anthrone pr
pentose by

All li
a Zeiss ph
for phase a

Phase Micro

Wet mo
100 X oil-i
film.

Chemical Characterization of Fibrils

Sodium dodecyl sulfate (SDS) polyacrylamide electrophoresis gels used to analyze fibril preparations were made according to Fairbanks (29) with the following modifications. Acid cleaned glass tubes were coated with dimethyl dichlorosilane (Sigma), allowed to dry and then rinsed with hot water, 95% ethanol, water and allowed to dry again. Gels (8 to 11 cm high) containing 7.5% polyacrylamide and 1% SDS were pre-electrophoresed at a constant amperage of 2 mA per tube. Protein samples containing 20 to 50 μg protein were boiled 5 min with 1% SDS and 2% mercaptoethanol, layered on the gels and run at 4 mA per tube. Coomassie blue-stained gels were scanned at a wavelength of 540 nm on a Gilford 2400-S Spectrophotometer. The molecular weights of standards had been determined by Weber and Osborn (106).

Protein was analyzed by Lowry's method (73), hexose by the anthrone procedure (2), DNA by the diphenylamine procedure (2), and pentose by the orcinol test (109).

Light Microscopy

All light microscopy and photomicrography was performed with a Zeiss photomicroscope. The automatic exposure control was used for phase and darkfield photography.

Phase Microscopy

Wet mounts of cells were observed with phase optics using a 100 X oil-immersion objective and photographed using Kodak Plus-X film.

Darkfield

When

the light

included

lens with

Fluorescen

For f

a high pre

necessary

developmen

staining c

and fixed

diethyl et

and some c

5 X crysta

stained fo

After rins

slide and

in the pro

tution of

7.4) for a

E.C. No. 3

For v

and one dr

buffer, pH

Agar coate

for photog

Darkfield Microscopy

When mounts of cells were observed by darkfield microscopy, the light source was a high-pressure mercury lamp and the optics included a cardioid condenser and a 100 X oil immersion objective lens with an iris diaphragm.

Fluorescence Microscopy

For fluorescence microscopy, the microscope was equipped with a high pressure mercury lamp. Exposure times of 2 to 15 min were necessary with Kodak High Speed Ektachrome film pushed in its development to an ASA of 640. In the procedure used for fluorescent staining of fixed cells (5), smears on coverslips were air dried and fixed overnight in Carnoy's solution and in 95% ethanol:95% diethyl ether (1:1). After fixation, the smears were rehydrated and some of them were treated with bovine pancreas ribonuclease 5 X crystallized (Nutritional Biochemicals). All smears were stained for 20 min in acridine orange McIlvaine's buffer (pH 6.0). After rinsing, the wet coverslip was placed, cells down, on a clean slide and the edges were sealed with nail polish. Many variations in the procedure were tried. The major ones included the substitution of euchrysine (in potassium-sodium phosphate buffer, pH 7.4) for acridine orange and the inclusion of deoxyribonuclease I, E.C. No. 3.1.4.5 (Sigma) after the RNase incubation.

For vital staining, a wet mount was prepared containing culture and one drop of a 0.02% solution of acridine orange in McIlvaine's buffer, pH 2.4 to 6.0, or euchrysine in phosphate buffer, pH 7.4. Agar coated slides helped to slow or stop the motion of the cells for photography.

Electron Microscopy

Scanning Electron Microscopy

Cells were collected on a 0.2 μm Nucleopore filter and fixed in 2% glutaraldehyde or in 2% glutaraldehyde plus 1% osmium tetroxide. The fixatives were dissolved in 0.067 M phosphate buffer (pH 7.2), with or without 0.05 M or 0.15 M NaCl. After dehydration in an alcohol series (5 min each in 50%, 70%, 95% and 100% ethanol), the cells were dried in a Sorvall critical-point dryer and then sputter-coated with gold. Cells were observed and photographed with an ISI Super Mini-SEM scanning electron microscope.

Negative Stains

All transmission electron micrographs were taken with a Philips EM-300 electron microscope operating at 80 Kv. For negative staining, cells were put on a carbon-Formvar grid and stained with a drop of stain. Isolated fibrils were stained on a thin carbon or Parlodian coated grid by floating the grid on the stain. The concentrations of stains used, unless otherwise noted, were: 0.5% phosphotungstate, pH 7.5 (PTA); 0.5% silicon tungstate, pH 7.0; 2% ammonium molybdate, pH 7.5; 0.4% uranyl acetate in 0.05 M HCl, and 0.5% uranyl oxalate, pH 6.8 (UOx).

DNA Spreading

A variation of the Kleinschmidt spreading technique was used for visualization of treponemal DNA (23). Various cell preparations in 0.5 M ammonium acetate, 0.1 mg/ml cytochrome c (Nutritional Biochemicals) were dropped onto the surface of 0.25 M ammonium acetate

in a paraf
was picked
ethanol an
ethanol.
shadowed w
evaporator.

Thin Secti

Cells
0.22 μm Mi
according
in 3% glut
embedded i
LKB Ultrot
uranyl ace
solution (

Shadowing

Isola
Platinum-ca
vacuum eva

in a paraffin coated glass petri plate. The cytochrome c monolayer was picked up on a carbon-Parlodian coated grid, dehydrated in 50% ethanol and stained for 30 sec with 0.002% uranyl acetate in 90% ethanol. Occasional grids were also stained with PTA or rotary shadowed with platinum in a Denton Vacuum DV-502 high vacuum evaporator.

Thin Sections

Cells to be embedded for thin sectioning were collected on a 0.22 µm Millipore filter, embedded in agar and fixed with osmium according to the Ryter-Kellenberger procedure (65). Pre-fixation in 3% glutaraldehyde was used only occasionally. The cells were embedded in Epon and sectioned with a DuPont diamond knife on a LKB Ultrotome III ultramicrotome. Sections were stained with 2% uranyl acetate for 30 min and 0.5% lead citrate in a sodium hydroxide solution (about pH 12) for 5 min.

Shadowing

Isolated fibrils on carbon-Parlodian grids were shadowed with platinum-carbon at an angle of 15° in a Denton Vacuum DV-502 high vacuum evaporator.

Nephe

cultures (

existed be

hr portion

phase was

Table 2. C
c

Age of
3 d
9 d
21
8 m

generation

Growth did

although th

inoculated

to normal s

RESULTS

Growth Curves

Nephelometry was used to record the growth of *T. refringens* cultures (Figure 1). It was assumed that a direct relationship existed between bacterial numbers and nephelos units (28). A 48 hr portion of each growth curve representing the exponential growth phase was used to calculate the generation time (Table 2). The generation time was longer when older cultures were used as inoculum. Growth did occur when a 20-month-old culture was used as inoculum, although the stationary phase was quickly reached. The culture inoculated with the 20-month-old population appeared to have returned to normal since when it, in turn, was used as inoculum, the culture

Table 2. Generation times of cultures inoculated with populations of varying ages

Age of inoculum	Time period used in calculation	Generation time
3 days	Day 1 to day 3	23 hours
9 days	Day 2 to day 4	35 hours
21 days	Day 2 to day 4	40 hours
8 months	Day 6 to day 8	49 hours

Fig
inocula
vals by
of inocu

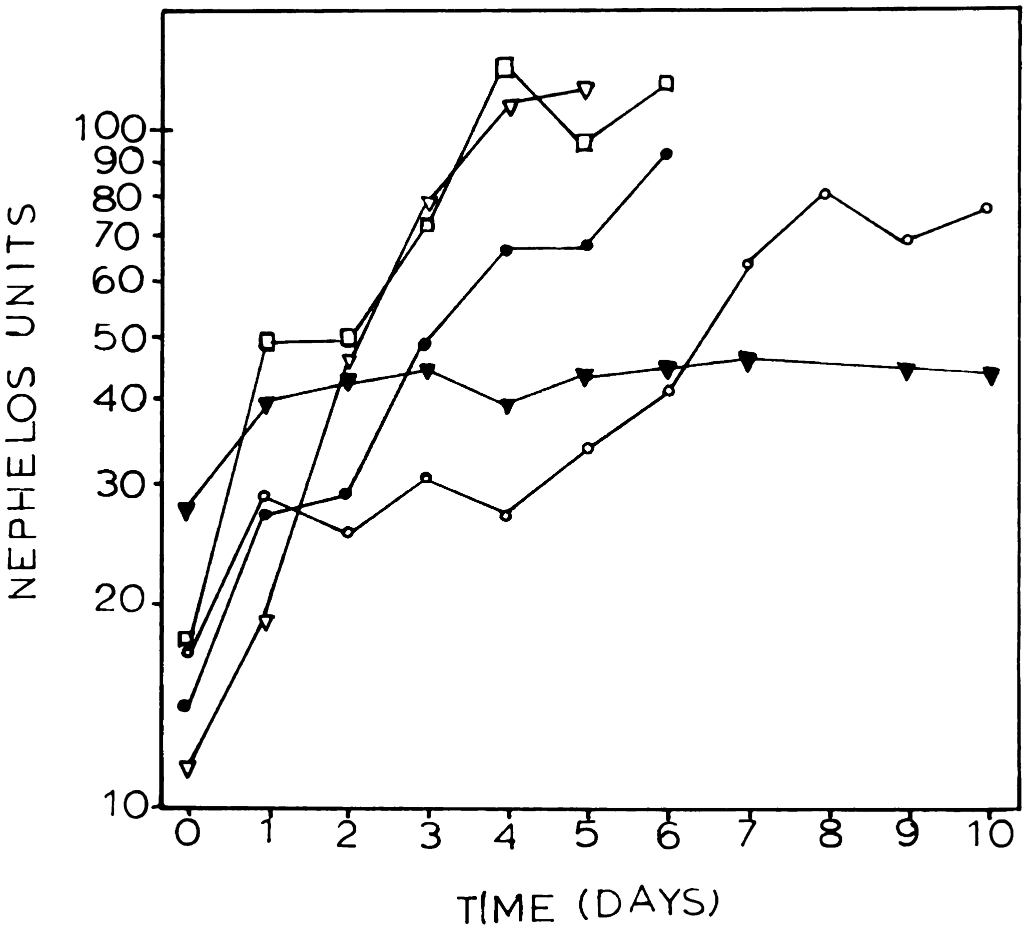

Figure 1. Growth curve showing growth of cultures using inocula of various ages. The growth was measured at one-day intervals by nephelometry of a 1 to 10 dilution of each culture. Age of inocula denoted by:

- ▽ 3 days
- □ 9 days
- ● 21 days
- ○ 8 months
- ▼ 20 months

grew a
regula
J
genic
appare
which
day 1
result
above.
time o

Determ

Th
resolu
field
becaus
best m
acridi
observ
(see G

Va
vation
raldeh
phosph
mate o
(35) to

grew at a rate comparable to that of a culture inoculated with regularly transferred stock (Figure 2).

Jackson (50) reported the generation time of Nichols nonpathogenic *T. pallidum (T. refringens)* as 45 hr. However, this was apparently calculated from the earliest part of the growth curve, which probably included the lag phase. A calculation based on day 1 to day 3 of her graph, which is part of the exponential phase, resulted in a generation time of 24 hr, similar to the value reported above. L. Martin (personal communication) found that the generation time of this organism is 20 hr.

General Ultrastructure

Determination of Optimal Microscopy Techniques

The diameter of *Treponema refringens* approaches the limit of resolution of the light microscope, making observation with brightfield microscopy difficult. Phase contrast and darkfield microscopy, because of the increased contrast they provide, were found to be the best modes for light microscopy studies. Fluorescent microscopy of acridine orange- or euchrysine-stained cells proved useful for the observation of RNA, but was of little value in the study of DNA (see General Ultrastructure: DNA and Cytoplasm).

Various procedures were tested in order to gain adequate preservation of the cells for scanning electron microscopy (SEM). Glutaraldehyde, in some cases followed by osmium tetroxide, was used in phosphate buffer, with or without NaCl added to produce the approximate osmotic conditions (0.3 osmolal) determined by Hardy and Nell (35) to preserve best the typical shape of treponemes. The cells

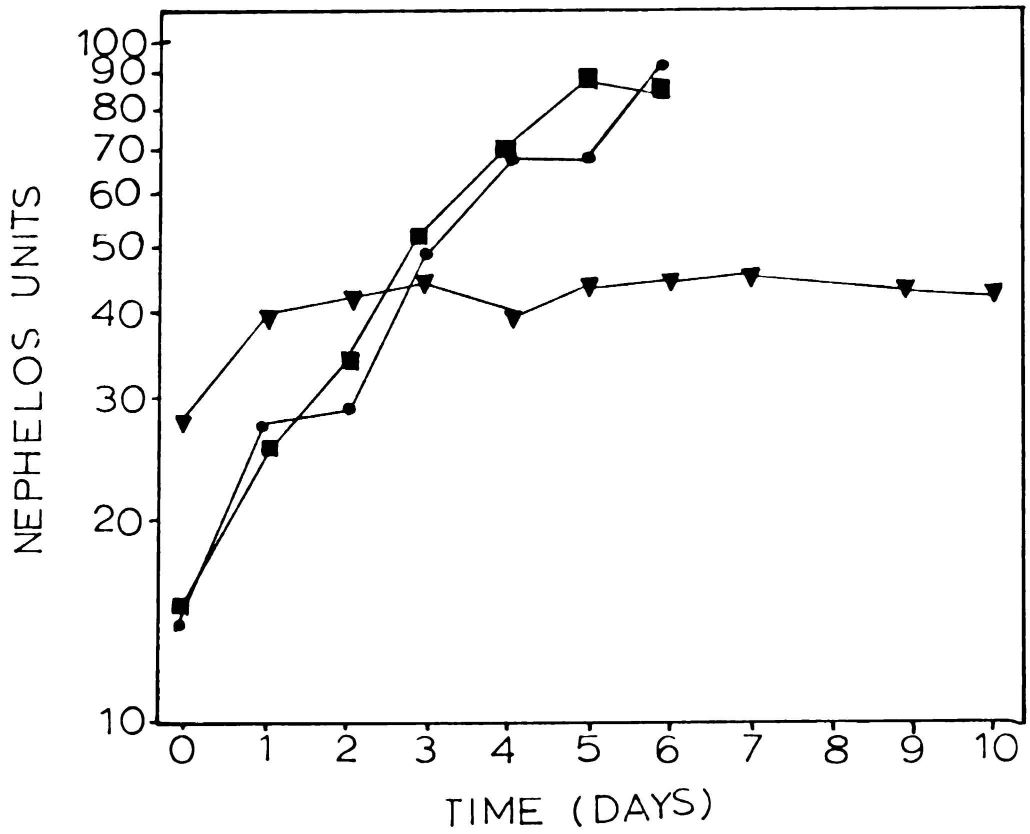

Figure 2. Growth curve showing slow growth of culture inoculated with 20-month-old culture and its recovery when transferred. Minimal growth occurred when a 20-month population was used as inoculum (▲). When the culture which had been inoculated with the 20-month population was itself used as inoculum after 16 days (■) it grew as well as a culture inoculated with a regularly transferred 21-day population (●).

were then dehydrated in an alcohol series and subjected to critical-point drying. The majority of cells in all preparations were relatively straight, but some cells in each preparation were helical. Those specimens fixed with both glutaraldehyde and osmium had the highest percentage of well preserved cells, regardless of the osmotic conditions.

Phosphotungstic acid (PTA), silicon tungstate and ammonium molybdate, at varying pH values, were all satisfactory negative stains for study of the cells by transmission electron microscopy (TEM). Various fixation procedures were tested in the preparation of thin sections for TEM. When the Ryter-Kellenberger fixation procedure was preceded with glutaraldehyde fixation, the membranes were well fixed, but the cytoplasm was somewhat clumped. Neither the DNA nor the cytoplasmic fibrils was well defined. Much better fixation of the cell contents resulted when the Ryter-Kellenberger procedure was repeated using a shorter time for osmium fixation and deleting the glutaraldehyde prefixation. The cytoplasm was evenly distributed, the fibrils were clearly visible, and fine strands were seen in an electron lucent space typical of the nuclear area in Ryter-Kellenberger fixed bacteria. When lanthanum nitrate was substituted for the Ryter-Kellenberger uranyl acetate post-fixation, the DNA clumped inside the nuclear area. One drawback to Ryter-Kellenberger fixation was that the outermost membrane, known in treponemes as the outer envelope, was farther away from the cell than when glutaraldehyde was used prior to the Ryter-Kellenberger procedure.

Shape and Size of Typical Cells

Typical living treponemal cells viewed by darkfield or phase microscopy were undulate (Figures 3 and 4). This appearance was determined by electron and light microscopy to be analogous to the projection of a three-dimensional helix onto a two-dimensional screen. Under the light microscope the lower portion of each turn of the helix appeared out of focus when the upper part was in focus (Figure 3). Furthermore, the wavy appearance was maintained on all sides as the cells rotated (due to water currents or cell motility).

Cells thin sectioned for TEM were occasionally cut in such a plane that their helical nature was apparent. The cell in Figure 5 winds back and forth and also passes out of and re-enters the plane of the figure. SEM micrographs were even more conclusive as to the helical nature of the cells and also demonstrated that the helix is right-handed (Figures 6 and 7). Considerable variation of wavelength and amplitude was noted from cell to cell and often even within the same cell. The mean wavelength was about 880 nm and the mean amplitude was about 170 nm. Negatively stained cells were dried and flattened onto the surface of the supporting film and consequently were not suitable as evidence for the helical nature of the cells.

SEM, light microscopy, and TEM of negative stains disclosed various other information about the shape of treponemes. The terminal portions of cells were often straight (Figures 6 and 7; see also Figures 3 and 4) with tapered ends (Figure 8). Occasional parts of an otherwise helical cell were also straight (Figure 7), often near division points.

F
partia
of ce
cells
visib

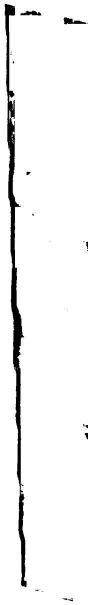

f

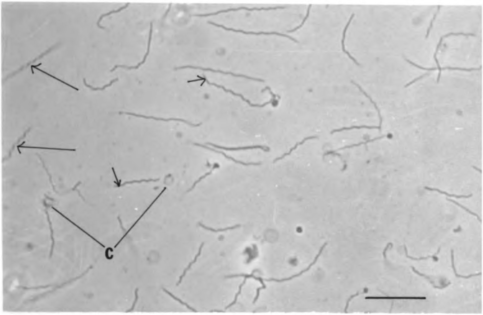

Figure 3. Phase micrograph of *T. refringens*. Note partially out of focus cells which indicate spiral nature of cells (long arrows), and the straight ends on some cells (short arrows). Occasional convoluted cells are visible. Bar = 10 µm.

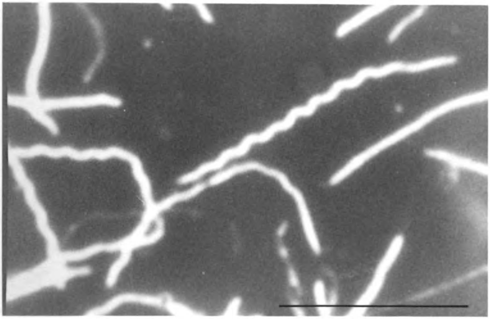

Figure 4. Darkfield micrograph of *T. refringens* from a 6 day culture. Bar = 10 µm.

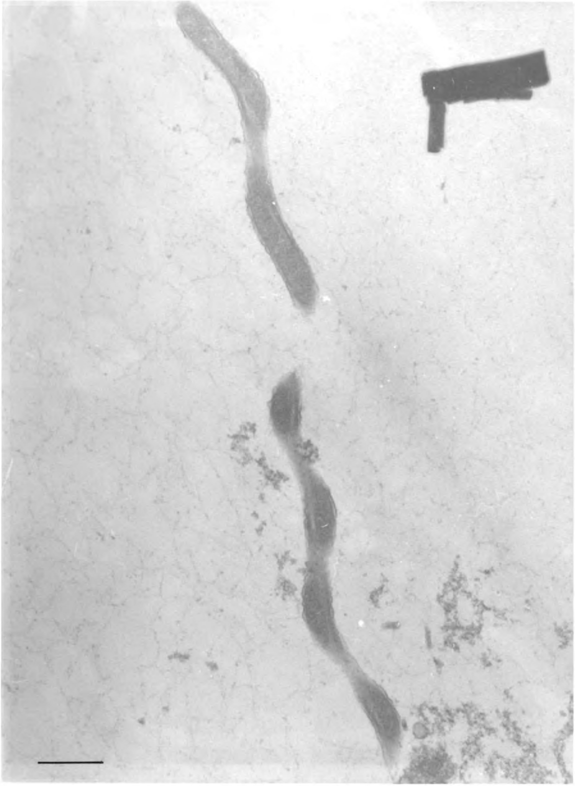

Figure 5. Longitudinal section through cell from 3 day culture. Bar = 0.5 µm.

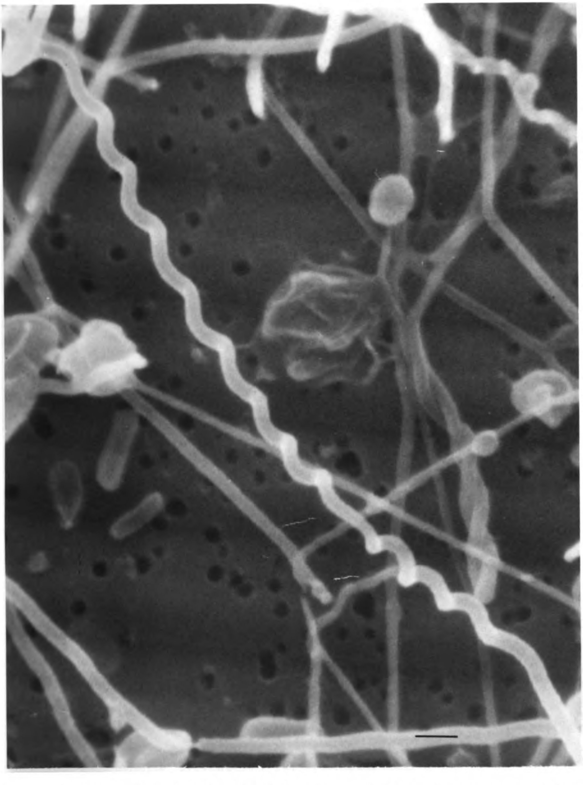

Figure 6. Scanning electron micrograph of helical treponeme among straighter cells. Bar = 0.5 μm.

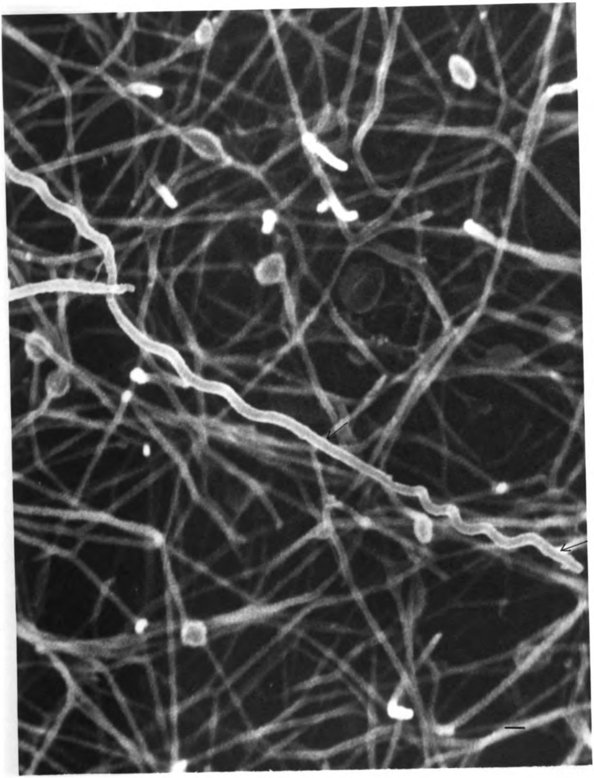

Figure 7. Scanning electron micrograph of helical treponeme among straighter cells. Note straight areas of cell (arrows). Bar = 0.5 µm.

Fig
Note tap

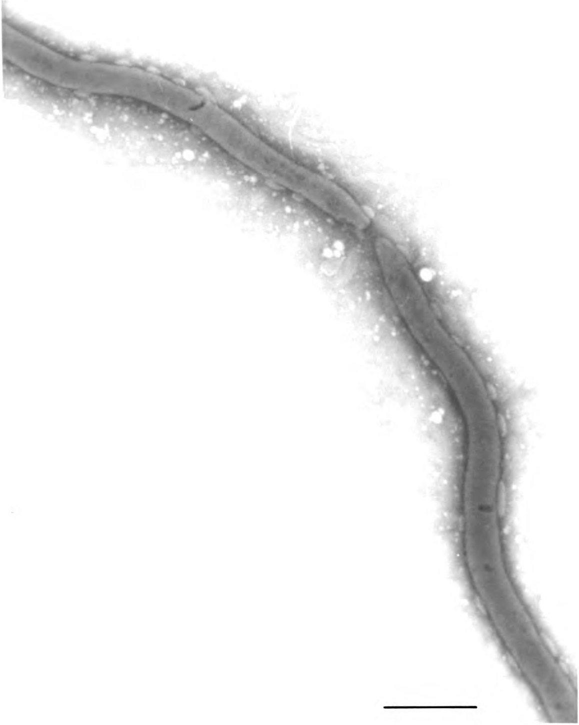

Figure 8. PTA-stained cells which have recently divided. Note tapered ends. Bar = 0.5 µm.

Tabl

sectioned

scanning

Table 3.

Preparatio
Thin secti
Negatively
Critical-p

enormously

Cell lengt

tip) from

(2 to 7 da

cells from

from 8 to

Cell Envel

Outer

(CM) are t

thin secti

which are

by a dark

to be 7.3 +

Table 3 shows the diameter of the cell as measured from thin sectioned cells, negatively stained cells and cells viewed with the scanning electron microscope. The length of the cells varies enormously, especially in the exponential growth phase cultures. Cell lengths (measured on phase micrographs from cell tip to cell tip) from 6 to 20 μm were more common in actively growing cultures (2 to 7 days) and occasionally much longer cells were seen. The cells from a 15-day culture were found to be more uniform, varying from 8 to 16 μm, with a mean length of about 12 μm.

Table 3. Mean diameter of normal cells as measured from micrographs produced by transmission electron microscopy (TEM) and scanning electron microscopy (SEM)

Preparation of cells	Microscope	Diameter (nm)	Number of cells measured
Thin sectioned	TEM	263 ± 4	66
Negatively stained	TEM	226 ± 9	11
Critical-point dried	SEM	196 ± 17	11

Cell Envelope

Outer envelope (OE), peptidoglycan, and cytoplasmic membrane (CM) are the components of the treponemal cell envelope visible in thin sections (Figure 9). Both OE and CM are trilaminar membranes which are composed of an electron light layer bounded on each side by a dark layer. The mean width of the OE and CM were calculated to be 7.3 ± 0.2 nm and 7.0 ± 0.4 nm, respectively. The CM was

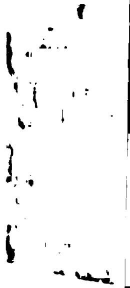

Fig
layers o
(OE), pe
the fibr

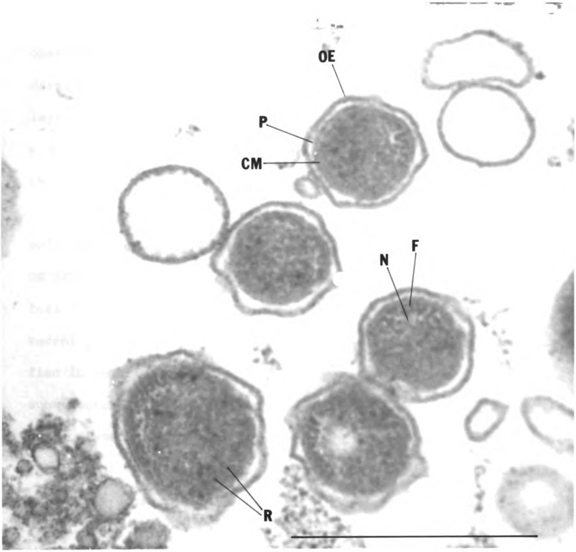

Figure 9. Thin section of cells from a 5 day culture. The layers of the cell envelope are clearly visible: outer envelope (OE), peptidoglycan (P) and cytoplasmic membrane (CM). Note also the fibrils (F), nuclear area (N), and ribosomes (R). Bar = 0.5 μm.

difficult to measure accurately because the adjacent cytoplasm obscured its inner boundary. The empirical ratio of the width of dark:light:dark components was about 2:3:2 for both membranes. The layer assumed to be peptidogylcan was a uniformly dense band (6.0 ± 0.4 nm wide) lying in direct contact with the outer layer of the CM.

Prior to complete separation of dividing cells, the OE was the only structure connecting the two cells. After division, a tail of OE often remained (Figure 10). The identification of the membrane tail as OE was confirmed by examination of a thin section of a recently divided cell (Figure 11). OE could sometimes be identified in negative stains of cells or membrane vesicles by its unique substructure. This consisted of electron dense particles about 8 nm in diameter which were hexagonally packed and separated by approximately 2 nm of electron light space (Figures 25 and 54). Vesicles of OE from disrupted cells were also occasionally found joined in large masses (Figure 12).

These masses of OE vesicles usually were connected to branched or unbranched tubules with distinctive striations and terminal knobs (Figure 12). Striated tubules were occasionally associated with the OE surrounding normal cells (Figure 13), and more often with the OE surrounding disrupted cells (Figure 46). Striated tubules had a fairly uniform diameter of 35 ± 2 nm in both negative stains and thin sections. In negative stains, dark bands with a periodicity of 4.0 to 5.5 nm extended across the central dark area (lumen) of the tubule and into part of the lighter area on each edge (Figure 13). Striated tubule substructure was more apparent in thin sections,

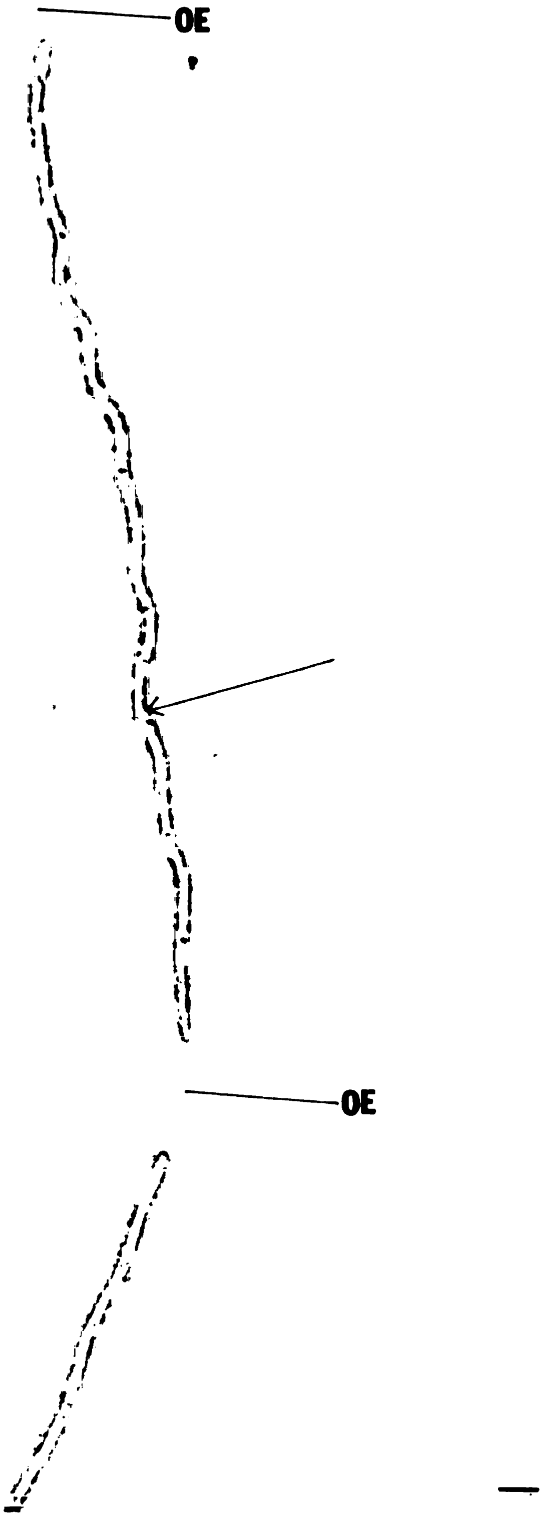

Figure 10. PTA-stained divided cells (from a 3 day culture) still bridged with outer envelope (OE). Both daughter cells have membranous structures (arrows) and one has a tail of OE remaining from previous division. Bar = 0.5 µm.

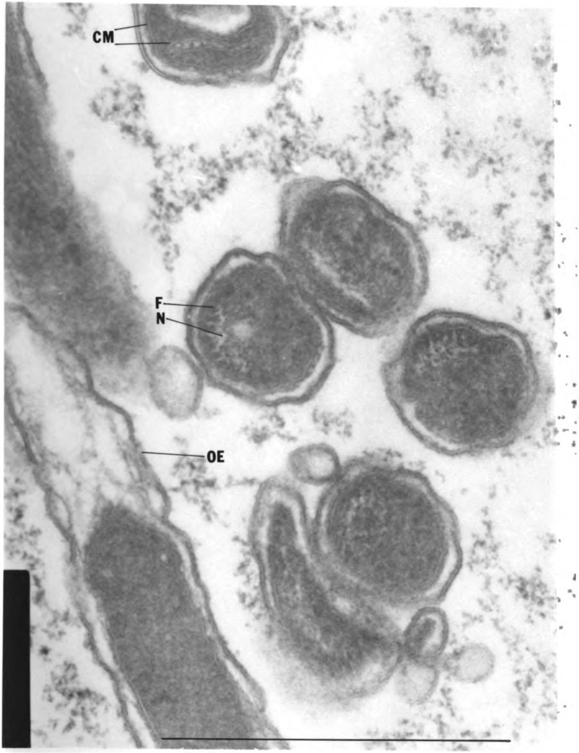

Figure 11. Thin sections of cells from a 5 day culture. OE extends past end of one cell. Cross sections show fibrils (F) and nuclear area (N). The internalized membrane is continuous with the cytoplasmic membrane (CM). Bar = 0.5 μm.

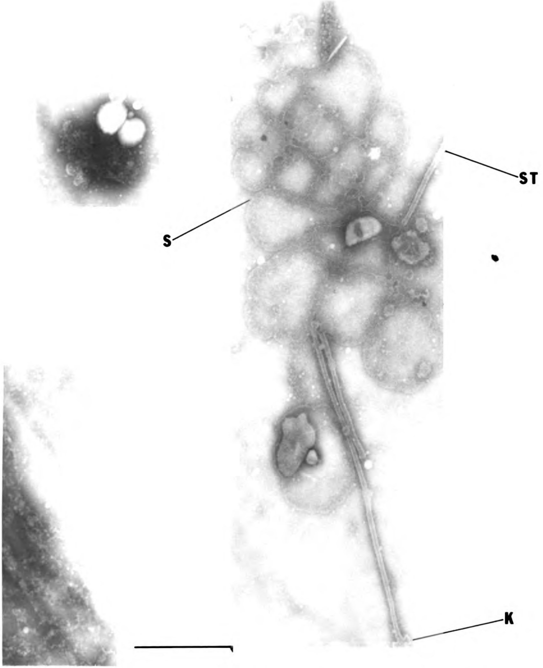

Figure 12. Outer envelope vesicles and striated tubules (ST) with knobbed ends (K) from population of cells disrupted with guinea pig serum in Tris. Outer envelope substructure (S) is visible. Negatively stained with ammonium molybdate. Bar = 0.5 µm.

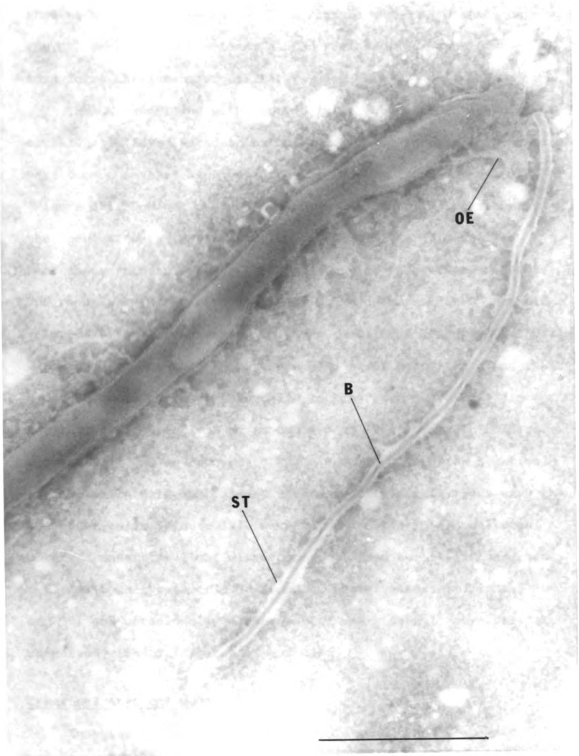

Figure 13. PTA-stained cell with a striated tubule (ST) extending from its outer envelope (OE). Dark bands (B) cross the tubule but do not extend completely across the outer white area. Bar = 0.5 μm.

showing membrane (presumably the structure which is continuous with the OE) surrounding the inner banded region of the tubule which in turn forms the lumen (Figure 14).

The CM, sometimes with peptidoglycan fragments attached, occasionally invaginated into the cell. These internalized membranes were common in thin sections of cells from 5- and 9-day cultures (Figure 15), but not in 3-day cultures (Figure 5). Occasionally the opening to the periplasmic space was visible (Figure 11). Membranous structures were also apparent (at an average of about 760 nm apart) in negative stains of cultures more than 3 days old (Figure 16) and occasionally in younger cultures (Figure 10). Cells with these structures had more negative stain deposited along their sides and were narrower than cells lacking such structures (in negative stains, 153 ± 8 nm as opposed to 226 ± 9 nm; in thin sections 245 ± 7 nm as opposed to 263 ± 4 nm). The narrow negatively stained cells with membrane structures were generally less wavy than the wider cells (Figure 17), as were many cells in old cultures observed under the light microscope. Divided but still connected cells of both types could be found in negative stains (Figures 10 and 18) and occasionally a narrow cell and wide cell were still connected with OE (Figures 18 and 23).

Spherical Atypical Cells

In aging cultures and under certain conditions described below, normal *T. refringens* cells converted to two types of spherical atypical cells 2 to 6 µm in diameter: a convoluted form and a spheroplast-like form (Figures 19 and 20).

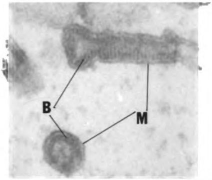

Figure 14. Thin sectioned striated tubules. The banded region (B) is covered with a membrane (M), presumably outer envelope. Bar = 0.5 μm.

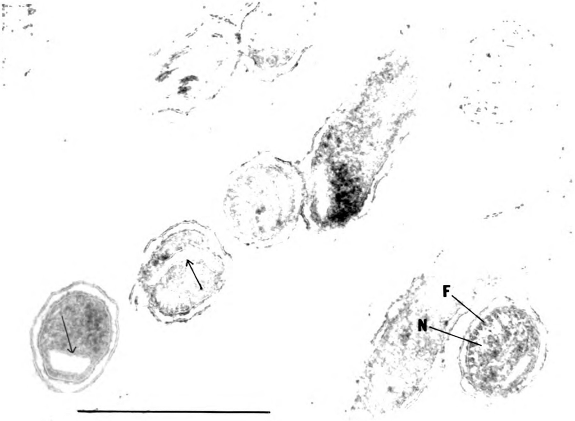

Figure 15. Thin sectioned cells, from a 9 day culture, which have internal membrane structures (arrows). Note also the fibrin (F) and nuclear area (N). Bar = 0.5 μm.

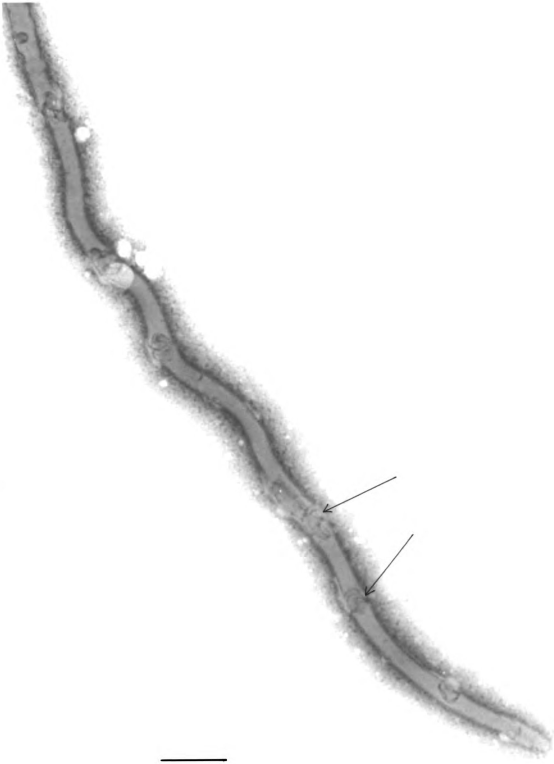

Figure 16. PTA-stained cell, from a 4 day culture, with numerous membrane structures (arrows). Bar = 0.5 μm.

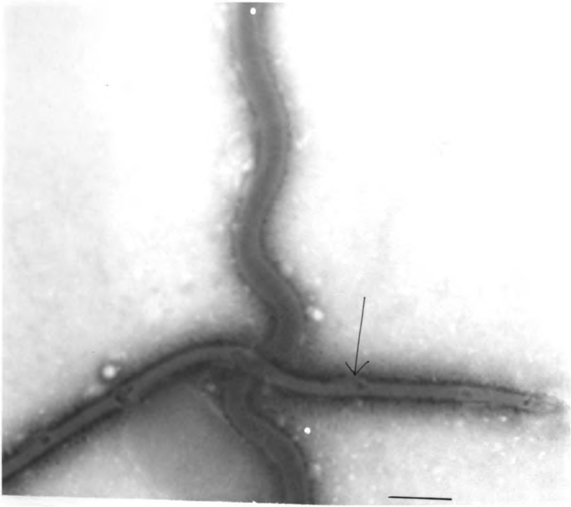

Figure 17. PTA-stained cells from a 4 day culture. One is wide, the other is narrow with membrane structures (arrow). Bar = 0.5 µm.

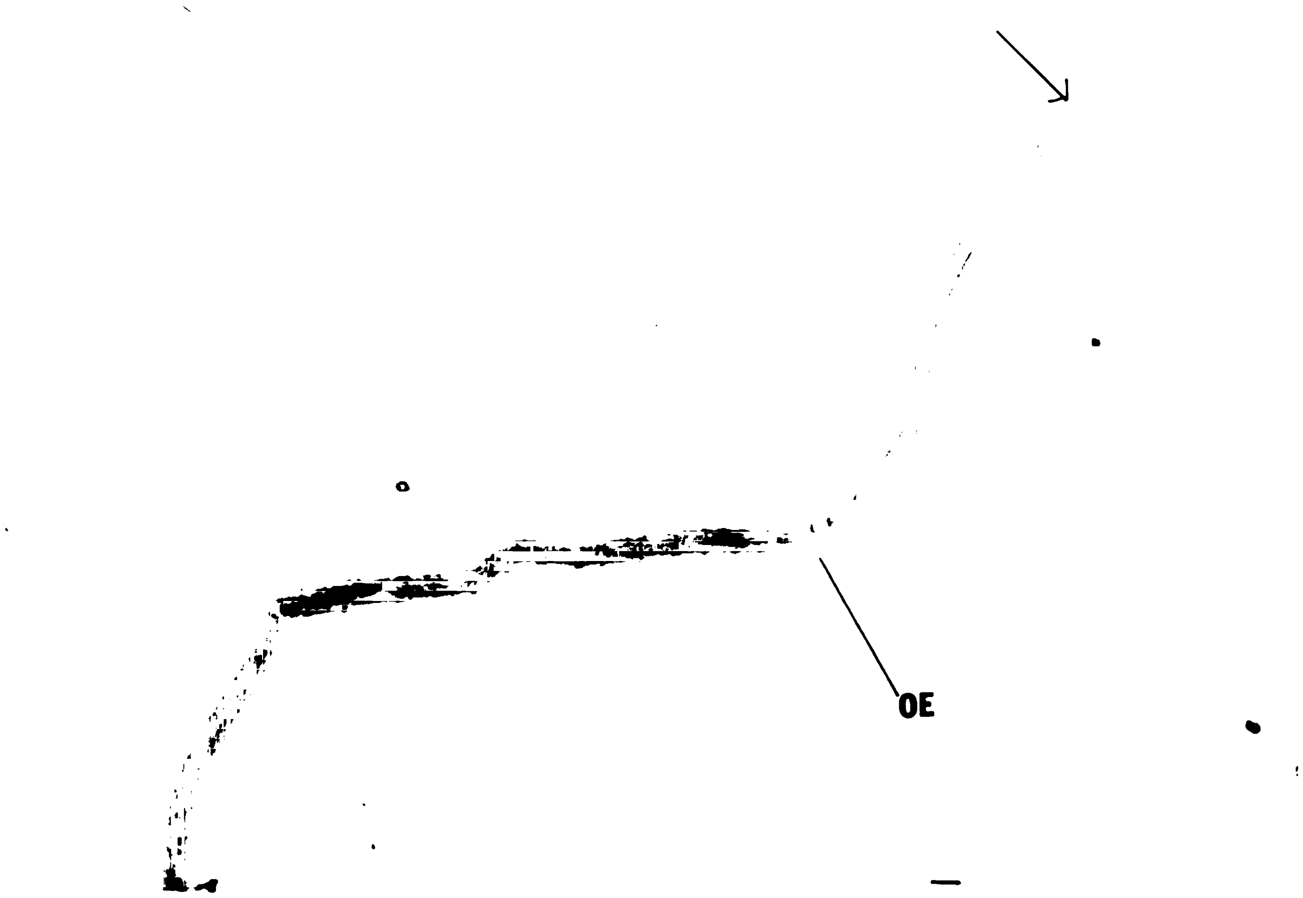

Figure 18. Three PTA-stained cells, two wide and one narrow, bridged with outer envelope (OE). The narrow cell has membrane structures (arrows). Bar = 0.5 μm.

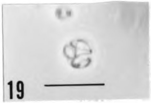

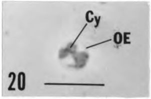

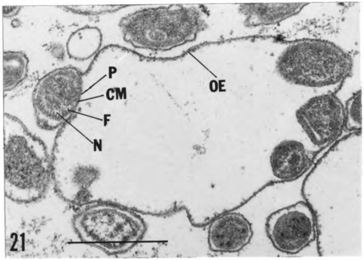

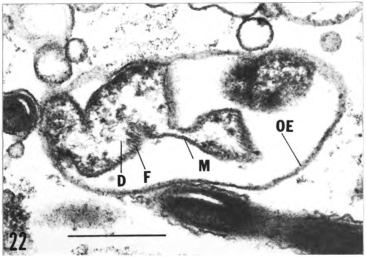

Figure 19. Phase micrograph of convoluted cell. Bar = 10 µm.

Figure 20. Phase micrograph of spheroplast-like cell. Outer envelope (OE) surrounds disrupted cytoplasm. Bar = 10 µm.

Figure 21. Thin sectioned convoluted form. Outer envelope (OE) surrounds the sections of cytoplasmic cylinder bounded with cytoplasmic membrane (CM) and peptidoglycan (P). Bar = 0.5 µm.

Figure 22. Thin sectioned spheroplast-like cell surrounded with OE. Disrupted cytoplasm is bounded by cytoplasmic membrane (CM). Note fibril bands (F) and strands of DNA (D). Bar = 0.5 µm.

The convoluted spheres formed when the protoplasmic cylinder, bounded by the CM and peptidoglycan, curled up inside the outer envelope. A negative stain of two partially convoluted cells and one completely convoluted cell is shown in Figure 23. Thin sections through a convoluted form revealed the expanded outer envelope surrounding the curled-up cytoplasmic cylinder which is bounded by CM and peptidoglycan (Figure 21). The cytoplasm of spheroplast-like cells was disrupted, in the form of one or more small spheres within the ballooned-out sphere of OE (Figure 20). From the outer layer inward, thin sections of these cells revealed an expanded OE, CM with traces of peptidoglycan attached and, finally, disrupted cytoplasm (Figure 22).

Cultures incubated three to four weeks or longer were found to contain large numbers of spheroplasts. It should be noted that attempts to induce these forms in younger populations with lysozyme or penicillin failed. A few convoluted forms were present in normal cultures of any age (Figure 3) and were readily induced, especially in cultures beyond the exponential growth phase (see Induction of Spherical Forms).

Axial Filaments

The axial filament was composed of a basal body, a hook and a filament. The filament portion was wavy much like bacterial flagella and consisted of a core and a sheath (Figure 24) which together had a diameter of approximately 20 nm. The core alone measured about 13 nm in diameter. The hook connecting the basal body and filament was not sheathed and had the same diameter as the core as well as a

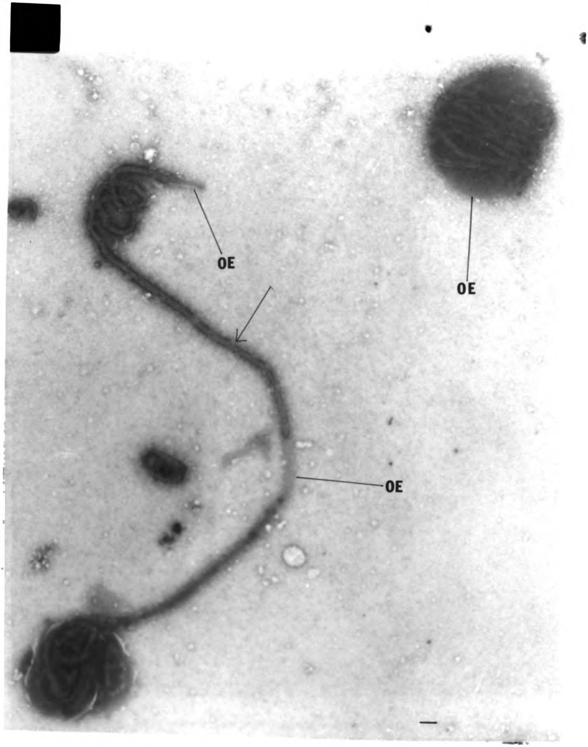

Figure 23. Two partially convoluted cells and a completely convoluted cell, stained with PTA. The convoluted portion of each cell is completely surrounded with outer envelope (OE). One cell has membrane structures (arrows) along its length. Bar = 0.5 μm.

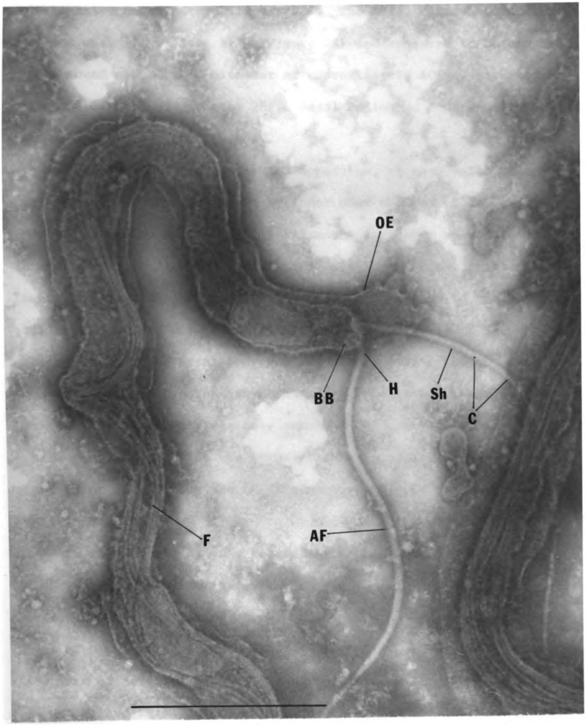

Figure 24. Ammonium molybdate-stained cell which was disrupted with guinea pig serum and lysozyme. Fibrils (F) are visible within the cell. Axial filaments (AF) with basal bodies (BB) and hooks (H) emerge through break in OE. The sheath (Sh) is not present on the distal part of either axial filament, thus revealing the core (C). Bar = 0.5 μm.

distinctive substructure (Figure 26). The basal body was mushroom-shaped when viewed laterally (Figure 24) and appeared to be composed of a round cap, with a diameter of approximately 50 nm, situated on the end of the hook (Figure 25). Basal bodies no longer attached to hooks are present in Figure 27.

The basal body, or insertion apparatus, of each axial filament was rooted in the cytoplasmic cylinder near the end of the cell. Usually one, two or three axial filaments were seen at each end of a cell. Figure 24 shows a disrupted cell in which the axial filaments appear released from the OE but still attached to the cytoplasmic cylinder. It was difficult to determine on the basis of negative stains whether the basal body was actually in the cytoplasm, with the axial filament extending through the cytoplasmic membrane, or whether the basal body was only embedded in a pocket in the CM, while remaining outside the membrane (Figure 58). The basal body appears to lie outside the CM in a micrograph of a thin sectioned cell in Figure 28.

In thin sections, one, two or three axial filaments were sometimes seen just inside the OE within the periplasmic space of typical cells (Figures 28, 29 and 30) or between the OE and the CM of either type of atypical spherical cell (Figure 31). However, many cross sections of normal cells did not contain any axial filaments (Figures 15 and 9) and axial filaments not in the cell, but simply enclosed in trilaminar membrane were also seen in longitudinal or cross section (Figure 32; see also Figures 29 and 30). Occasionally a connection between this membrane tube and cellular OE was visible (Figure 32; see also Figure 29) indicating that the axial filament

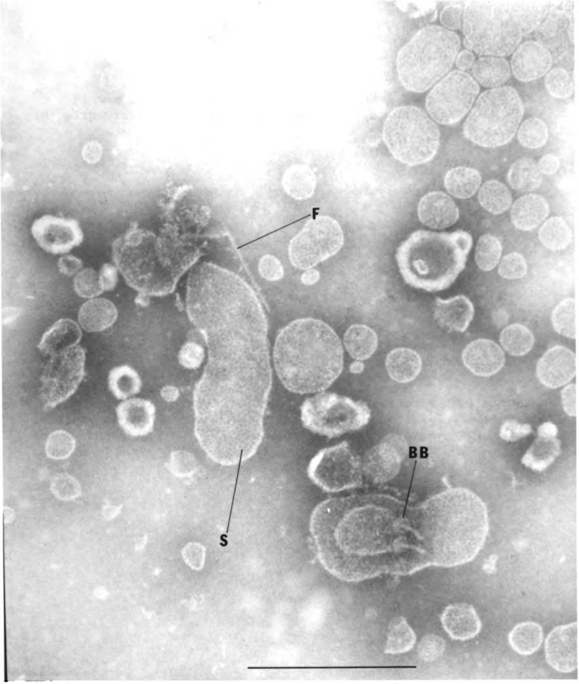

Figure 25. Negative stain of band A of Renografin gradient. Note outer envelope vesicles with substructure (S), axial filament hooks with basal bodies (BB) and a fibril (F). Bar = 0.5 μm.

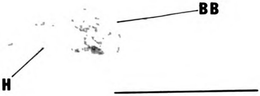

Figure 26. Uranyl oxalate-stained basal body (BB) and hook (H) with visible substructure. Bar = 0.1 μm.

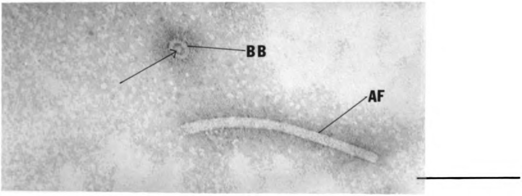

Figure 27. Uranyl oxalate-stained basal body (BB) which has stain deposited around the point at which the axial filament hook was attached (arrow). A fragment of axial filament (AF) is also present. Bar = 0.1 μm.

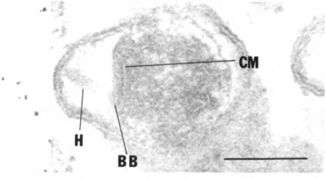

Figure 28. Thin sectioned cell with axial filament hook (H) and basal body (BB) apparently embedded in pocket of cytoplasmic membrane (CM). Bar = 0.1 μm.

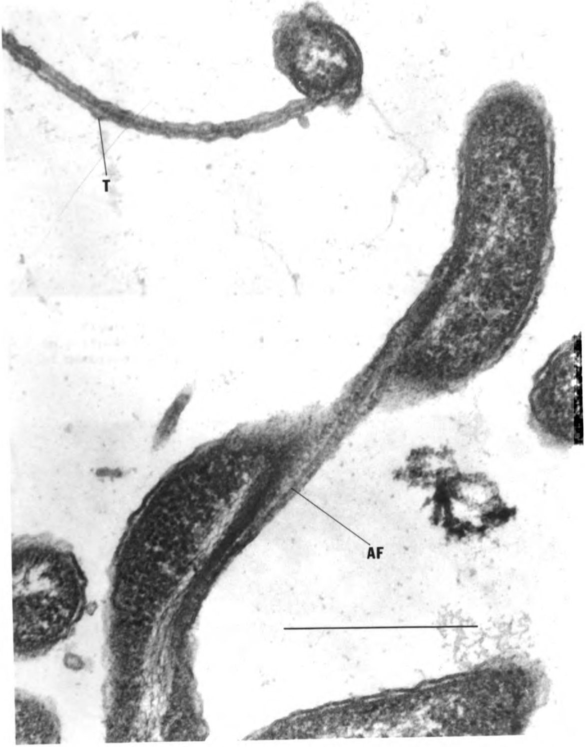

Figure 29. Longitudinal sections of axial filaments in periplasmic space (AF) and within a tube of membrane (T). Bar = 0.5 µm.

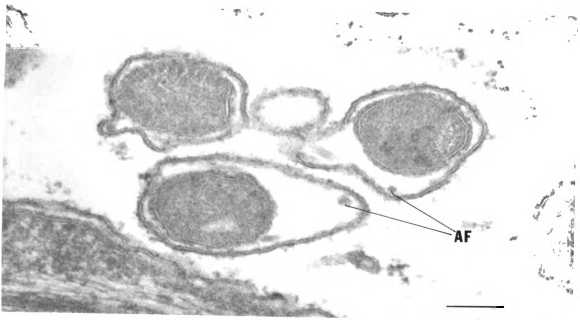

Figure 30. Cross sections of cell with axial filaments (AF) in periplasmic space. Also present is a cross sectioned tube (T) of membrane enclosing an axial filament. Bar = 0.1 µm.

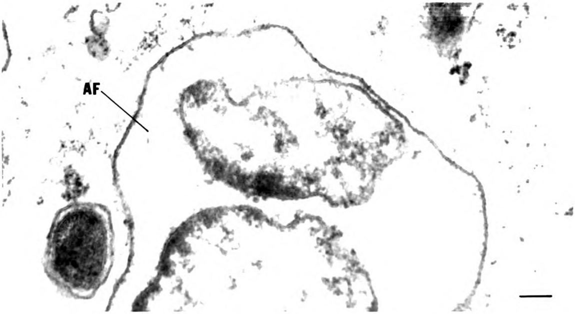

Figure 31. Thin sectioned axial filament (AF) in space between outer envelope and cytoplasm of spheroplast-like form. Bar = 0.1 µm.

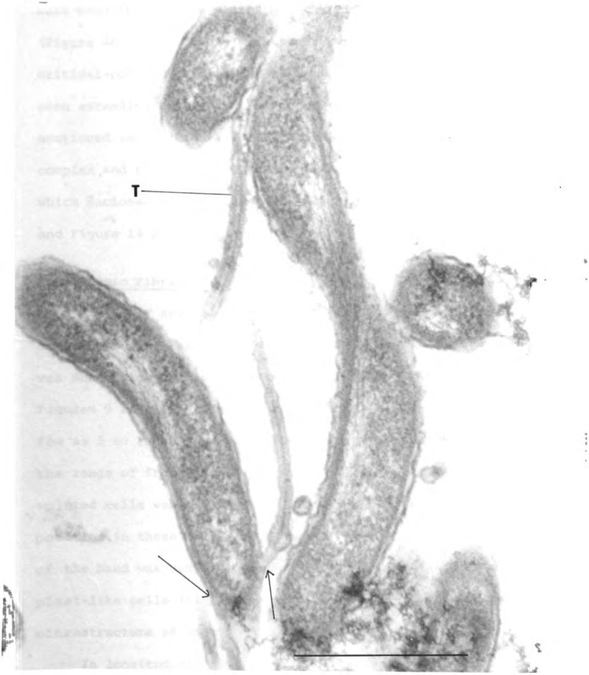

Figure 32. Thin sections of cells and tubes of membrane (T) containing axial filaments. The membrane of the tube is continuous with cellular OE at the arrows. Bar = 0.5 µm.

was protruding away from its normal position next to the cytoplasmic cylinder while still enclosed in OE. Such tubes of membrane surrounding axial filaments were commonly seen in thin sections but were seen in negative stains of only old (Figure 33) or disrupted (Figure 48) cells. They were never seen in cells subjected to critical-point drying for SEM. Striated tubules were occasionally seen extending from the OE of normal negatively stained or thin sectioned cells (Figure 13). Their substructure was clearly more complex and their diameter more uniform than the simple tubes of OE which enclosed axial filaments. Compare Figure 13 with Figure 48 and Figure 14 with Figure 32.

Cytoplasmic Fibrils

A band of several cytoplasmic fibrils ran through the cell adjacent to the inner side of the CM; the location of these fibrils was most evident in cross sections of cells (Figure 15; see also Figures 9 and 11). The number of fibrils per cell varied from as few as 5 to as many as 21. The most predominant numbers fell in the range of from 6 to 10 (Figure 34). Since the cytoplasm of convoluted cells was undisturbed, the fibrils were in their normal position in these cells (Figure 21). More than one cross section of the band was usually present on the inside of the CM of spheroplast-like cells (Figure 22). Details concerning the size and ultrastructure of fibrils are reported in a later section.

In longitudinal sections, the fibrils lay adjacent to the CM, crossing from one side of the section to the other (Figure 35). Fibrils invariably lay along the inside of the curves in those

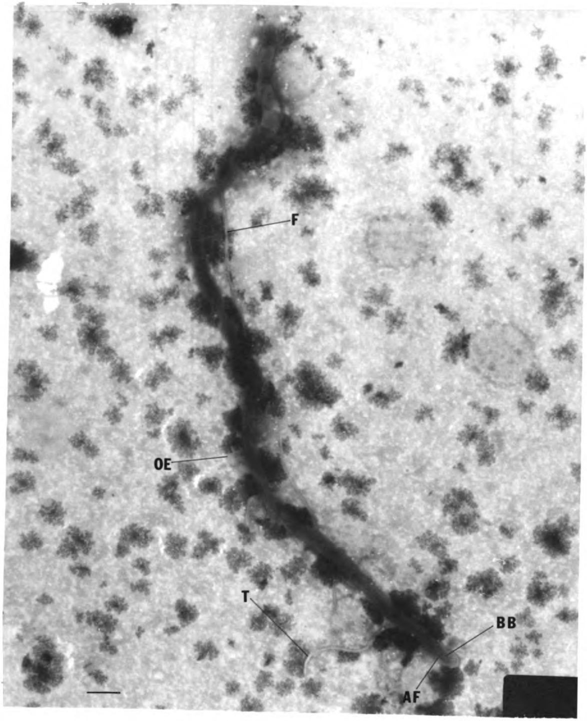

Figure 33. Negative stain of cells from a 2 month culture. Axial filaments (AF) arising from basal bodies (BB) near the end of each cell remain within the periplasmic space or extend away from the cell within a tube (T) of outer envelope (OE). Fibrils (F) can be seen within each cell and extending away from the cells. Stained with 0.5% PTA pH 6.7. Bar = 0.5 μm.

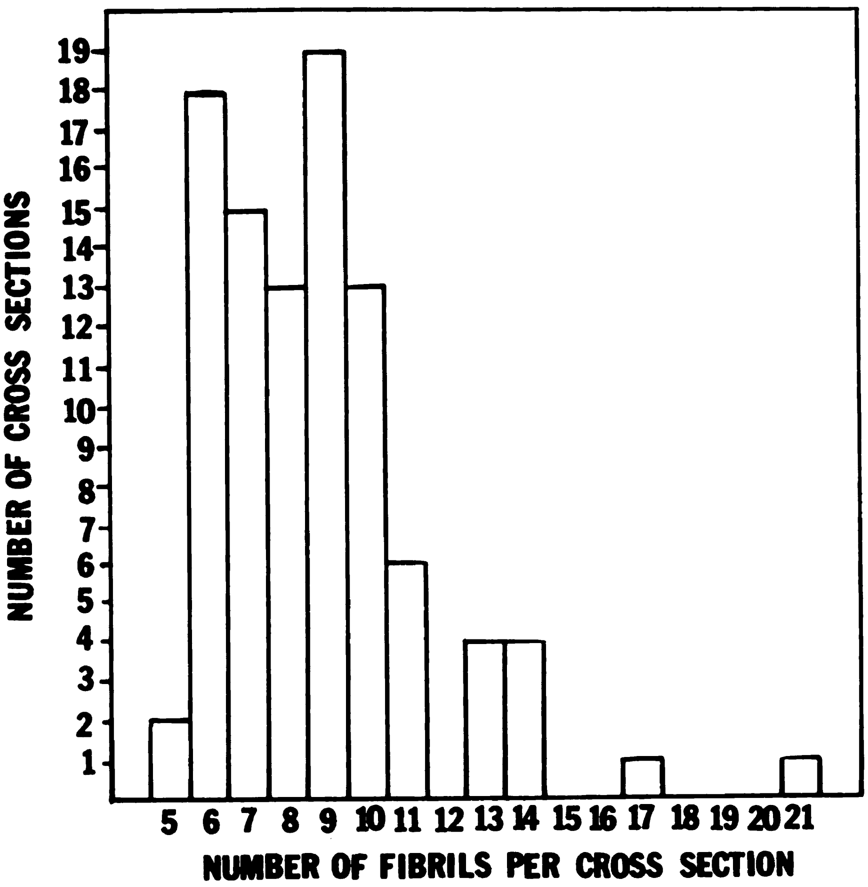

Figure 34. Distribution of the number of fibrils per cross section of cell. The number of fibrils was counted in 98 treponemal cross sections in which the fibril band was clearly visible.

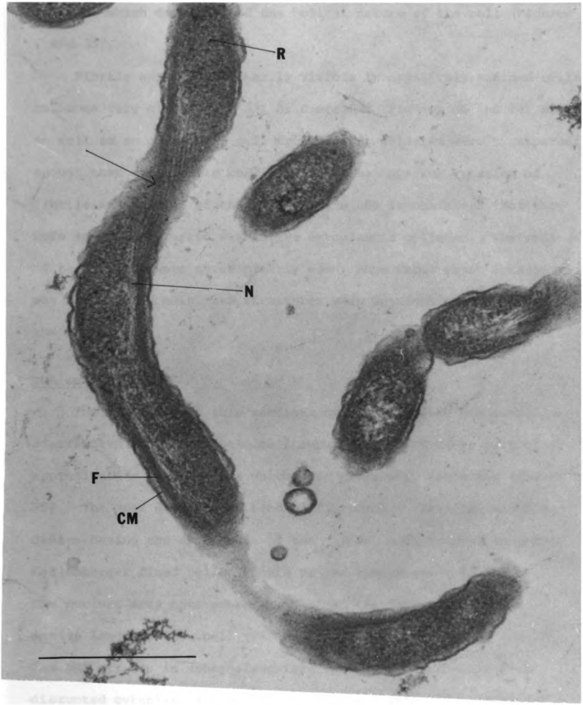

Figure 35. Longitudinal section of cell with fibrils (F) adjacent to inner edge of cytoplasmic membrane (CM). Nuclear area (N) is found next to the fibrils at several points along the cell. At arrow, fibrils cross from the inside of one curve of the section to the inside of the next curve. Ribosomes are visible within the cell. Bar = 0.5 μm.

sections which demonstrated the helical nature of the cell (Figures 5 and 35).

Fibrils were not ordinarily visible in negatively stained cells but some very old (Figure 33) or disrupted (Figures 36 and 24) cells as well as an occasional cell from younger cultures were transparent enough that the fibrils were visible. The apparent crossing of fibrils at the edge of the cell (Figure 36) demonstrated that they were spirally arranged within the cytoplasmic cylinder. The ends of the fibrils were never clearly seen; thus their exact location was unclear. Specialized structures were apparently not present on the fibril ends.

DNA and Cytoplasm

The cytoplasm in thin sections of *T. refringens* was evenly distributed and often included irregularly shaped dense particles approximately 14.5 nm wide which were presumably ribosomes (Figure 35). The area next to the band of fibrils was fibrillar and less dense--having the appearance of the typical nuclear area in Ryter-Kellenberger fixed cells (Figure 9; see also Figures 15 and 21). The nuclear area most probably adjoined the fibrils along the entire length of the cell (Figure 37; see also Figures 29 and 32). The DNA strands in spheroplast-like forms and other cells with disrupted cytoplasm appeared to be directly attached to fibrils (Figures 38, 39 and 22).

Fluorescence microscopy was employed as another means of studying the location of DNA and RNA in the cell. Smears of treponemes were made on slides, fixed, and stained with acridine orange or

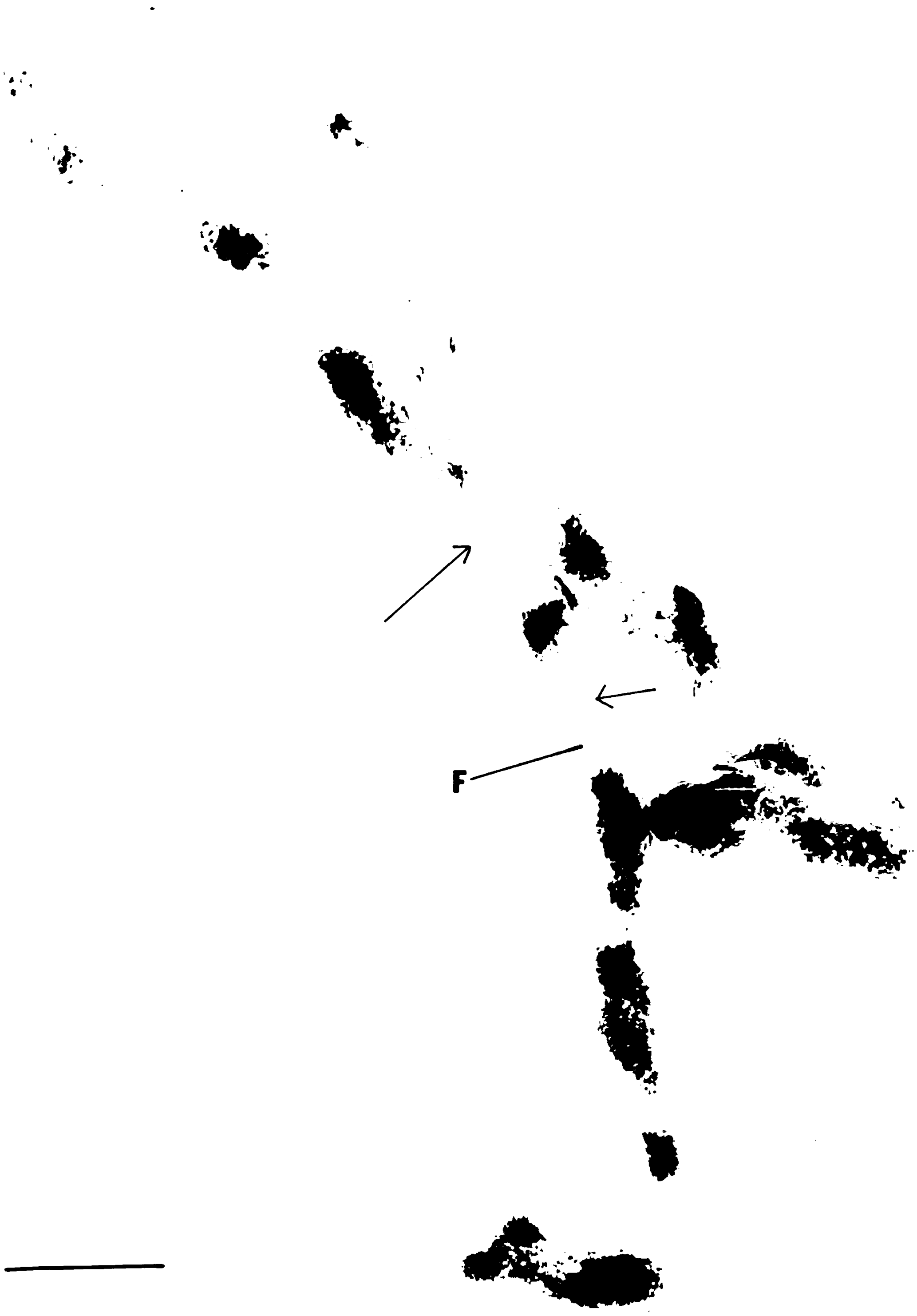

Figure 36. PTA-stained cell disrupted with guinea pig serum and lysozyme. The cytoplasm is unevenly distributed and fibrils (F) are visible within the cell. Note apparent crossing of fibrils at edge of cell (arrows). Bar = 0.5 µm.

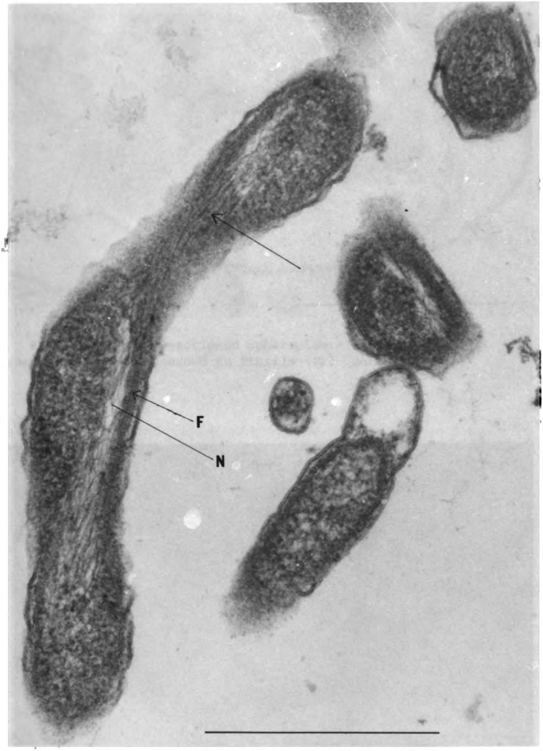

Figure 37. Thin sectioned cell with fibrils (F) and nuclear area (N) visible. The longitudinally sectioned fibril (arrow) adjacent to the cytoplasmic membrane resembles a trilaminar membrane. Bar = 0.5 μm.

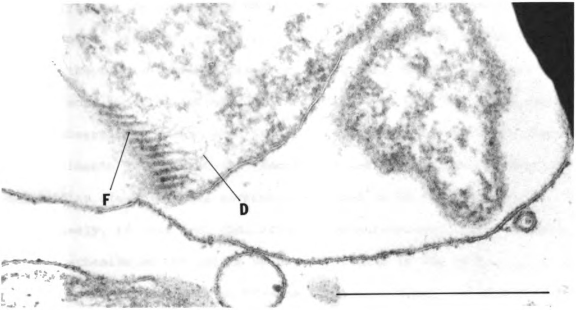

Figure 38. Thin sectioned spheroplast-like cell. Note strands of DNA (D) attached to fibrils (F). Bar = 0.5 μm.

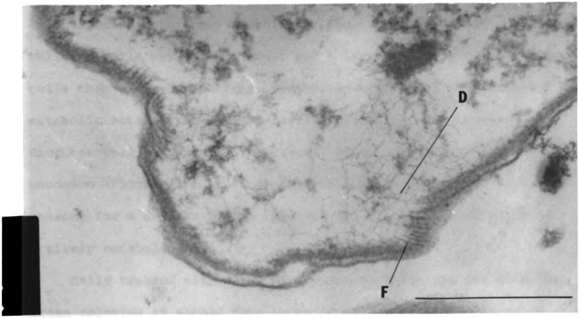

Figure 39. Thin sectioned spheroplast-like cell. Note strands of DNA (D) attached to fibrils (F). Bar = 0.5 μm.

euchrysine. The alternate method was to stain unfixed cells in a wet mount. Similar results were obtained with either method except that the fluorescence of fixed cells was less intense and faded much more rapidly. Vitally stained cells were used for photography and observation except when it was necessary to fix the cells for experiments with nucleases. Euchrysine was usually used instead of acridine orange because euchrysine-stained cells fluoresced more intensely, if less red, than acridine orange-stained cells, while the mechanism of the action of the two stains is the same.

Cells stained with euchrysine fluoresced green, various shades of orange (Figure 40), or orange alternating along the cell length with green (Figure 41). Cells treated with RNase and stained with euchrysine were green rather than yellow or orange, indicating that when present RNA stained orange as expected. Cultures in the exponential growth phase contained a higher percentage of orange cells or cells with orange areas and a lower percentage of all-green cells than older populations, presumably because of the increased metabolic activity in younger cells. Dividing cells in which one daughter cell contained more orange than the other were not uncommon (Figure 42). This is difficult to explain since it is unusual for a cell to divide into two cells, only one of which is actively metabolising.

Cells treated with DNase subsequent to RNase did not lose the green coloring as should have happened if the green fluorescence was due to DNA. Both before and after DNase treatment, the outer envelope extending between divided cells, as well as the membrane and cytoplasm of spheroplast-like cells, stained green (Figure 43).

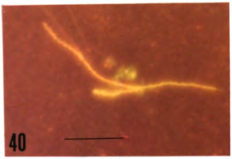

40

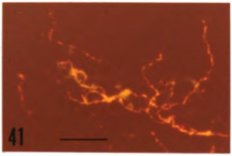

41

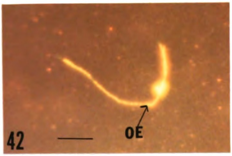

42

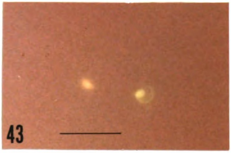

43

Figure 40. Two wet-mounted cells stained with euchrysine. One cell is orange, the other yellow-green. Bar = 10μm in Figures 40 through 43.

Figure 41. Wet-mounted cells stained with euchrysine. Cells are orange and green alternately along their lengths.

Figure 42. Two recently divided cells stained with euchrysine. Cell on left has alternating orange and green areas whereas cell on right is mostly orange. They are connected with green outer envelope (OE).

Figure 43. Wet-mounted spheroplast-like cell stained with euchrysine.

Since the green fluorescence did not prove to be specific for DNA, acridine orange- or euchrysine-staining was not appropriate for determining whether DNA extended the entire length of the cell.

Induction of Spherical Forms

As a first step in cell lysis or for visualization of DNA by the Kleinschmidt technique it was desirable to produce a population of osmotically sensitive spheroplast-like forms.

Treatment with Penicillin

Penicillin was added in various amounts to 3- or 4-day cultures grown in the regular medium, with or without 10% (w/v) sucrose, 25% (w/v) sucrose or 1 M ammonium acetate. When 0.1 U penicillin per ml was used, the culture turbidity increased at the normal rate, but many of the cells were extremely long (up to 10 times the mean length) and without visible division points. Little or no growth was evident in penicillin concentrations of 1 U per ml or 10 U per ml. The population included a high percentage of convoluted forms, with some emaciated and normal cells, but few spheroplasts.

Treatment with Lysozyme

Attempts to induce spheroplasts with lysozyme resulted instead in convoluted forms. The result was not specific to lysozyme treatments, as seen below. A culture was centrifuged and the pellet resuspended in buffer or water, with or without an osmotic stabilizer, EDTA or lysozyme. Phase microscopy was used to examine the cells after one to two hours as well as after 24 hours. Convoluted forms developed more readily in cultures that were beyond the exponential phase of growth, even when cultures were only centrifuged and resuspended in buffer or water. The results are summarized in Table 4.

Lysozyme-EDTA in Tris and sucrose appeared to induce all cells of any age culture to convolute. Lesser but quite severe effects were seen in any other lysozyme solution (Figure 44) or whenever Tris was present, with or without lysozyme. These effects were more pronounced after one day than after one hour. The number of spheroplast forms did not increase under any of these conditions; nor did severe cell disruption or lysis occur.

Cell Lysis

The attempt to isolate cytoplasmic fibrils from treponemes required that they be lysed. Guinea pig serum was tried as a lytic agent because Nevin and Guest (77) had reported that the complement and lysozyme present in guinea pig serum had a lytic effect on several treponemal strains.

Treatment with Guinea Pig Serum

The addition of guinea pig serum (GPS), with or without added lysozyme, to cell suspensions produced mangled or emaciated cell forms. Blebs were often evident at points along the cell (Figure 45). Electron microscopy confirmed that this treatment disrupted the cells more than any other lysozyme solution although most cells were still enclosed in outer envelope and not fragmented into smaller pieces. In the least disrupted cells, the cytoplasm appeared unevenly distributed in a striped pattern and the cells were more transparent so that fibrils became visible within them (Figure 36). In some cases, the outer envelope was affected, with striated tubules

Table 4. Inductions of convoluted forms by suspension of treponemes in lysozyme solutions and buffers. The culture was centrifuged and the pellet resuspended in a lysozyme solution or buffer, with or without an osmotic stabilizer, butanol or EDTA. Phase microscopy was used to determine the number of convoluted forms after 1 hr and after 24 hrs.

Resuspension solutions	Effect of solution on cells in exponential phase cultures (2-7 days)[a]		Effect of solution on cells in older cultures (12-21 days)	
	1 hr	24 hrs	1 hr	24 hrs
100 µg/ml lysozyme in following solutions:				
0.1 M EDTA, 5 M ammonium acetate in water, pH 8.0	-	+	++	
0.1 M EDTA, 25% (w/v) sucrose in water, pH 8.0			++	
2% butanol, in 0.067 M phosphate buffer, pH 7.8	++	+++		
2% butanol, 25% (w/v) sucrose, in 0.067 M phosphate buffer, pH 7.8	++	+++		
0.01 M Tris, pH 8.1	+	+++		
2% butanol, in 0.01 M Tris, pH 8.1	+++			
0.01 M EDTA, 25% (w/v) sucrose in 0.01 M Tris, pH 8.1	++	++++		
0.01 M EDTA, 40% (w/v) sucrose in 0.01 M Tris, pH 8.1	++	++++		
control solutions				
Water	-		+	
0.067 M phosphate buffer, pH 7.0			+	
0.067 M phosphate buffer, pH 7.8	-	-		
0.01 M Tris, pH 8.1	+	+++	+++	
25% sucrose in 0.067 M phosphate buffer, pH 7.8	-	-		
25% sucrose in 0.01 M Tris, pH 8.1	+	+++	+	+++
0.01 M EDTA, 25% (w/v) sucrose in 0.01 M Tris, pH 8.1	++	+++	++	+++

[a] Experimental suspensions were compared with normal cultures by phase microscopy. The number of convoluted cells in experimental suspensions was recorded as follows: - no change, + less than 50% of the cells were convoluted, ++ approximately 50% of the cells were convoluted, +++ more than 50% of the cells were convoluted, ++++ all visible cells were convoluted.

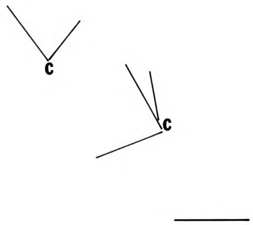

Figure 44. Phase micrograph of 5 day culture suspended in 0.067 M phosphate buffer, pH 7.8, with 2% n-butanol and 100 g/ml lysozyme. After one day, most of the cells had convoluted (C). Compare with normal culture in Figure 3. Bar = 10 μm.

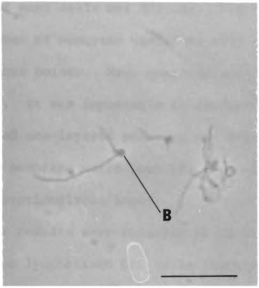

Figure 45. Phase micrograph of a 5 day culture suspended in 0.067 M phosphate buffer, pH 7.8, and guinea pig serum. After one day, many of the cells had blebs (B). Bar = 10 μm.

or vesicles of OE extending from the cell (Figures 46 and 47). Masses of outer envelope and striated tubules were also present apart from the cells (Figure 12). The blebs visible with the phase microscope were seen also with the electron microscope (Figure 48).

Some cells were more severely disrupted than those just described, as they were no longer cylindrical (Figure 49), or had holes in the cytoplasmic membrane and outer envelope through which fibrils or axial filaments extruded (Figures 50 and 24). A few cells were so disrupted that nothing was visible but a band of fibrils and membrane vesicles, some of which had the substructure of outer envelope (Figure 51). The fibril bands often retained a spiral configuration (Figure 52).

Cells treated with guinea pig serum and lysozyme were embedded for thin sectioning. Many spheroplast-like forms were seen and the cytoplasm of most cells was diffuse. Scattered among the cells were a large number of membrane vesicles, many of which were discontinuous at one or more points. Many membrane vesicles were not trilaminar (Figure 53). It was impossible to determine from the pictures if this isolated one-layered membrane was originally outer envelope or cytoplasmic membrane which lost its three-layered appearance or if it was the peptidoglycan layer.

Similar results were observed in cells resuspended in either reconstituted lyophilized GPS or in fresh-frozen GPS and also in amounts of GPS varying from 0.03 ml to 1.0 ml per ml of suspension. This covered a range of 0.01 to 1.7 ml GPS per ml of original culture. The best disruption was seen at pH 8.0, whereas at pH 6.5 most cells were unaffected. The amount of lysozyme added (from 0.02 to 1.5 mg

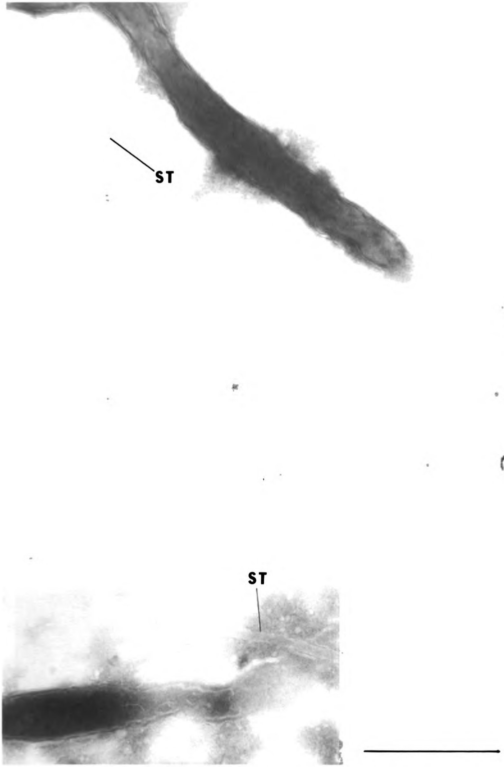

Figure 46. Cells disrupted with guinea pig serum and negatively stained with uranyl acetate. Striated tubules extend from cells. Bar = 0.5 μm.

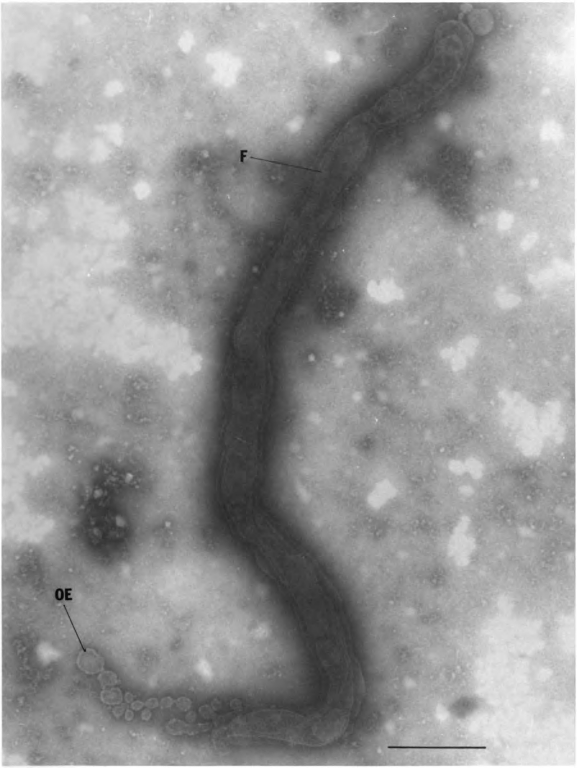

Figure 47. Cell disrupted with guinea pig serum and negatively stained with ammonium molybdate. Note fibrils visible within cell (F) and vesicles of outer envelope. Bar = 0.5 µm.

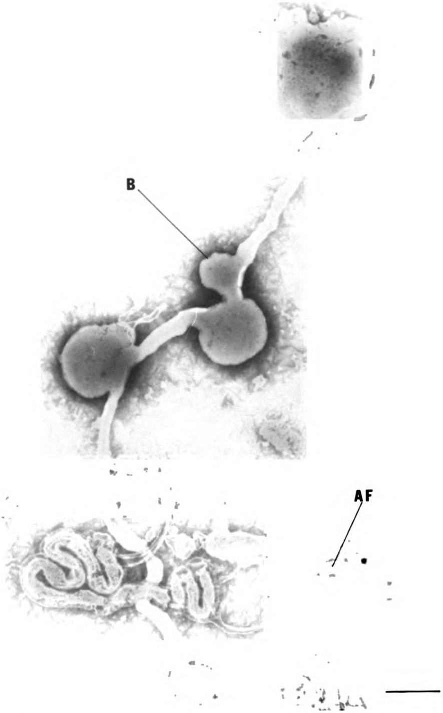

Figure 48. Cells disrupted with guinea pig serum and lysozyme and negatively stained with PTA. Several blebs (B) have formed on one cell. Axial filaments in a tube of outer envelope (AF) are visible in another cell. Bar = 0.5 μm.

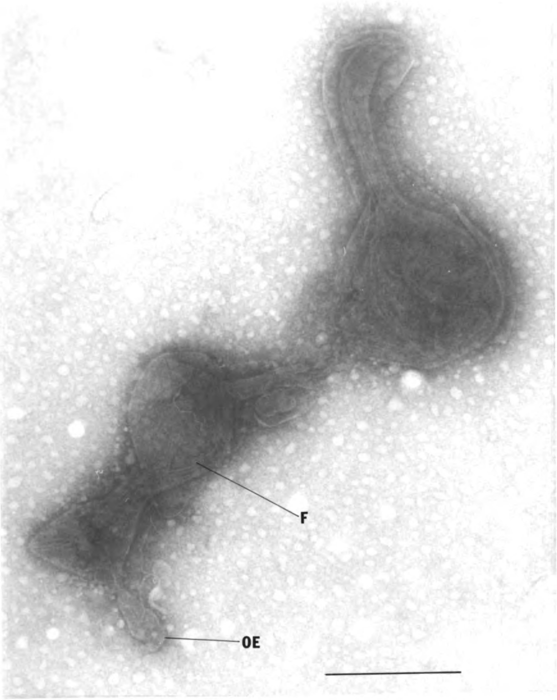

Figure 49. Cell disrupted with guinea pig serum and lysozyme and negatively stained with 0.5% PTA pH 6.7. Outer envelope (OE) and fibrils (F) are visible. Bar = 0.5 μm.

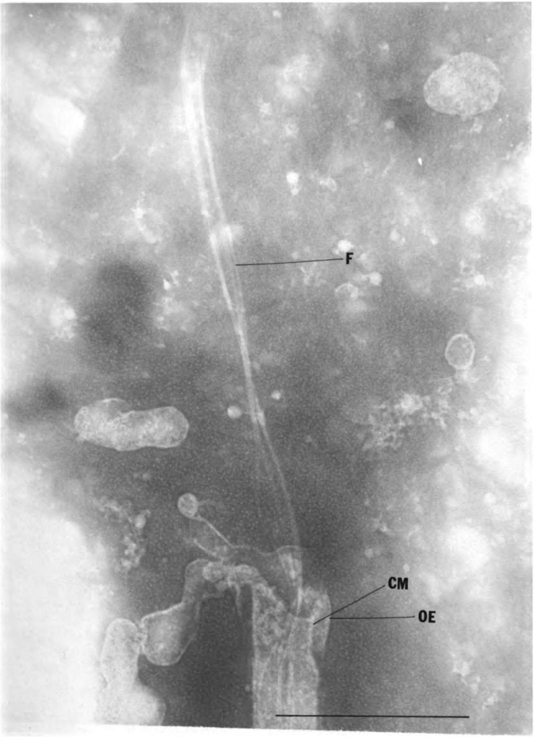

Figure 50. Cell disrupted with guinea pig serum and lysozyme and negatively stained with PTA. Fibrils (F) emerge from the end of the cell through holes in the cytoplasmic membrane (CM) and outer envelope (OE). Bar = 0.5 μm.

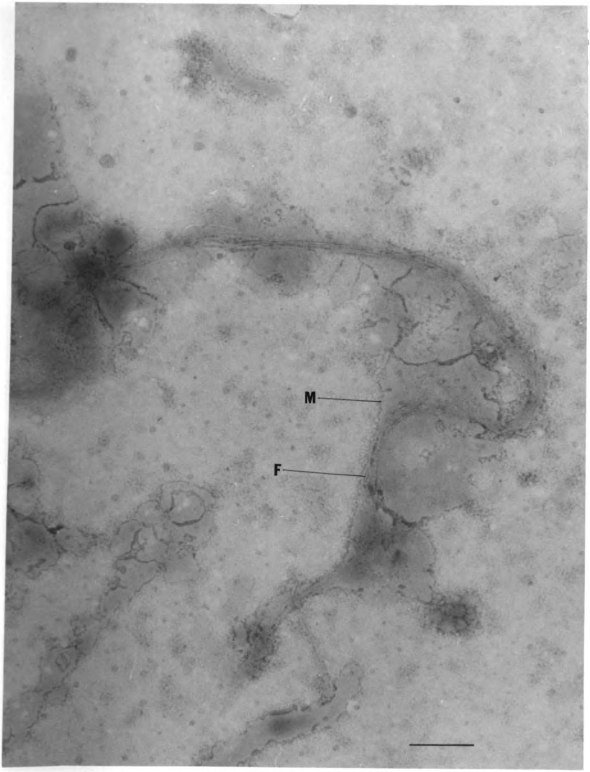

Figure 51. Cell disrupted with guinea pig serum and lysozyme and negatively stained with PTA. Membrane (M) and fibrils (F) remain. Bar = 0.5 µm.

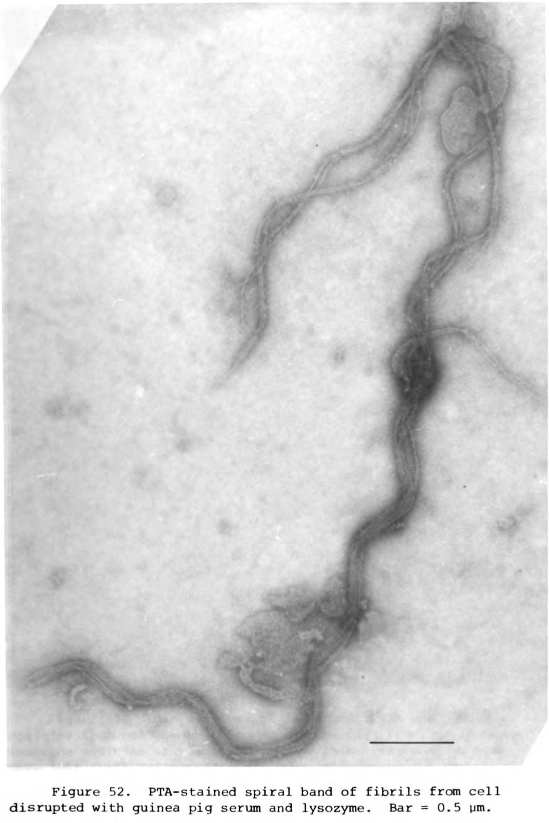

Figure 52. PTA-stained spiral band of fibrils from cell disrupted with guinea pig serum and lysozyme. Bar = 0.5 μm.

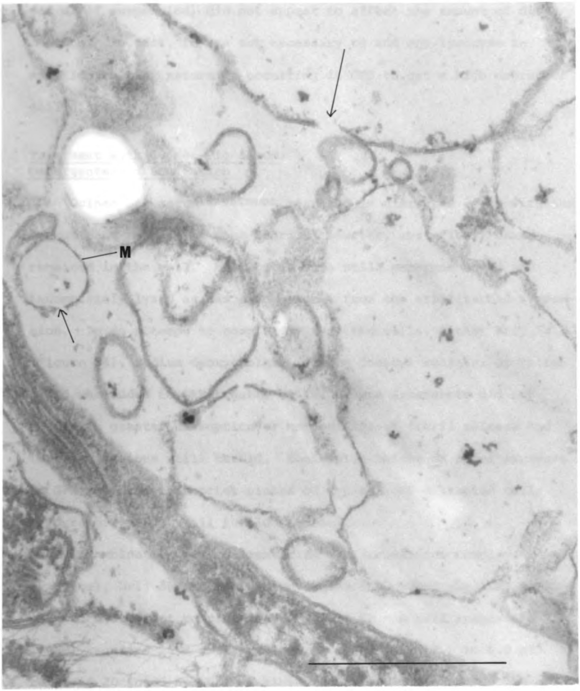

Figure 53. Thin sections of disrupted cells and membrane vesicles from culture treated with guinea pig serum and lysozyme. Membrane vesicles are discontinuous at points (arrow) and some have lost their trilaminar appearance (M). Bar = 0.5 μm.

per ml of suspension) did not appear to affect the amount of disruption. In fact, it was not necessary to add any lysozyme in addition to that naturally occurring in GPS to get a high degree of cell disruption.

Treatment with Guinea Pig Serum, Detergents and Sonication

Guinea pig serum treatment resulted in disrupted cells with the concomitant release of some fibrils; however, most fibril bands remained in the cell. Most cells were still membrane bound and incompletely lysed as was also evident from the still turbid suspension. In an attempt to completely lyse the cells, either Brij 58 (Figure 54), sodium deoxycholate, sodium dodecyl sulfate, or Triton X-100 was added to GPS-treated cells. These detergents did not result in greater disruption or more efficient fibril release and left suspensions still turbid. Sonication before or after exposure to GPS resulted in shorter pieces of typical GPS-disrupted cells (Figure 55) and a still turbid suspension.

A combination of treatment with GPS (containing complement and lysozyme), Brij 58 and sonication, hereafter called the CLBS procedure, did effect complete lysis (Table 5). A cell suspension of 1.6 ml required 15 s sonication while a volume of 2.5 to 6.0 ml required 20 to 35 s. Vortex mixing in place of sonication did not clear the suspension and sodium deoxycholate could not replace Brij t8. CLBS-treated cells viewed under the electron microscope revealed free fibril bands of varying lengths, clumps of individual fibrils, and axial filaments.

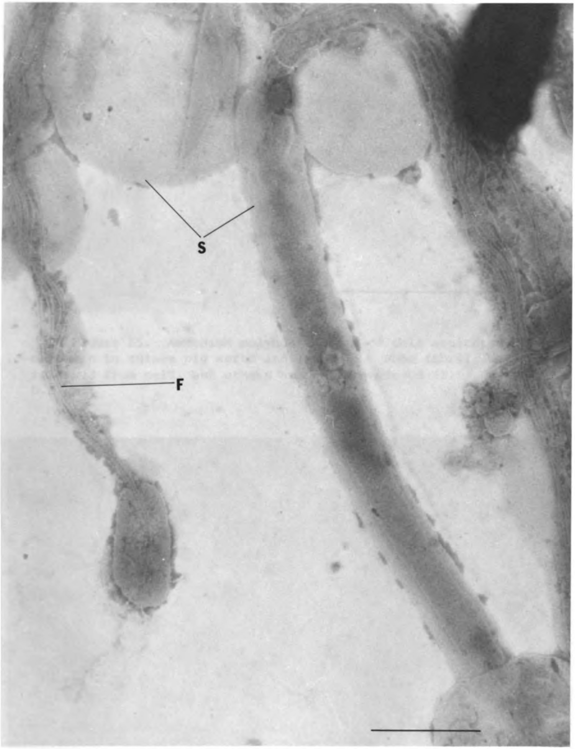

Figure 54. Cells disrupted with guinea pig serum and Brij 58 and negatively stained with PTA. Fibrils (F) are partially released from cell and outer envelope substructure (S) is visible. Bar = 0.5 μm.

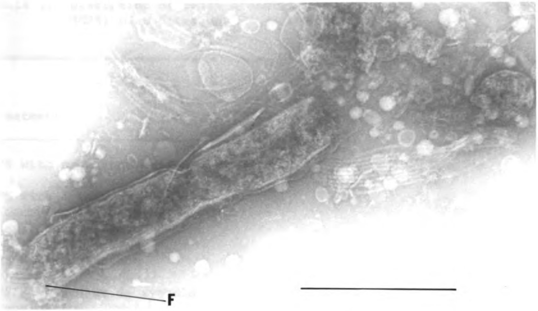

Figure 55. Ammonium molybdate stain of cell sonicated after exposure to guinea pig serum and lysozyme. Some fibrils have been released from cell, but others are still enclosed (F). Bar = 0.5 μm.

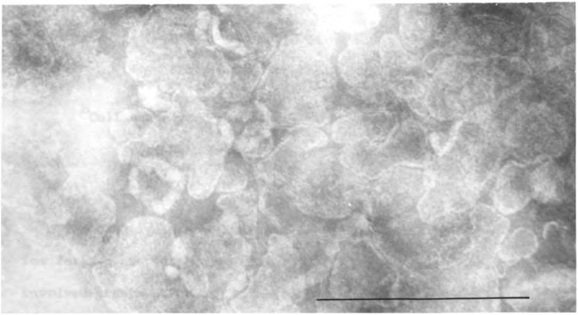

Figure 56. Silicon tungstate-stained material from Renografin gradient band A. Bar = 0.5 μm.

Table 5. Disruption of cells after treatment with guinea pig serum (GPS) plus detergent or sonication or both

Treatment	Condition of majority of cells[a]	Clearing of turbidity of cell suspension[b]
GPS with or without added lysozyme	+	-
GPS with detergent (Brij 58, sodium deoxycholate, sodium dodecyl sulfate, or Triton X-100)	+	-
GPS with sonication	++	-
GPS with sodium deoxycholate and sonication	++	-
GPS with Brij 58 and sonication (CLBS)	+++	+

[a] Cells were observed by electron microscopy and rated according to the following criteria:

-	No disruption
+	Mildly disrupted cells still surrounded with outer envelope
++	Short pieces of mildly disrupted cells
+++	Cells completely lysed; fibrils freed

[b] Cell suspension was visually observed for loss of turbidity.

-	Suspension remained turbid
+	Suspension became clear

The CLBS lysis procedure was determined to be the best treatment for further use in the isolation of the fibrils. Routine preparation involved treatment of 440 ml of culture. Under identical conditions, when three times this volume (1320 ml) was treated, lysis was not effected. Sonication of small portions of this GPS-Brij 58-treated suspension failed to clear the suspension.

Fibril Isolation

Sucrose Gradients

Treponeme preparations treated with GPS and lysozyme were placed onto a gradient of from 5 to 40% (w/v) sucrose and centrifuged for 10 min at 48,000 x g in an attempt to isolate fibrils. Fractions collected by puncturing the bottom of the tube were dialyzed and negatively stained for electron microscopic observation. Although most membrane was found near the top of the gradient, membrane fragments or vesicles as well as fibrils were scattered throughout the upper half of the gradient. The lower half contained axial filament and membrane fragments, with whole treponemes and large protoplasmic cylinder fragments near the bottom. When similar cell preparations, with or without DNase treatment, were centrifuged under the same conditions on a 5 to 25% (w/v) sucrose gradient, whole cells and large fragments pelleted while the distribution of other cell components resembled that described above. Visible bands were sometimes formed in these gradients, dependent upon the degree of cell disruption and the mass of cells put onto the gradient. These bands were not homogeneous accumulations of any particular cell component.

Cells treated with GPS, lysozyme and DNase were further disrupted by detergent treatment (sodium deoxycholate or Triton X-100), sonication or both. Distribution of the cell components on a 5 to 25% sucrose gradient was similar to that found in earlier gradients with one difference: no pellet of whole cells formed when cells were disrupted with GPS, lysozyme and sonication, with or without

detergent. Treatment with GPS, lysozyme and detergent resulted in a small pellet.

When the CLBS lysis procedure was used to disrupt the cells, on a 5 to 25% gradient a pellet of fibrils and membrane was formed with no whole cells. When centrifuged on a 5 to 67% sucrose gradient from 15 min to 2 hr at 106,000 x g, the cell lysate was not distributed into distinct bands. This gradient was collected on a fraction collector while the absorption at 280 nm was simultaneously read. The top 1/8 of the gradient was dominated by contaminating proteins including DNase, lysozyme, and serum components. One distinct protein absorbance peak was detected near the bottom of the gradient in the portion containing large cell fragments and clumps of fibrils.

Renografin Gradients

When cells were disrupted with CLBS and DNase and centrifuged on Renografin density gradients, the cell components were more clearly resolved than on comparable sucrose gradients. A low speed centrifugation step was not used on the lysate prior to gradient centrifugation because separation of fibrils from unlysed cells did not occur. Fibril clumps pelleted with whole cells at low speeds while many individual fibrils remained in suspension.

CLBS-treated cells centrifuged on gradients of 0-76% Renografin at 130,000 x g formed distinct bands. Since the position of the bands changed with further centrifugation after 1 1/2 hr, but not after 2 hr, it was determined that equilibrium was reached at 2 hr. The average position and size of the two main bands (A and C) can be seen in Figure 57. Band C was flocculent, while band A was more homogeneous. Smaller bands, often with diffuse edges, were seen between band A and band C as well as directly below band C. Their presence, size, and location in relation to the major bands varied with minor changes in the procedure (e.g., length of sonication, volume of disrupted cells placed on the gradient).

Band A consisted largely of membrane vesicles (Figure 56; see also Figure 25), much of which had the substructure typical of outer envelope. Occasional fibrils, axial filaments and striated tubules were present. Light bands and diffuse material between band A and band C did not contain major amounts of any particular cell component other than membrane. Band C was composed of fibrils with varying numbers of small membrane vesicles as well as occasional axial filament hooks and basal bodies (Figure 58). Although a few fibrils were seen in other parts of the gradient, most were concentrated in band C. There was considerable variation of fibril length with most fibrils shorter than those found in situ.

One or two narrow, fairly distinct bands were usually seen immediately below band C. These could be distinguished from band C only if the gradient covered a sufficiently narrow density range. The content of these bands was similar to that of band C, with more membrane and a higher percentage of long fibrils (Figure 59). A gradient of 0-57% Renografin allowed adequate separation of bands, while still retaining the whole spectrum of bands.

The location of bands A and C in 34 0-76% Renografin linear gradients from 10 experiments employing almost identical disruption procedures (CLBS and DNase) were recorded. Since the mean density

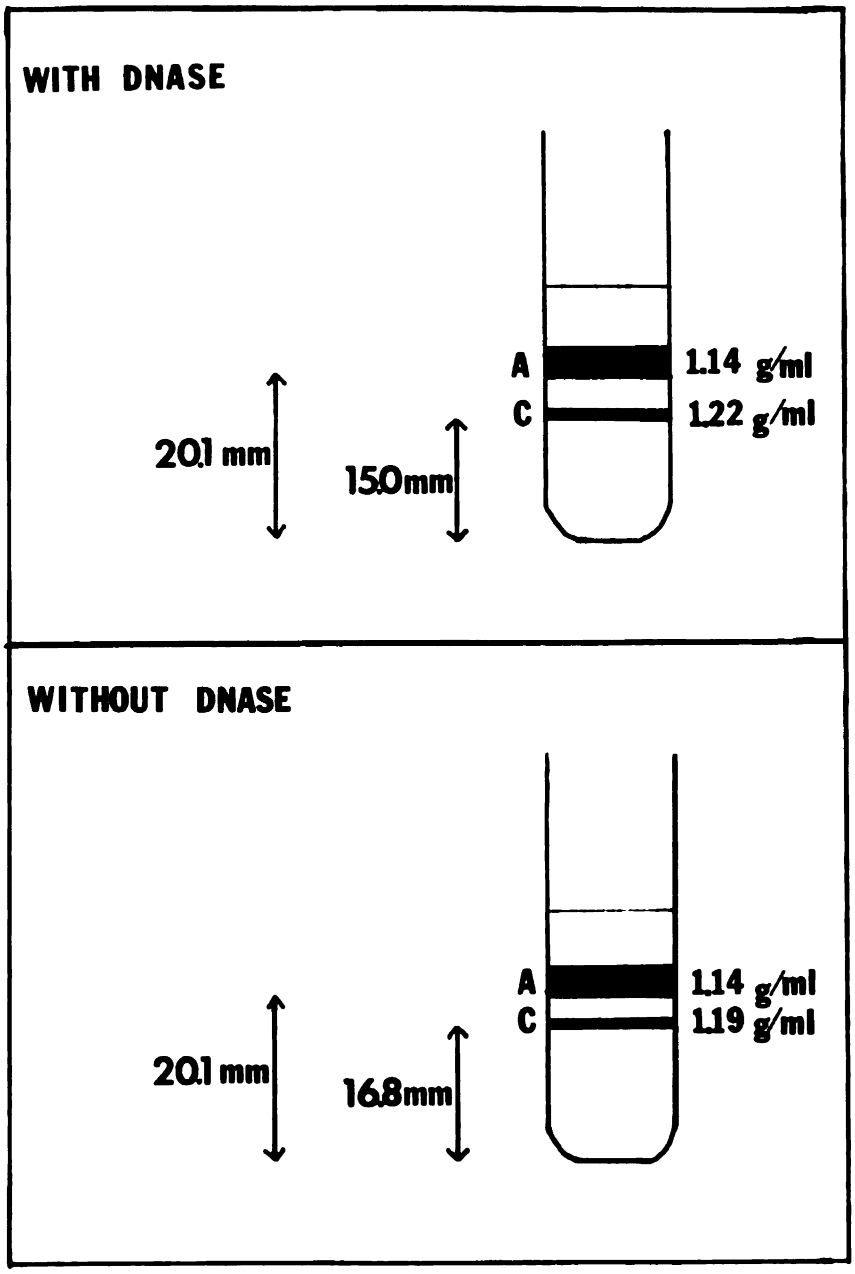
WITH DNASE
A
C
1.14 g/ml
1.22 g/ml
20.1 mm
15.0mm
WITHOUT DNASE
A
C
1.14 g/ml
1.19 g/ml
20.1 mm
16.8mm

Figure 57. Average position of bands A and C when cell lysate, with or without DNase, was centrifuged to equilibrium on 0 to 76% Renografin gradients. Average height of lower edge of each band and average buoyant density is recorded.

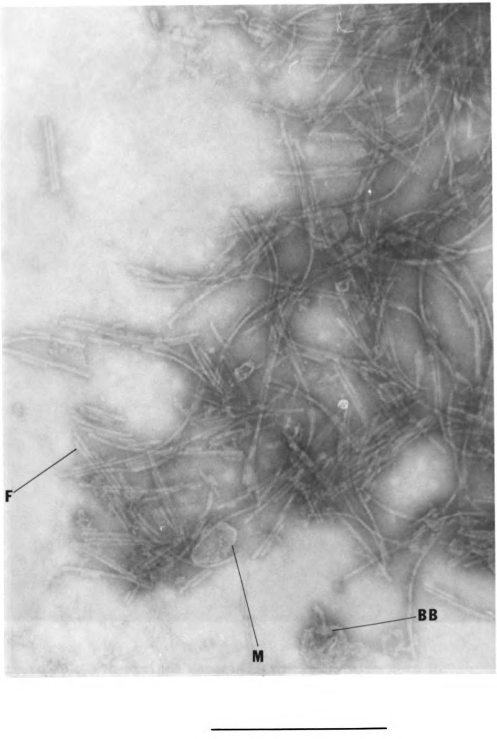

Figure 58. Ammonium molybdate-stained material from Renografin band C. Membrane (M), fibrils (F), and an axial filament hook with basal body (BB) are visible. Bar = 0.5 µm.

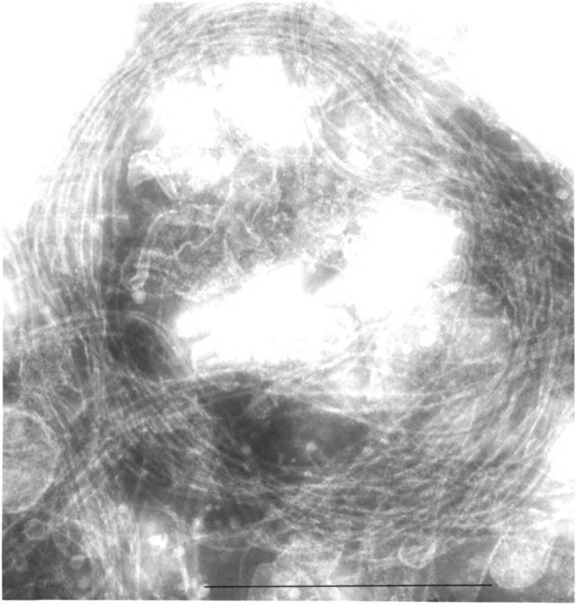

Figure 59. PTA-stained material from Renografin band D. Membrane and long fibrils are present. Bar = 0.5 µm.

of 76% Renografin had been measured (1.435 ± .009 g/ml), the buoyant density of a particular band could be calculated from its position in the linear gradient. By this method the average buoyant density of the lower edge of band A was found to be 1.14 ± 0.02, while that of band C was 1.22 ± 0.01 g/ml (Figure 57).

The use of DNase in the disruption procedure directly affected the position of band C, but not that of band A. The buoyant density of band C on gradients when DNase had not been used was 1.193 ± 0.003 g/ml, as compared to 1.22 ± 0.01, the average buoyant density of band C with DNase (Figure 57).

Even after dialysis, band C was very flocculent, especially when DNase had not been used in the disruption procedure. The fibrils and membrane settled to the bottom of a test tube from suspension in only a few minutes. The resuspended fibrils, when viewed with the electron microscope, were in large clumps (Figure 60). In order to determine a method of disrupting the clumps, the fibrils were treated by various chemical and physical procedures before electron microscopy. Aggregation was still apparent after the treatments listed in Table 6.

For further purification of the fibrils, band C was dialyzed to remove the Renografin and treated with DNase. Triton X-100 was also added because it solubilizes both the outer and cytoplasmic membranes of *Escherichia coli* (31). After the suspension was centrifuged a second time on a Renografin gradient (Figure 61), the band C which formed contained fibrils with less membrane contamination than band C on the previous gradient. When band C was treated again with DNase and Triton X-100, and centrifuged on a Renografin gradient

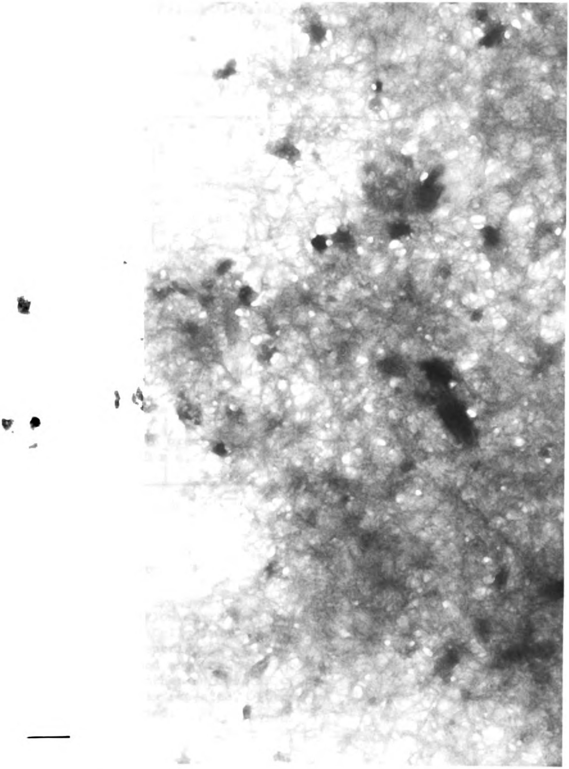

Figure 60. PTA stain of large clump of fibrils from Renografin band C. Bar = 0.5 μm.

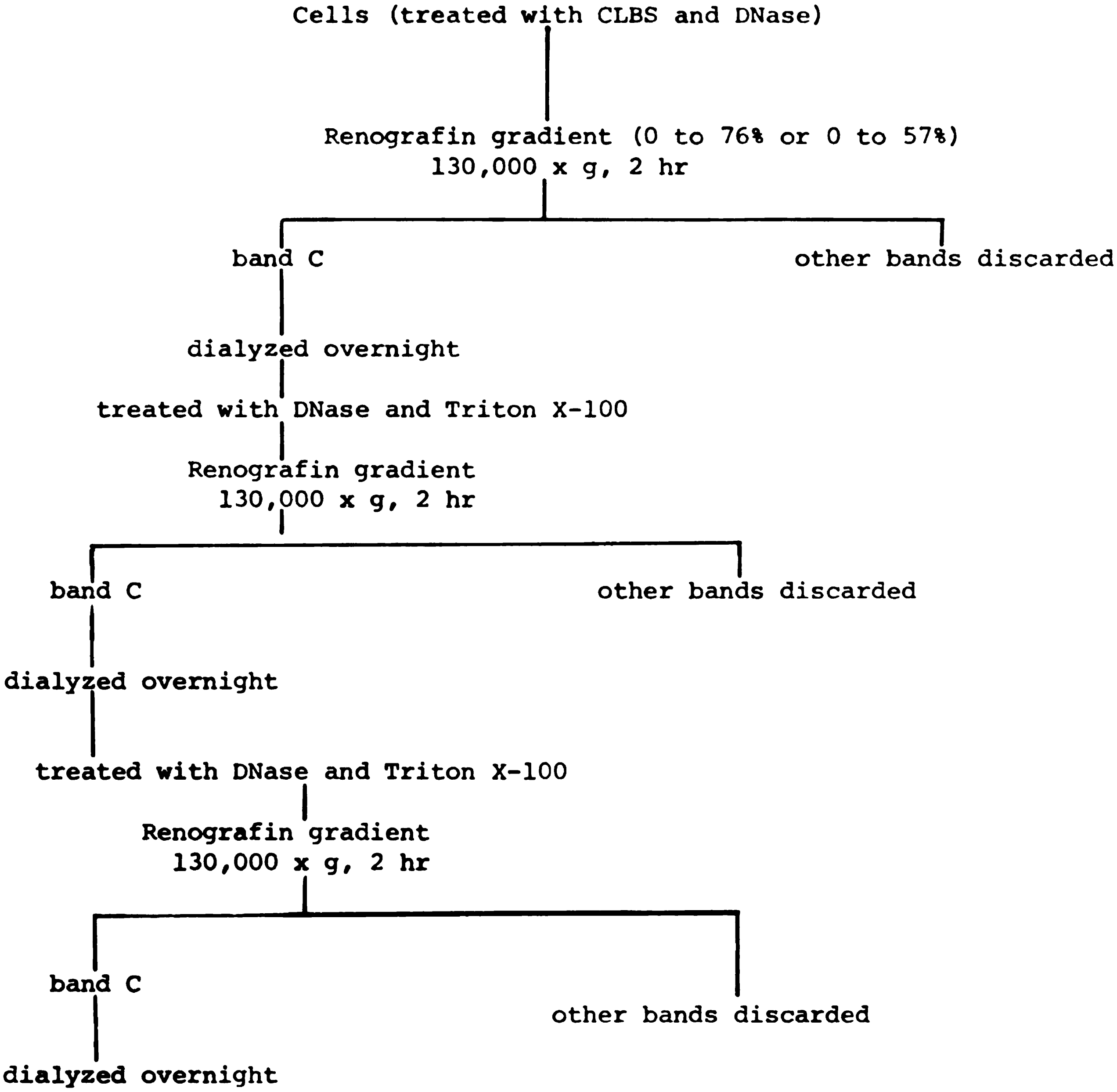
Cells (treated with CLBS and DNase)
Renografin gradient (0 to 76% or 0 to 57%)
130,000 x g, 2 hr
band C
other bands discarded
dialyzed overnight
treated with DNase and Triton X-100
Renografin gradient
130,000 x g, 2 hr
band C
other bands discarded
dialyzed overnight
treated with DNase and Triton X-100
Renografin gradient
130,000 x g, 2 hr
band C
other bands discarded
dialyzed overnight

Figure 61. Flow chart of procedure for isolation of fibrils from treponemes. Cells lysed with guinea pig serum, Brij 58 and sonication were centrifuged on a Renografin gradient. Band C was collected, dialyzed and treated with DNase and Triton X-100 and centrifuged on another Renografin gradient. Band C was collected and the process was repeated. After the third centrifugation band C was again dialyzed.

Table 6. Treatments which did not disaggregate clumps of fibrils, as determined by electron microscopy

Sonication
2% Triton X-100
0.01 N HCl (pH 2)
0.025 M ammonium acetate buffer at pH 5.0
0.5 to 1 M ammonium acetate at pH 7.5
0.5 to 1 M ammonium acetate at pH 8.6
0.5 to 1 M ammonium acetate at pH 9.5
0.1 to 2 M NaCl
0.1 to 2 M NaCl and sonication
1 M $CaCl_2$
50% chloroform-methanol
33% ethanol
33% ethanol and sonication
2 M urea

a third time, the resulting band C was a fairly purified preparation of fibrils with few or no visible contaminants (Figure 62). This type of preparation was used for chemical studies on fibrils.

Chemical Characterization of Fibrils

Several fibril preparations which had been purified three times on Renografin gradients were put onto SDS polyacrylamide electrophoresis gels. One major band of molecular weight 97,000 (96,960 ± 1180) and several minor bands were resolved after staining the gels with Coomassie blue (Figure 63a). On less purified preparations, the 97,000 molecular weight peak was proportionately smaller in comparison to the other peaks (Figure 63b). Renografin-prepared band A, containing mostly membrane with occasional fibrils, had only a small peak at the molecular weight of about 97,000 (Figure 63c).

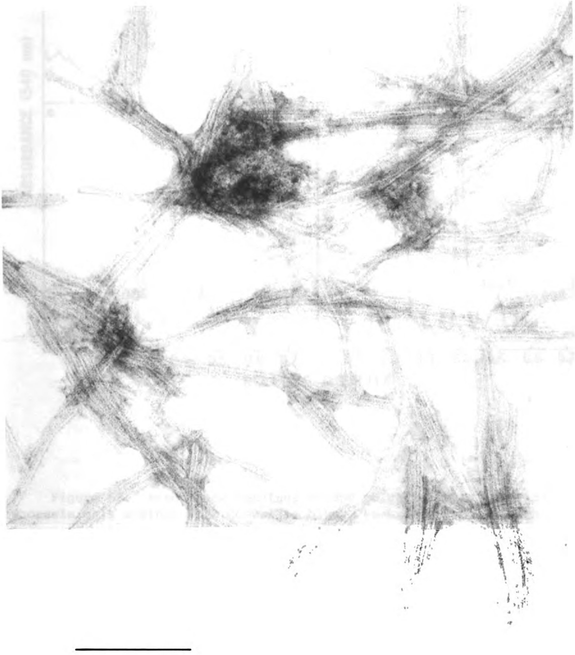

Figure 62. Uranyl oxalate-stained band C from third Renografin gradient. Bar = 0.5 μm.

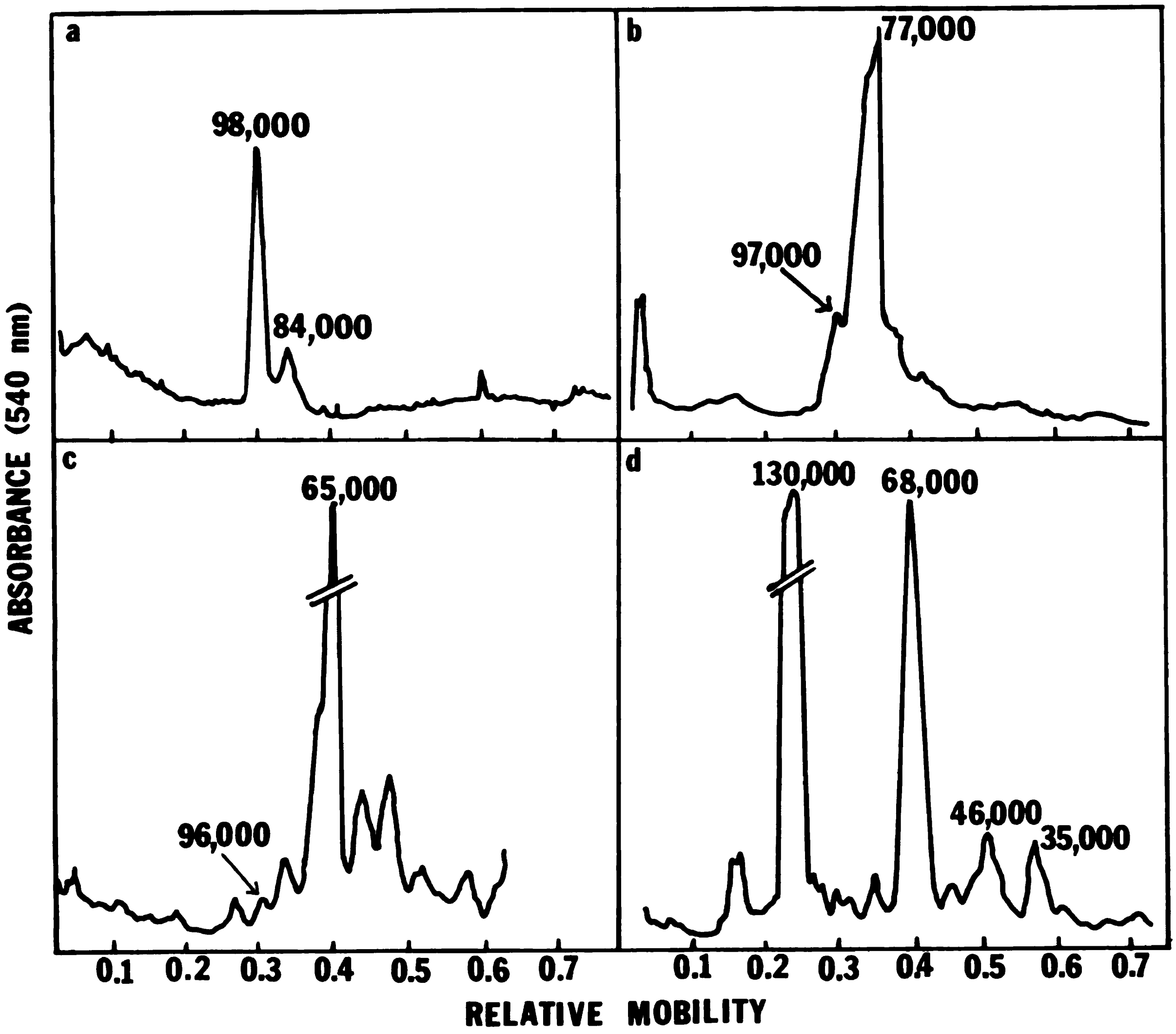

Figure 63. Absorbance readings of SDS polyacrylamide electrophoresis gels stained with Coomassie blue. Peaks are labeled with molecular weights obtained by comparison with standards.

a. Fibril preparation purified on three Reongrafin gradients.
b. Fibril preparation purified on two Renografin gradients.
c. Band A from a Renografin gradient.
d. Molecular weight standards:

β-galactosidase (130,000)
bovine serum albumin (68,000)
ovalbumin (46,000)
pepsin (35,000)

The yield was estimated by Lowry's protein analysis of dialyzed fibril preparations. Approximately 125 to 320 μg protein were found in band C after one Renografin centrifugation of 120 ml of CLBS-treated culture. After two more Renografin centrifugations there were only about 30 μg protein. Using Jackson's calculation of the dry weight of these treponemes (50), it was calculated that the protein in the purest fibril preparation represented about 0.2% of the total dry weight of the cells.

Fibrils purified by three centrifugations on Renografin gradients were subjected to further chemical analyses. The preparation was first dialyzed overnight with several changes of water. Analysis by Lowry's method indicated about 50 μg/ml protein in this particular preparation. Hexose was not detected by the anthrone method, but it must be noted that the smallest amount detectable in this test is 25 μg/ml. The diphenylamine test revealed approximately 10 μg DNA/ml, while the orcinol test indicated pentose at a concentration of 34 μg/ml. The determination of the ratio of absorbance at 280 nm to the absorbance at 260 nm gave inconclusive results because Renografin absorbs light very strongly at both wavelengths and is difficult to dialyze away completely.

DNA-Fibril Connection

Further evidence for the apparent relationship between DNA and fibrils noted in thin sectioned cells was pursued by the aqueous spreading technique for electron microscopy of disrupted cells and by gradient centrifugation of cells labeled with ^{3}H-thymidine before disruption.

Aqueous Spreading Technique for Electron Microscopy

The Kleinschmidt spreading technique for electron microscopy was used on various cell preparations to visualize a direct connection between fibrils and DNA. DNA strands on the electron micrographs were identified by comparison with control preparations of T_4 DNA (Figure 64) and by the absence of these strands in cell preparations treated with DNase.

Strands of material (probably DNA) were seen emerging from the ends of cells disrupted with GPS or the CLBS procedure (Figure 65). In such cases the cytoplasmic fibrils were still inside the cell, making it impossible to note any connection between fibrils and DNA. The DNA was spread out from bands of fibrils (or from the cellular material surrounding fibrils) of more disrupted cells (Figure 66). The DNA strands often extended directly from the broken end of a fibril band (Figure 67).

^{3}H-Thymidine Labeling

An alternative method of determining the attachment of DNA to fibrils is to demonstrate that DNA segregates in gradients with fibrils rather than with membrane. Detection of DNA would then be possible by growing cells in a medium containing a radioactive DNA precursor. Incorporation of ^{3}H-thymidine by *T. refringens* was demonstrated by adding 1, 5, 10 or 50 μCi of ^{3}H-thymidine to 12 ml of a 2-day-old culture. The cells contained the maximum radioactivity after 3 more days of growth in 50 μCi ^{3}H-thymidine and thereafter lost radioactivity until the 6-day level was equal to that at 6 hr.

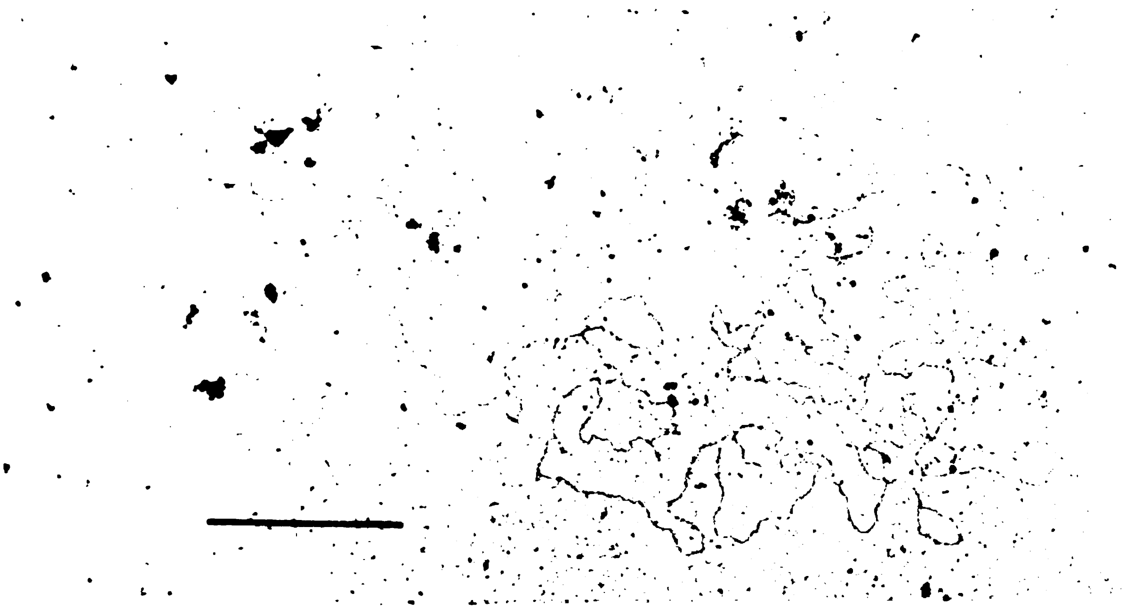

Figure 64. DNA from T_4 bacteriophage. Isolated DNA was prepared for electron microscopy by the Kleinschmidt spreading technique and stained with uranyl acetate. Bar = 1 µm.

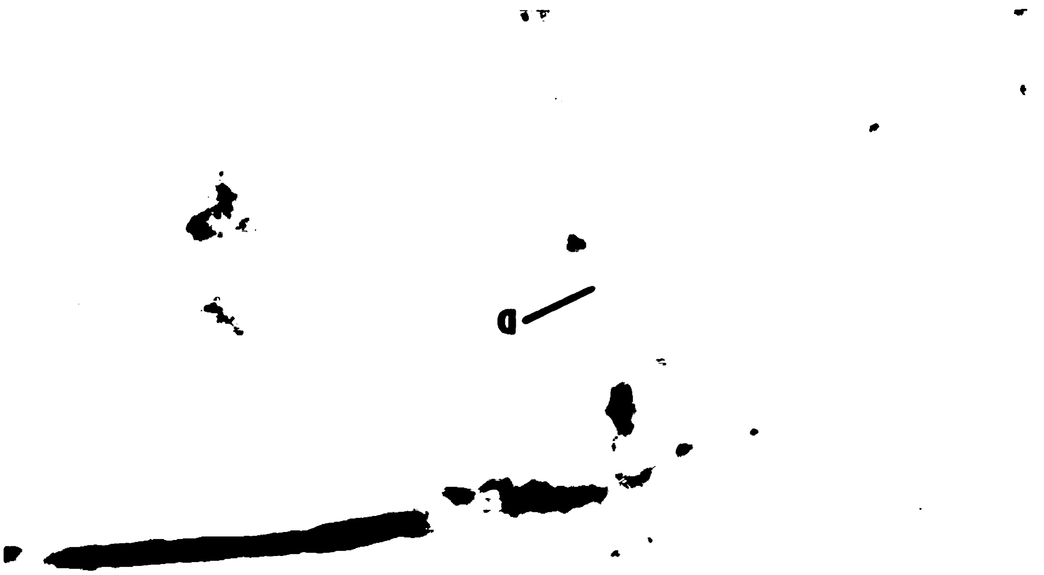

Figure 65. Cell disrupted with guinea pig serum, prepared for electron microscopy by the Kleinschmidt spreading technique and stained with PTA and uranyl acetate. Strands of DNA (D) emerge from the cell. Bar = 1 µm.

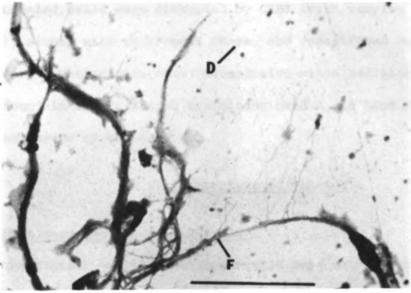

Figure 66. Cells disrupted with CLBS, prepared for electron microscopy by the Kleinschmidt spreading technique, stained with uranyl acetate and rotary shadowed with platinum. DNA (D) emerges from near fibrils (F). Bar = 1 μm.

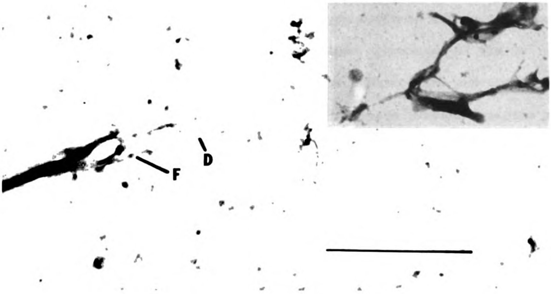

Figure 67. Cell disrupted with CLBS, prepared for electron microscopy by the Kleinschmidt technique and stained with uranyl acetate. DNA (D) emerges from near fibrils (F). Bar = 1 μm.

Labeled cells were disrupted by CLBS (with varying sonication times), either with or without DNase, and centrifuged on Renografin gradients. The results were inconclusive since radioactivity peaks were found in the fractions containing band A and band C as well as in other areas of the gradient.

Ultrastructure of Fibrils

Thin Sectioned and Shadowed Fibrils

The fibrils in thin sectioned cells were studied to gain additional information about their shape, substructure and location in the cell. It was apparent in any slightly oblique or cross sectioned cell that the fibrils were directly adjacent to the inner boundary of the cytoplasmic membrane, but for information on the shape and substructure of the fibrils it was necessary that the section be cut perpendicular to the fibrils. These sections were not common and could be identified by the trilaminar appearance of the CM adjoining the fibrils (Figure 68). The substructure and shape of cross sectioned fibrils varied, but there were certain features which all or most sections had in common. The width of the fibril section changed from its base (next to the CM) to its tip (the part extending furthest into the nuclear area of the cell), forming a shape resembling a pentagon (Figures 68 and 69a). Almost all fibrils had a cap, or narrower area, at their tip. The widest part of the fibrils was usually just below the cap and the base was sometimes, but not always, narrower than this. The base of the fibril averaged 10.8 nm and the base-to-base interval between fibrils about 3.5 nm. The height of the fibril section from the CM to the tip averaged

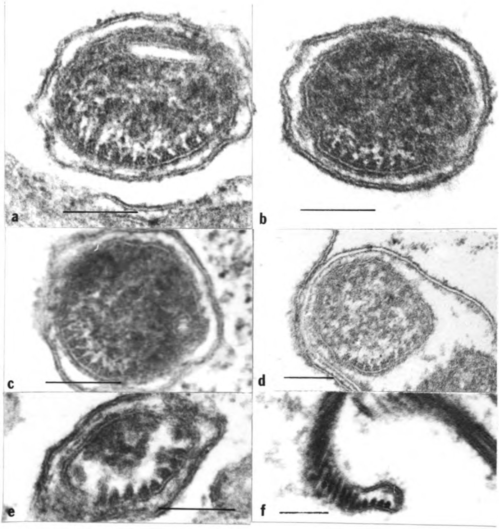

Figure 68. Direct cross sections of fibrils in normal cells (a,b,c), a convoluted cell (d) and disrupted cells (e,f). The substructure of the fibrils is visible, as is the nuclear area into which they project. The trilaminar appearance of the adjoining cytoplasmic membrane indicated that the fibrils were cut approximately perpendicular to their length. Bar = 0.1 μm.

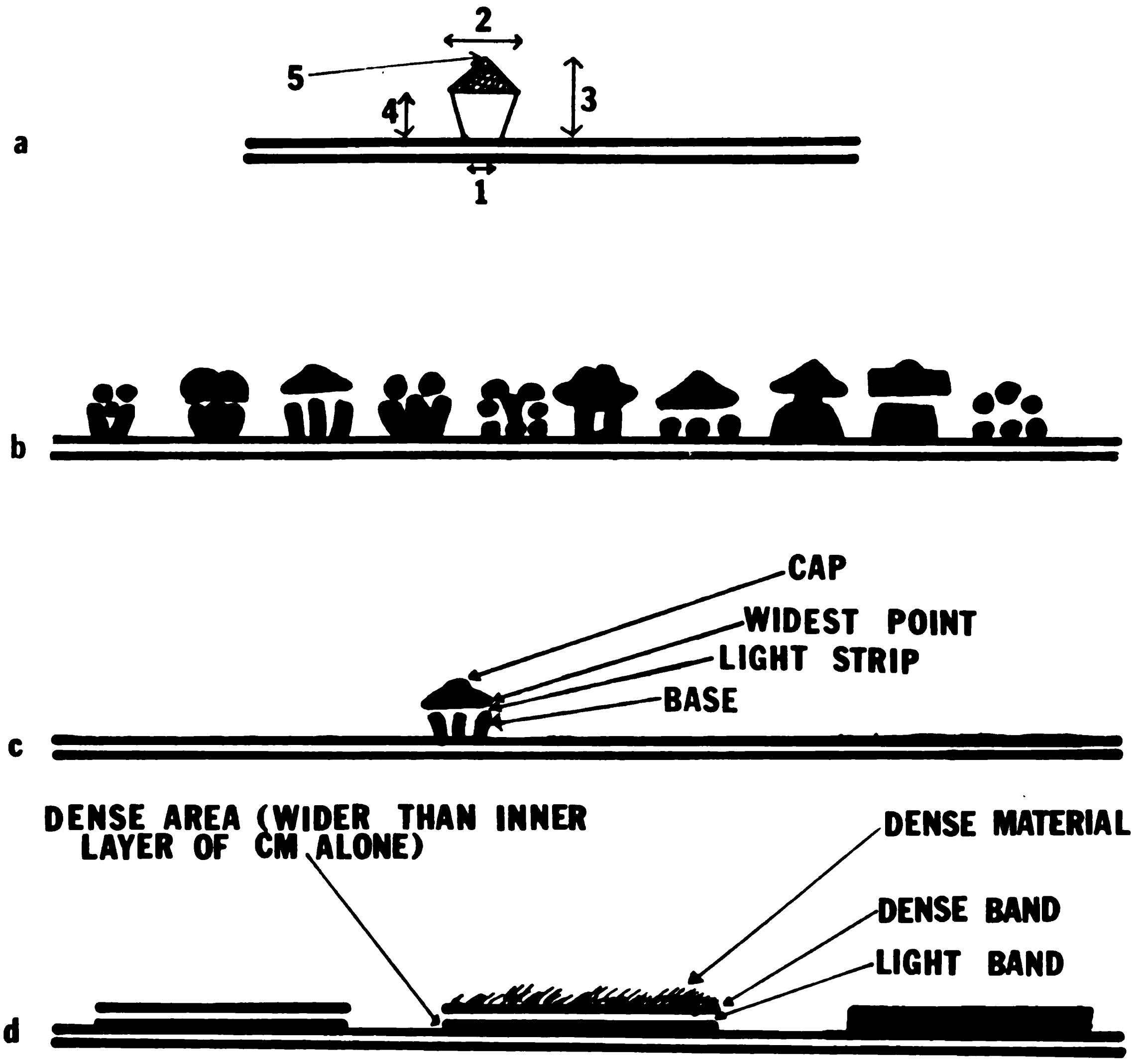
a
1
2
3
4
5
b
c
CAP
WIDEST POINT
LIGHT STRIP
BASE
d
DENSE AREA (WIDER THAN INNER LAYER OF CM ALONE)
DENSE MATERIAL
DENSE BAND
LIGHT BAND

Figure 69. Drawings of sectioned fibrils drawn approximately to scale and positioned on the cytoplasmic membrane.

a. Generalized shape of sectioned fibril. The terms used in the text and Table 7 to describe the parts of the sections are defined:

1. width of base
2. width of widest point
3. height
4. height, excluding cap
5. tip

hatched area; cap

b. Substructure of various cross sectioned fibrils.

c. Cross sectioned fibril which includes the elements common to most sectioned fibrils in which substructure is visible.

d. Substructure of various longitudinally sectioned fibrils.

14.5 nm but was difficult to determine accurately since DNA or other cellular material often obscured the tip and there was no clear distinction between the base of the fibril and the inner dark layer of the CM. Measurements of various dimensions of sectioned fibrils as well as fibrils prepared by other electron microscopic techniques are summarized in Tables 7 and 8.

Table 7. Means of various fibril dimensions measured from fibrils in thin sectioned cells (see Figure 69 for clarification of terms)

Dimension measured	Mean measurement (nm)	Number of fibrils measured
Cross sections of fibrils		
Width at base of fibril	10.8 ± 0.6	37
Width of fibril at widest point (if wider than base)	14.0 ± 1.5	16
Height of fibril from cytoplasmic membrane (CM)	14.5 ± 0.9	48
Height of fibril from CM, excluding cap	9.6 ± 0.4	15
Fibril-to-fibril interval between bases	3.5 ± 0.5	29
Longitudinal sections of fibrils		
Height of fibril including dark band	7.3 ± 0.2	28
Height of fibril including dark band and dense material outside band	16.2 ± 1.7	21
Cross sections of loose fibrils inside disrupted cells		
Widest dimension	12.6 ± 5.8	6
Dimension perpendicular to widest dimension	12.4 ± 4.0	6

Table 8. Mean measurements of various dimensions of negatively stained fibrils. Fibrils were stained with phosphotungstate (PTA) or uranyl oxalate (UOx) (see Figure 76 for clarification of terms)

Dimension measured	PTA-stained fibrils Mean measurement (nm)	PTA-stained fibrils Number of fibrils measured	UOx-stained fibrils Mean measurement (nm)	UOx-stained fibrils Number of fibrils measured
Negative stains of isolated fibrils				
Width of wide fibril	12.7 ± 0.2	138	11.9 ± 0.3	239
Width of narrow fibril	8.4 ± 0.3	121	7.7 ± 0.3	97
Width of strand of wide fibril	3.4 ± 0.3	41	2.2 ± 0.2	39
Width of strand of narrow fibril	3.1 ± 0.7	37	3.8 ± 0.8	30
Width of ribbon alongside wide fibril	5.4 ± 0.4	30	4.3 ± 0.5	31
Width of fibril in band of fibrils	8.4 ± 0.4	35		
Interval between fibrils in band	4.3 ± 0.6	30		
Periodicity of striations on wide fibrils			3.0 ± 0.3	12
Fibrils within negatively stained cells				
Width of fibrils	7.6 ± 0.6	34		
Interval between fibrils	3.5 ± 0.9	10		

The electron density varied with some of the sectioned fibrils. The pattern of this substructure varied but some fairly common elements included: a base made up of three (or two) dark areas and an electron light strip just below the widest point (Figure 69b, 69c). Fibrils were sometimes free from the CM in disrupted cells (Figure 70). Dense areas were visible, but the fibrils' dimensions varied (Table 7) and they offered no clarification of fibrillar structure.

Longitudinal sections of fibrils were rare and even more difficult to measure accurately than cross sections. Adjacent to the inner dark layer of the CM, which was perhaps thicker than usual and included part of the CM, was sometimes seen a light band and then a dense band, resembling another trilaminar membrane (Figures 69d and 37). Often outside the dense band more dark material was found (Figures 37 and 35). Cross striations were seen only occasionally in longitudinally sectioned fibrils (Figure 71), but their periodicity (about 3 nm) was similar to the periodicity of negatively stained fibrils reported later.

Isolated fibrils were shadowed with platinum-carbon. The resolution attained did not allow a distinction to be made between different fibril orientations and did not reveal any substructure (Figure 72). The average height of the shadowed fibrils from the grid was 6.6 ± 0.4 nm.

Negatively Stained Fibrils

Negative stains of fibrils revealed the complexity of their substructure. The initial impression of PTA, silicon tungstate, or ammonium molybdate-stained fibrils was that they were tubular with stain penetrating into the lumen or lying in the center groove created by a collapsed tube (Figure 73; see also Figure 58). More careful inspection of negative stains revealed that some of the two-stranded fibrils were wider than the others (Figures 73 and 74).

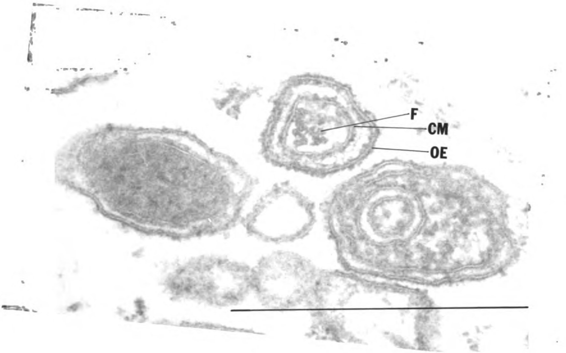

Figure 70. Sectioned disrupted cell containing fibrils (F) which have been freed from the cytoplasmic membrane (CM). The outer envelope (OE) still surrounds the cell. Bar = 0.5 µm.

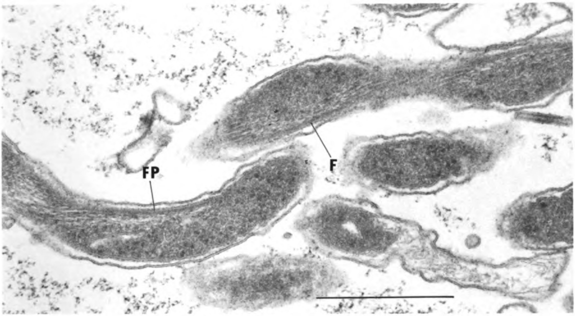

Figure 71. Longitudinally sectioned fibrils (F). A 3 nm periodicity is evident in one of the fibrils (FP). Bar = 0.5 µm.

Figure 72. Isolated fibrils which were shadowed with platinum-carbon in the direction of the arrow. Bar = 0.5 μm.

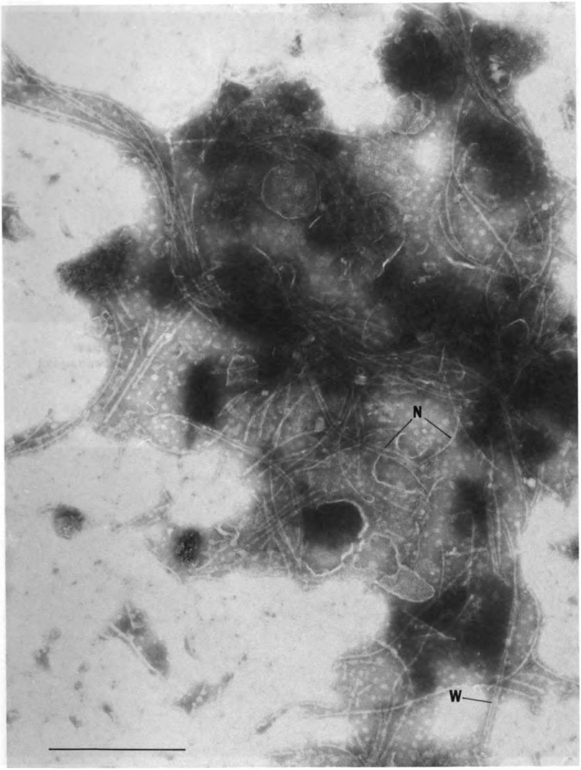

Figure 73. PTA-stained narrow (N) and wide (W) two-stranded fibrils. Bar = 0.5 µm.

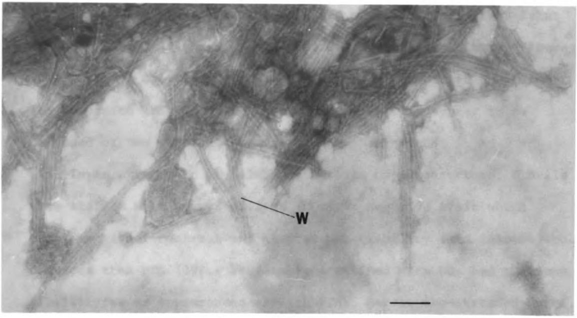

Figure 74. PTA-stained wide two-stranded fibrils (W) from preparation which had been kept frozen. Bar = 0.1 µm.

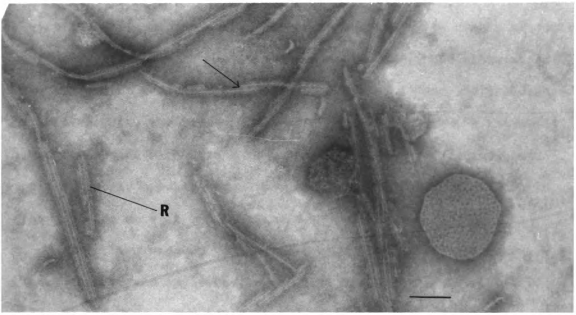

Figure 75. Silicon tungstate-stained wide fibrils with ribbon (R) of stained material lying on each side. One strand of some of the fibrils is broken (arrows). Bar = 0.1 µm.

Sometimes these wide fibrils were edged on both sides with a faint ribbon of material whose width varied from fibril to fibril (Figures 75 and 76a). One strand of the fibril was often broken away from its companion (Figure 75). This made the fibrils appear to be composed of two parallel strands rather than a tube.

In an attempt to reveal finer details of substructure, fibrils were stained with uranyl oxalate (UOx), a negative stain which provides higher contrast and greater penetrability into intramoleculr crevices than PTA (39). Preparations stained with UOx had the same fibril types or appearances as with PTA: narrow two-stranded forms, and wide two-stranded forms, with and without ribbons (Figures 77 and 78). In addition, very definite cross striations could be seen on the wide fibrils (Figures 77 and 76b). Small extensions with a periodicity of about 3 nm projected inward from each strand of the wide fibrils, meeting at the center of the fibril to create a ladder effect. When part of one strand was broken away, the other strand retained its periodic extensions (Figures 78, 79 and 76c), and when fibrils split, the break appeared in the center, leaving the small projections of each strand (Figures 78 and 76c). The cross striations usually appeared to be perpendicular to the strands, but in some places were at a slight angle.

Sometimes when one strand of a wide fibril was broken away, the other strand apparently twisted to reveal a narrow fibril (Figures 77, 80 and 76d). The inner strand of this narrow fibril was continuous with a strand from the wide fibril. The outer strand of the narrow fibril appeared to come from underneath the wide fibril strand

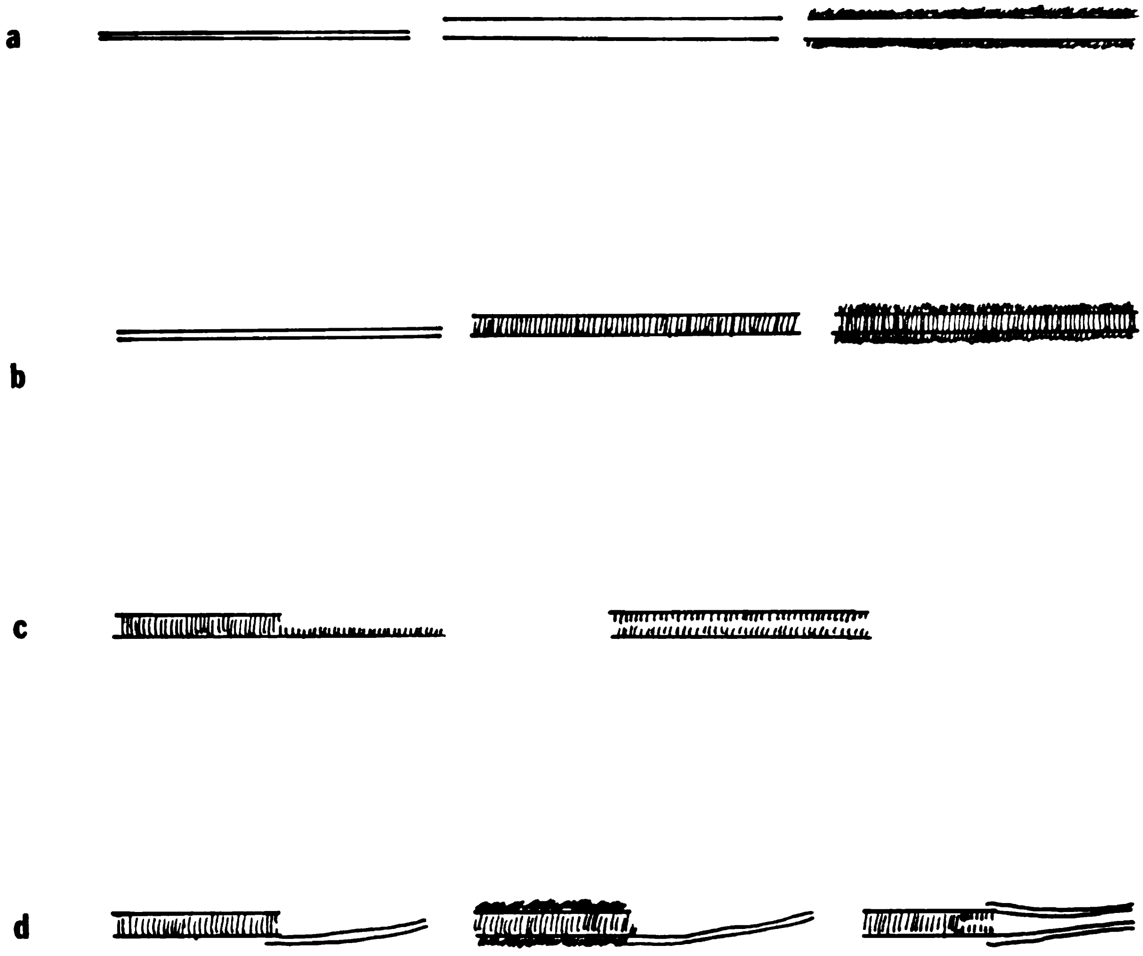

Figure 76. Drawings of fibril types and substructure seen in preparations of isolated fibrils stained with PTA or UOx. Fibrils are drawn approximately to scale. See Table 8 for measurements.

a. PTA-stained narrow fibril, wide fibril without ribbon and wide fibril with ribbon.

b. UOx-stained narrow fibril, wide fibril without ribbon and wide fibril with ribbon. Wide fibrils have cross striations.

c. UOx-stained wide fibril with one broken strand and wide fibril with strands split apart. Each strand retains its extensions.

d. UOx-stained wide fibrils (without and with ribbons) when one or both strands have twisted into what appears to be narrow fibrils.

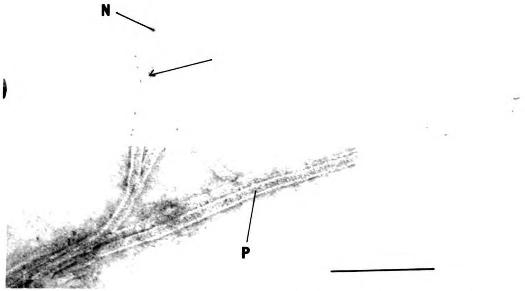

Figure 77. UOx-stained wide fibrils with periodic cross striations (P). A strand of one wide fibril appears to twist into narrow fibril (N) at point where other strand is broken away (arrow). Bar = 0.1 µm.

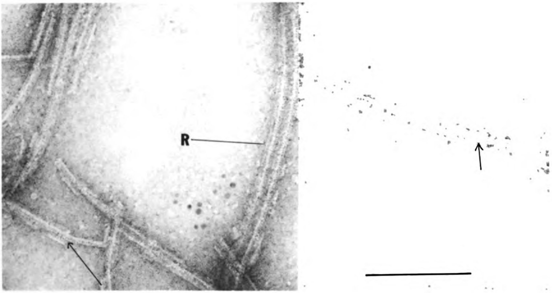

Figure 78. UOx-stained wide fibrils with ribbons (R) alongside. Each strand of wide fibrils retains its periodic projections when fibril splits (long arrow) or when one strand is broken away (short arrows). Bar = 0.1 µm.

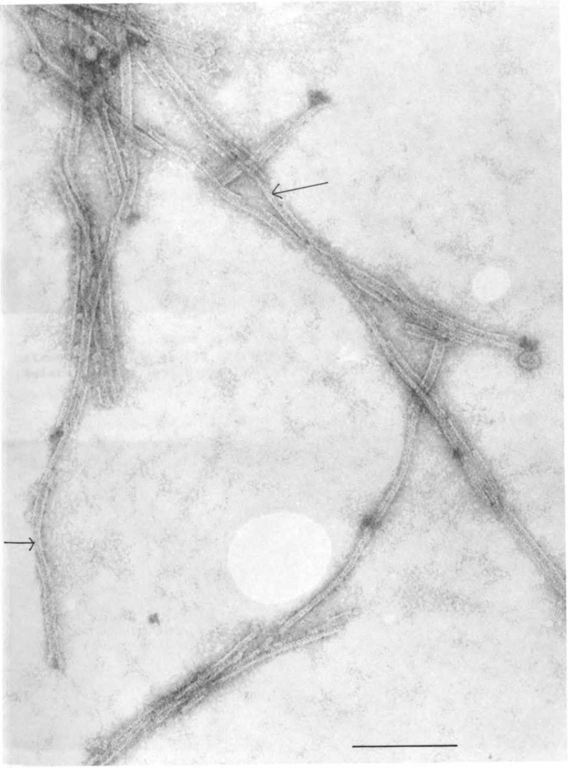

Figure 79. UOx-stained wide fibrils. Each strand of a fibril retains its periodic projections when the other strand is broken away (arrows). Bar = 0.1 μm.

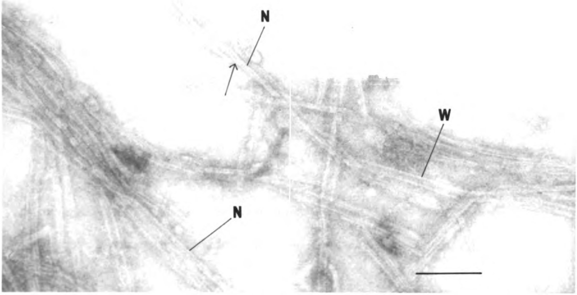

Figure 80. UOx-stained wide (W) and narrow (N) fibrils. One strand of a wide fibril splits away from the other strand and twists (arrow) into a narrow fibril. Bar = 0.1 µm.

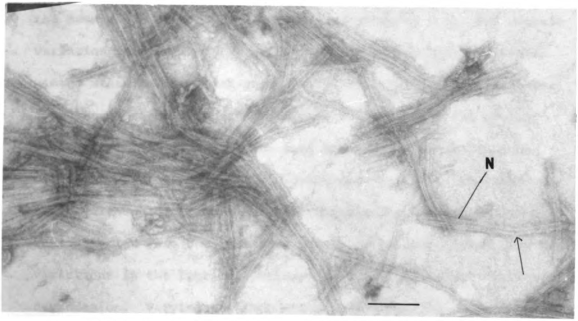

Figure 81. UOx-stained wide and narrow fibrils. Both strands of one fibril twist (arrow), resulting in two narrow fibrils (N). Bar = 0.1 µm.

or to extend from the dark ribbon alongside the wide fibril (Figure 76d). In Figure 81, both strands of a wide fibril twisted, after splitting apart, resulting in two narrow fibrils.

The widths of many fibrils, both the side and the narrow types, were measured after being stained with PTA or UOx. The mean widths of UOx-stained narrow and wide fibrils were significantly less than the respective mean widths of fibrils stained with PTA (or ammonium molybdate or silicon tungstate). The averages of the widths of several hundred wide and narrow fibrils are reported in Table 8.

The widths of both wide and narrow fibrils also varied widely within each stain group (Figures 82 and 83), but there was a normal distribution of widths in micrographs taken from each grid, and within each grid the ratio of the mean width of narrow fibrils to the mean width of wide fibrils remained close to 0.6. The overall variation in fibril widths was due to the normal distribution in widths measured from each grid as well as significant differences among means calculated from each grid (Figure 84). The average width of fibrils from even the same preparation would often be different when calculated from micrographs taken at different times. It could not be determined whether the differences among various grids were due to variations in stain penetration or actual variations in the fibrils, perhaps because of different degrees of degradation. Varying stain penetration was the less likely reason because when the same fibril preparation was stained on separate grids on the same day the fibril widths calculated from each grid were the same. No consistent correlation was found between any of

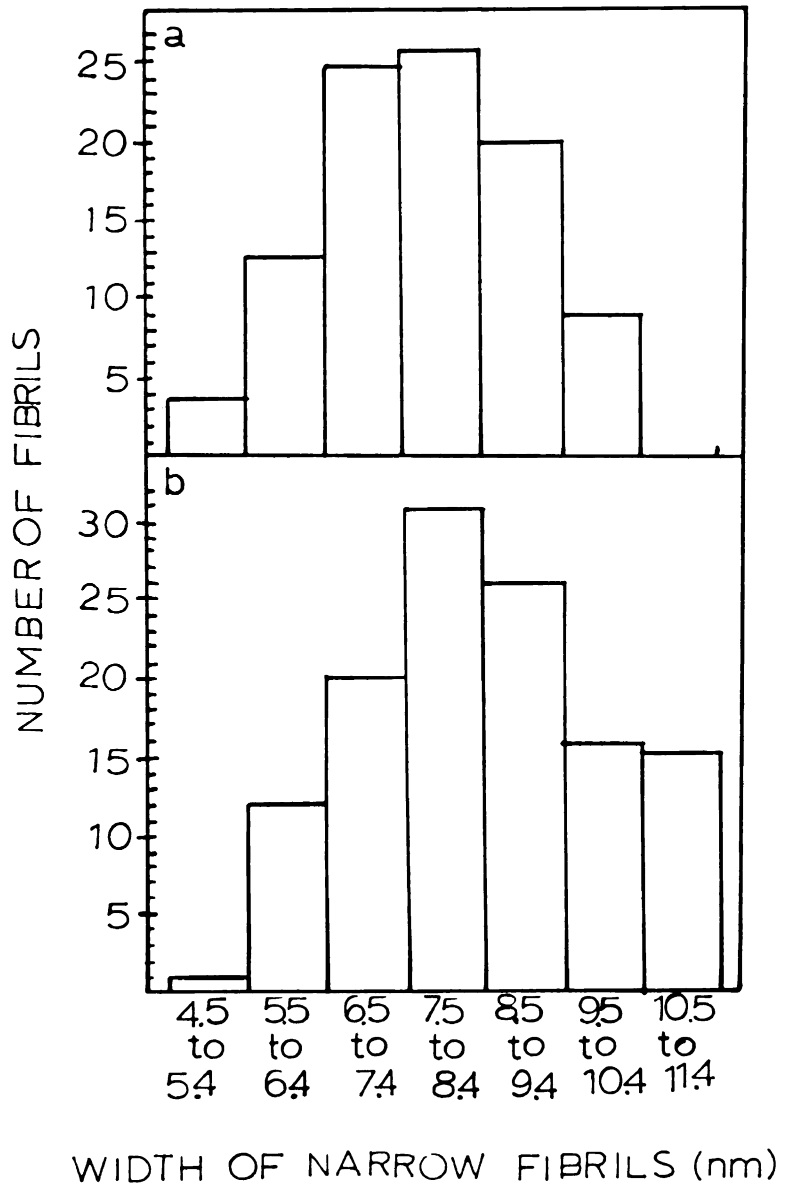

Figure 82. Distribution of widths of narrow fibrils.

a. Distribution of widths of 97 UOx-stained narrow fibrils from 42 micrographs.

b. Distribution of widths of 121 PTA-stained narrow fibrils from 36 micrographs.

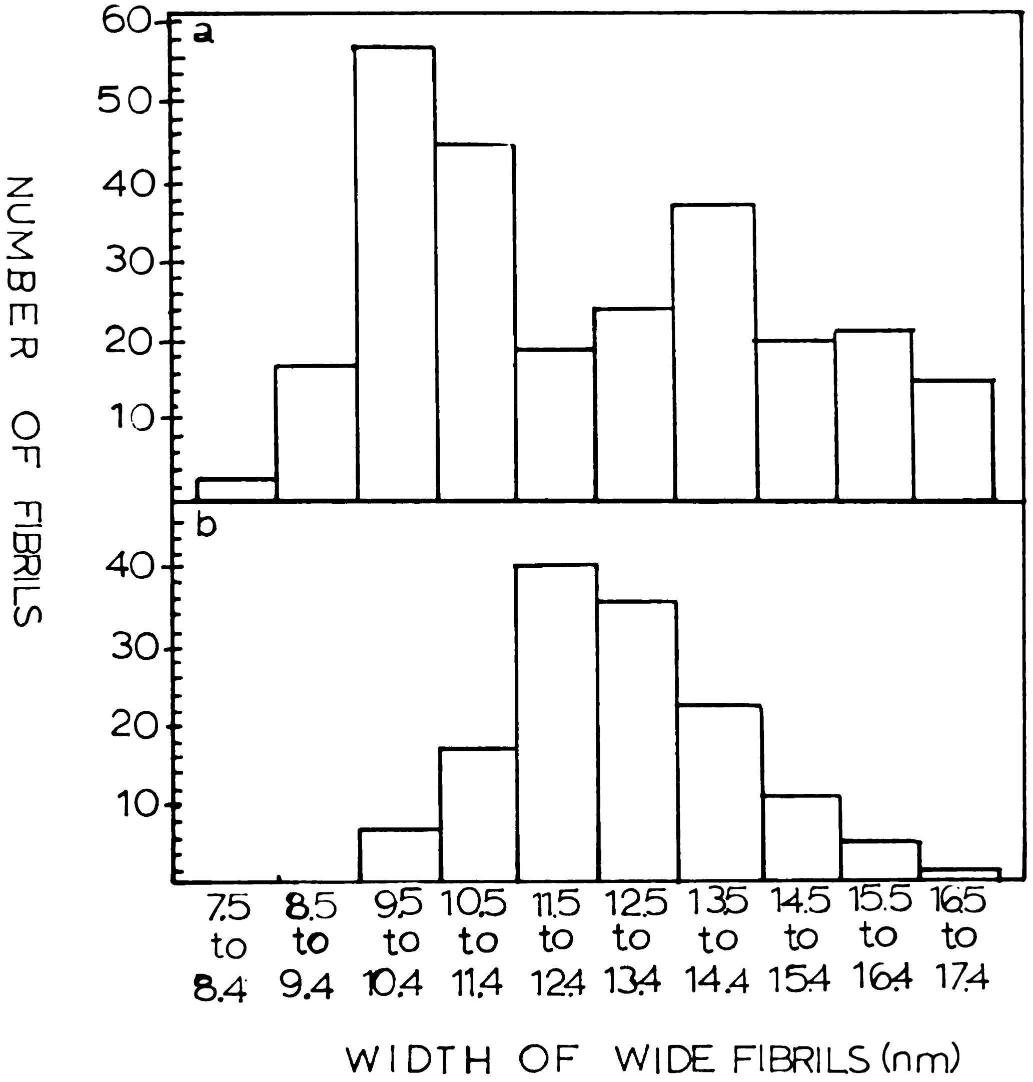

Figure 83. Distribution of widths of wide fibrils.

a. Distribution of widths of 239 UOx-stained wide fibrils from 67 micrographs.

b. Distribution of widths of 138 PTA-stained wide fibrils from 34 micrographs.

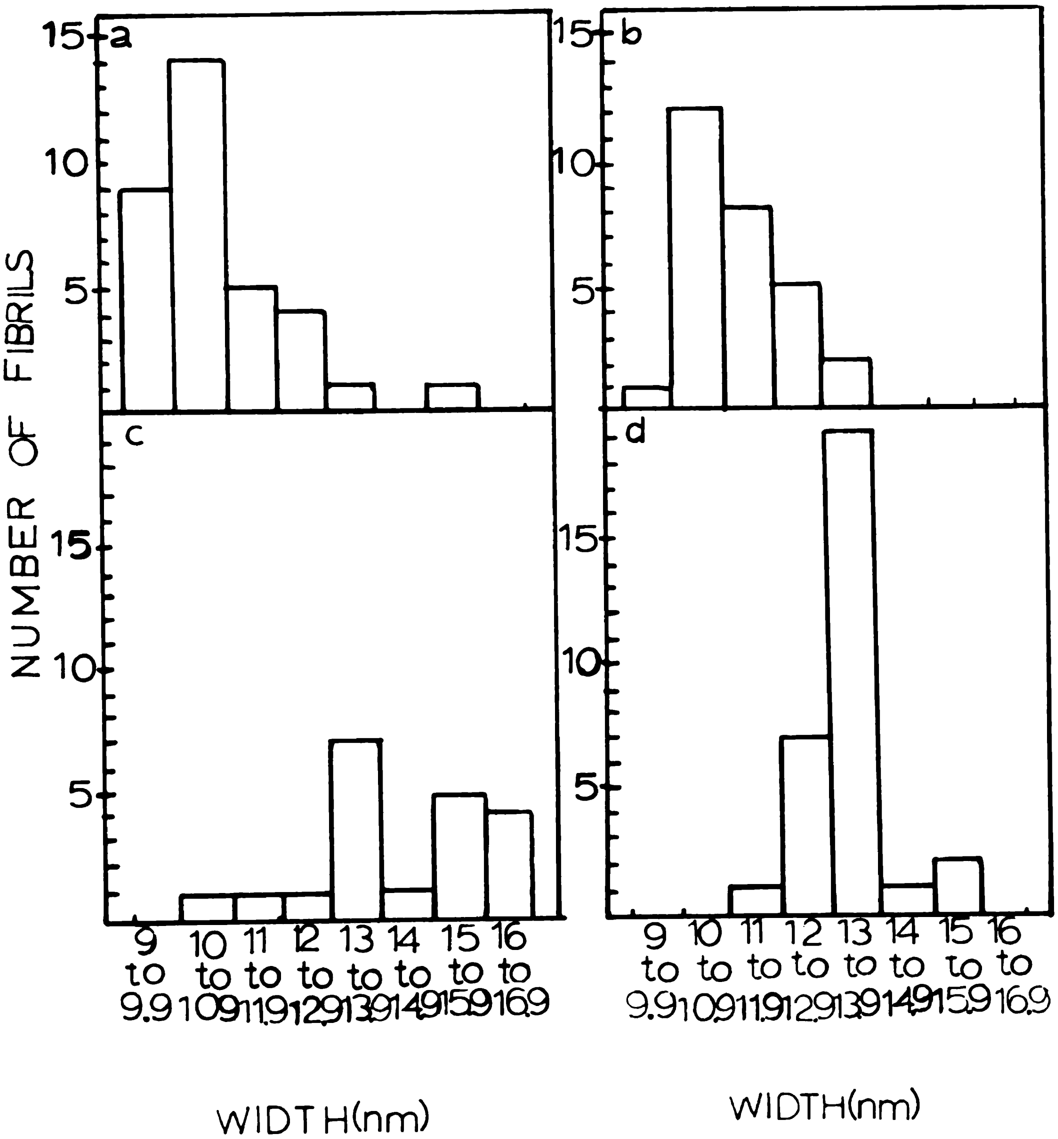

Figure 84. Each histogram shows the distribution of wide fibril widths from micrographs taken of one microscope grid. These examples were chosen because they are near the extremes of the range of means for each strain.

a. UOx-stained; mean width = 10.8 ± 0.5 nm
b. PTA-stained; mean width = 11.4 ± 0.4 nm
c. UOx-stained; mean width = 13.5 ± 1.5 nm
d. PTA-stained; mean width = 13.3 ± 0.3 nm

several factors and the variations in means. The factors considered were: age of culture, length of time from preparation of fibrils to electron microscopy, type or pH of buffer (water), variations in electron microscope magnifications, errors in print magnification, and magnification of prints used for measurement.

The strands composing the UOx-stained narrow fibrils were wider than those in the wide fibrils. PTA-stained strands of narrow fibrils, however, were not significantly different from those of wide fibrils (Table 8). The ribbons of material sometimes seen alongside the wide fibrils varied in width from 1.2 to 8.5 nm.

In micrographs of newly disrupted cells, the fibrils sometimes remained in bands (Figures 85 and 86). These bands were usually but not always still attached to membrane. The fibrils in bands were definitely of the narrow variety, since comparisons could be made with individual narrow and wide fibrils on the same micrograph (Figure 86). Also, the mean width of fibrils in bands was similar to that of individual narrow fibrils, as was the width of fibrils occasionally visible inside negatively stained cells (Table 8). The interval between fibrils in negatively stained bands compared favorably with that measured within negatively stained and cross sectioned cells (Tables 7 and 8).

Effect of Chemical, Physical or Enzymatic Treatment of Fibrils

One drop of a suspension of fibrils was mixed with one drop of any of various solutions and allowed to stand at room temperature for 10 to 45 minutes, after which the fibrils were negatively stained and viewed with the electron microscope. No effect was observed on

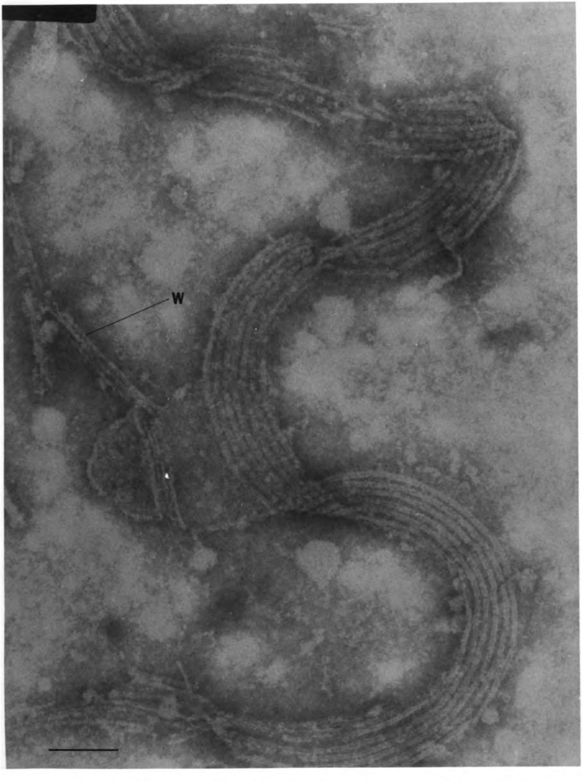

Figure 85. PTA-stained spiral band of narrow fibrils from fibril preparation which had been dried and resuspended. Note possible wide fibril (W). Bar = 0.1 μm.

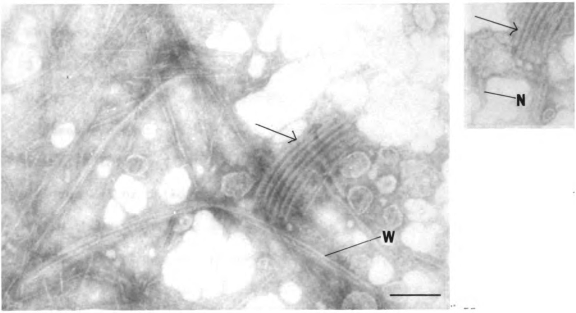

Figure 86. Negative stain of narrow fibrils in bands (arrows). Compare with wide (W) and narrow (N) fibrils. Stain was 2% PTA pH 6.7. Bar = 0.1 µm.

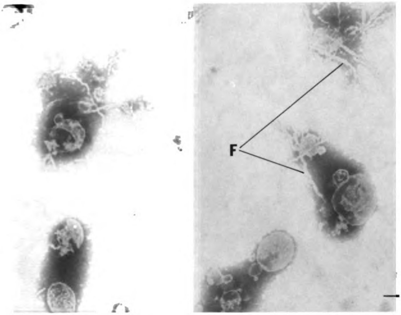

Figure 87. PTA-stained fibrils (F) disrupted with exposure to 4 M urea overnight. Bar = 0.1 µm.

fibrils in a final concentration of 33% ethanol, 50% chloroform-methanol, 2% Triton X-100, 2% sodium deoxycholate, 0.005 N HCl or 2 M urea. Fibrils were not visible after treatment with 1 N HCl, 0.005 N NaOH, 1.3% sodium dodecyl sulfate or 6 M urea. Fibrils exposed overnight to 4 M urea were still two-stranded but were wrinkled (Figure 87). Fibrils which had been frozen and thawed (Figure 74) or dried and resuspended (Figure 85) looked normal, while those which were repeatedly sonicated broke into shorter pieces. No change was observed a few minutes after fibrils were treated with 1% trypsin at pH 7.7, but after 1 hr at RT, no fibrils remained. One percent pronase at pH 7.7 destroyed the fibrils immediately.

DISCUSSION

Cell Envelope and Axial Filaments

The Ryter-Kellenberger fixation used in this study is not the ideal procedure for electron microscopic studies of bacterial cell envelopes, but nevertheless some comments can be made about the structure of the treponemal cell envelope based on these micrographs. The findings here confirm earlier reports that the treponemal cell envelope is similar to that of gram-negative cells (53,70,87, 88). The outer envelope was often expanded away from the cytoplasmic cylinder, but the expansion and separation of the outer membrane from the rest of the cell is not uncommon in osmium-fixed gram-negative bacteria. The preservation of the outer membrane can be improved when glutaraldehyde pre-fixation is used (75,84). Although this technique was tried on *T. refringens*, it proved undesirable for the observation of the intracytoplasmic structures that were the main targets of this research.

Membrane invaginations were observed only in old, degenerating cells. Ultrastructural studies to determine the conditions for the occurrence of these membrane structures, their possible function or their similarity to bacterial mesosomes would have to be done on cells fixed by various procedures, including glutaraldehyde pre-fixation.

Axial filaments have usually been reported to lie between the outer envelope and the cytoplasmic cylinder, but they have been seen in striated tubules (7,10,11,52,59,76) or in simple tubes of membrane (11,72). Listgarten and Socransky (72) reported that axial filaments attached to one end of the cell extended beyond the other end of the cell, within a sleeve of outer envelope, after cell division. In the present work, however, axial filaments were more often seen in tubes of membrane directed away from the cell than in their commonly reported position--wound around the cytoplasmic cylinder inside the outer envelope. Little significance can be ascribed to the position of these filaments because the fixation used was not optimum for preservation of the outer envelope. Negatively stained cells did not show these structures unless they had been previously disrupted.

Striated tubules may only form when the outer envelope is disrupted since they are often seen without axial filaments or in association with outer envelope vesicles. The preparation for electron microscopy may be important to their formation since they are more often seen in negatively stained cells than in thin sectioned cells. The functional significance of striated tubules or membrane sleeves and their relationships to axial filaments in normal cells is not known.

Researchers have reported that the basal body of an axial filament is inserted in the cytoplasm, with the filament protruding through a hole in the cytoplasmic membrane into the periplasmic space (43,48,52). This conclusion has been based mostly on the results of negative stains, in which the relationship between axial filaments and cytoplasmic membrane cannot be exactly determined. The few micrographs available of thin sectioned basal bodies (see Figure 28 above and Figures 7, 8 and 9 in Jackson and Black [52]) suggest that the basal body remains outside the cytoplasmic membrane, and that it is embedded in a pocket of cytoplasmic membrane rather than positioned inside the membrane. The innermost ring of the attachment apparatus of the bacterial flagellum is associated with the cytoplasmic membrane, but is not actually inside the membrane (26). Further evidence about the position of the axial filament basal body may increase understanding of the role of axial filaments in spirochetal motility.

It has been reported that fibrils are found on the same side of the cell as the axial filament (44,47,48,49,68,81,101). This relationship would be expected since the fibrils are found consistently on the insides of the curves of the cell where the "axial" filaments apparently are usually positioned (7,14,56,107). In this study no correlation was found between the positions of fibrils and those of the axial filaments in thin sectioned cells in which axial filaments were present. This is probably due to the displacement of the axial filament rather than the fibrils. The axial filaments could have been displaced due to inadequate fixation of the outer envelope or because the axial filaments of this strain of *T. refringens* are defective in some way.

Fibril Purification

For technical reasons it was practical to use no more than 440 ml culture at a time for fibril isolation. Thus only about 120

μg of fibrils were available from each preparation for use in chemical analysis, ultrastructural studies, etc. This small amount of fibrils available precluded getting more definitive results from the chemical analyses. The orcinol and diphenylamine tests did show that the RNA and DNA were not completely removed and, thus, the preparation was not chemically pure. A few protein peaks besides the 97,000 molecular weight peak were present on the tracing of the SDS acrylamide gel indicating that contaminating proteins were present, although little cellular contamination was visible with the electron microscope. It was not resolved whether fibrils are composed of only one large protein subunit (97,000 molecular weight) or more than one subunit, possibly including the 84,000 molecular weight peak. The possibility of carbohydrate or lipid components has not been excluded.

Isolated fibrils have a tendency to clump together, as evidenced by the flocculent appearance of a suspension of fibrils and the large aggregates visible under the electron microscope. Electron microscopy was used to gauge the disaggregation effect of various chemicals because, with the small amount of fibrils available, this could not be done by visual determination. It was noticed, however, that DNase reduced the rapid settling of fibril clumps. With electron microscopy, no chemicals were found to disaggregate the fibrils (Table 4), but it is possible that the clumps were dispersed only to reassemble as the dispersing agent dialyzed into the negative stain or as the suspension dried during preparation for electron microscopy. Thus, even though Triton X-100 did not appear to disaggregate fibril clumps, its success in the purification procedure may have been due to disaggregation of the clumps as well as to solubilization of membrane contaminants.

Fibril Location in Cell

Treponemal fibrils are found in a specific location in the cell--next to the cytoplasmic membrane on the inside of the curves of the cell. Fibrils in the cell follow the shortest route from one end of the cell to the other, staying on the inside of the cell's windings. Thus, the amplitude of the fibrils' helix would be less than that of the cell and the length of the fibrils which extend from end to end of a cell would be shorter than the cell's length. Long fibrils released from a cell often partially retain their spiral or curved shape, whether or not they are still organized in a band (Figures 59, 52 and 85). In no instances do the fibrils appear to be in a rigid helical form.

It is assumed that axial filaments are the agents of spirochetal locomotion but it is not known how they effect this motion. Many of the theories of the mechanism of translational movement in spirochetes are based on the phenomenon of waves traveling down the length of the spirochete (55,105). The apparently fixed position of fibrils on the inside of the treponemal waves argues against the traveling wave theory. Unless fibrils moved around the inside circumference of the cell membrane while waves traveled the cell, it would be expected that fibrils be seen also on the outer side of curves, as well as at all other positions.

No data were found to suggest that each cell contains two overlapping bands of fibrils, as was reported by Hovind Hougen

(44,45,47), rather than one band running the full length of the cell. Areas in which two bands of fibrils interdigitate were never seen in those negatively stained cells in which fibrils were visible. Such an area remains a possibility because fibrils in these cells are difficult to count accurately (Figure 36). All cross sections of cells contained only one band, but those with 13, 14 or more fibrils (Figure 34) could possibly have been cut through areas where two smaller bands interdigitated. It is possible that interdigitation of the fibrils occurs only at division points.

The observations here did not support the claim by some observers (4,66,79) that the fibrils are in two or three bands, all of which run the full length of the cell at different positions around the circumference. Some cite the visible crossing of fibrils in negatively stained cells as evidence that there are two separate bands (4,79), but this crossing is actually due to the flattening of one spiral band of cells (Figure 36).

Khorvat (66) apparently based his diagram showing three separate fibril bands on a micrograph of a band of isolated fibrils which had separated into three groups. This is flimsy evidence for such a theory, especially since the micrograph bears a remarkable similarity to one of Ovčinnikov and Delektorskij's pictures of axial filaments (79).

Fibril Ultrastructure

Some proposals can be made for the shape and structure of treponemal fibrils from the evidence produced by electron microscopy. The fibrils are more complex than simple tubules in both thin sectioned and negatively stained preparations.

In thin sectioned fibrils there are several common structures which can be found in both cross and longitudinally sectioned cells. It is likely that the dark band in longitudinal sections corresponds to the widest part of the cross sectioned fibril, whereas the light bands in longitudinal sections correspond to the light strips in cross sections (Figure 88). The base of the longitudinally sectioned fibril is indistinguishable from the edge of the inner layer of the cytoplasmic membrane. The material sometimes seen beyond the dark band in longitudinal sections could then be analogous to the cap. Measurements of these dimensions do not correspond exactly (height of cross sectioned cell excluding cap is 9.6 nm, height of longitudinally sectioned fibril from the cytoplasmic membrane through the dark band is 7.3 nm; height of cross sectioned fibril including cap is 14.5, height of longitudinally sectioned fibril including material above dark band is 16.2 nm) (Table 7), but because of the difficulties in knowing the exact orientation of the slice through the fibrils, especially longitudinally sectioned ones, these measurements compare closely enough for the above relationship to be feasible.

Both PTA-stained and UOx-stained fibril preparations contain two distinct fibril types or orientations: wide and narrow. Since the distribution of widths of narrow fibrils slightly overlaps that of the wide fibrils (Figures 80 and 81), it might appear that wide fibrils are simply fibrils on one end of a range of widths. However, the periodic striations seen on wide fibrils in UOx-stained preparations clearly distinguish wide fibrils from narrow ones. Thus there are definitely two separate fibril appearances or types.

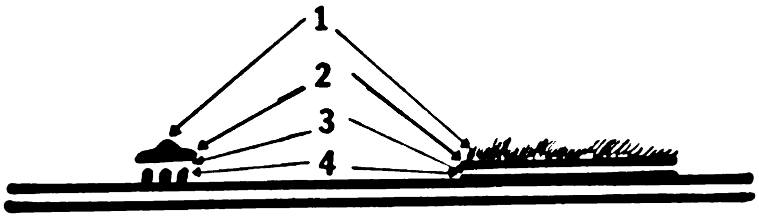

Figure 88. Relationship between components of cross and longitudinally sectioned fibrils.

1. cap
2. dark band
3. light area
4. base

It can be assumed that wide fibrils are either degraded forms of the narrow types seen in situ or that the wide and narrow fibrils are merely two different orientations of the same fibrils.

The narrow fibrils are seen in isolated fibrils preparations as well as within cells and in bands from disrupted cells while wide fibrils are seen only in isolated fibril preparations. The average fibril width reported by other researchers, who usually measured fibrils in situ, ranged from 6 to 9 nm, which corresponds to the narrow width. The fact that wide fibrils are seen only in preparations of isolated fibrils seems to support the hypothesis that they are degraded fibrils. If it is assumed that fibrils are tubules, despite the evidence from cross sections, the wide fibrils could be flattened tubules since the width of wide fibrils is approximately half the circumference of narrow fibrils. Other ways of explaining the wide fibrils as degraded narrow fibrils are possible, but the observation of wide fibril strands which twist and then appear as narrow fibrils is difficult to explain if wide fibrils are merely degraded narrow fibrils, and is a serious objection to this hypothesis.

The second hypothesis, that wide and narrow fibrils are two different views of the same type of fibril, is supported by more evidence and a model can be proposed on the basis of this evidence. Fibrils are probably not simple two-stranded structures or cylinders since they do not appear flat or circular in cross sections. The twisting of wide fibril strands is the most helpful observation when trying to construct a three-dimensional model of fibrils. Once a strand of a wide fibril is broken off (or the two strands are split apart), the other appears to be free to twist on its side, revealing that it was composed of two strands on top of one another. It is proposed, then, that each fibril is composed of four strands, each at a corner of a rectangular cross section. When the fibril is viewed from the narrow side, it has a narrow two-stranded appearance, and when viewed from the wide side, it has a wide two-stranded appearance (Figure 89a). The periodic projections visible on each strand of the wide pair apparently join together all four strands. The two strands of each narrow pair are held tightly together by means of the periodic components and, when the fibril splits in half, it does so between the two narrow pairs, each of which retains its periodic projections (Figure 89b). The periodicity can usually be seen only from the wide side, where the strands are far enough apart to allow stain penetration.

When fibrils inside a cell or in a band are viewed, they are seen on their narrow side because that is the side which is attached to the cytoplasmic membrane in this model. When fibrils are freed from the band, they are preferentially oriented on the grid support film on their wide side and only occasionally are they positioned on their narrow side. The height of shadowed fibrils is closer to the narrow than to the wide fibril width, giving further evidence that fibrils more often lie on their widest side. When one narrow pair of strands is broken away from the fibril, the remaining pair twists to lie flat (Figure 89c). The ribbons sometimes seen on wide fibrils are a little more difficult to explain, but these fibrils could be partially disorganized. If the pair of strands in contact with the grid were spread apart, without splitting completely apart, the lower

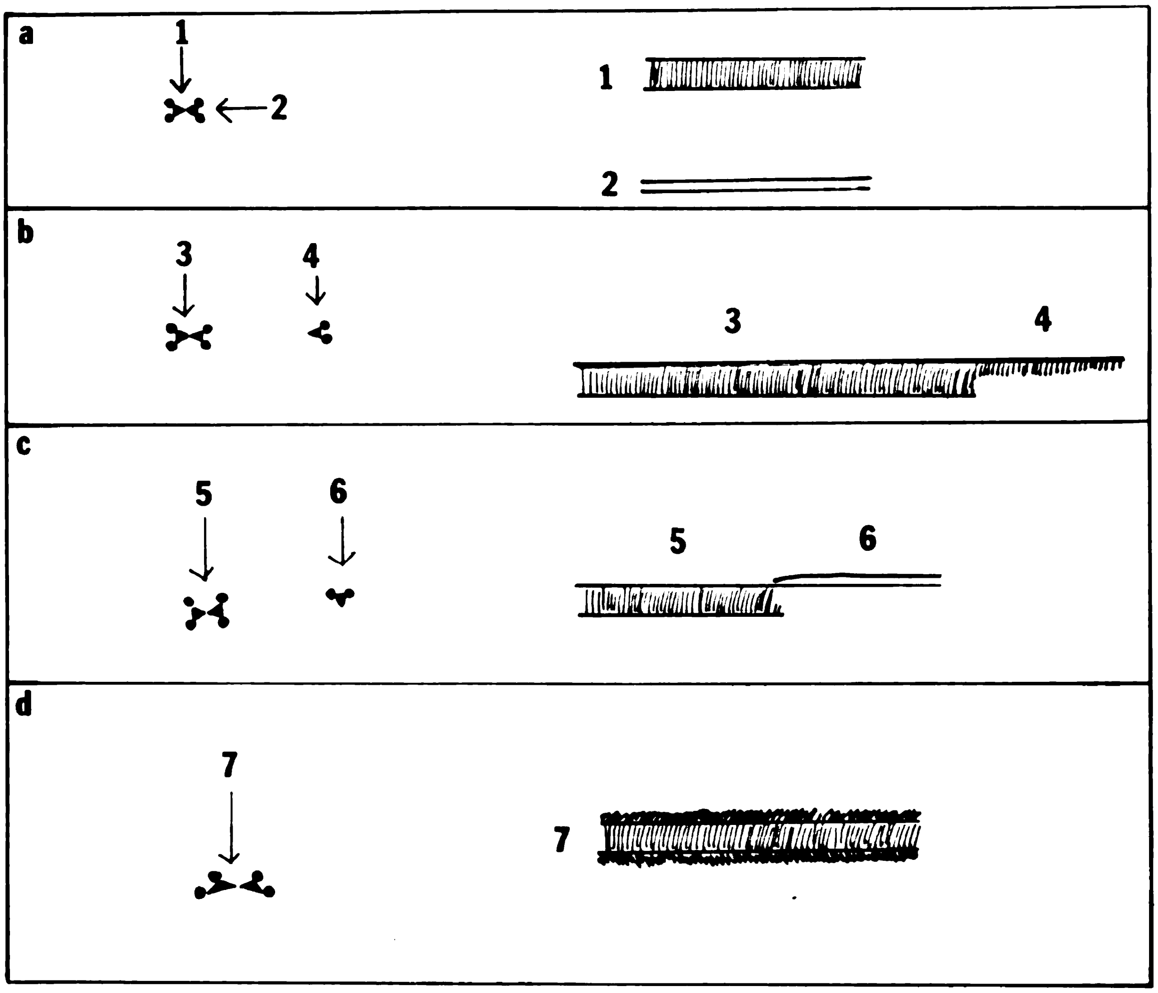

Figure 89. Model of ultrastructure of treponemal fibril as constructed from micrographs of negatively stained fibrils. Left-hand column cross sections through model. Right-hand column is what is seen when UOx-stained fibril is viewed in direction of arrow.

a. complete fibril
b. complete fibril, one strand of which has broken away
c. wide fibril in which one strand has twisted to reveal narrow fibril
d. wide fibril with ribbons on each side

strands would be covered with more negative stain than the upper pair (Figure 89d), resulting in a dark area of varying width along each side of the fibrils.

Certain difficulties arise in trying to correlate the above model with the appearance of thin sectioned fibrils. The narrowest side of the cross sectioned fibrils faces the cytoplasmic membrane, both in these micrographs and in Wiegand's (107), as it does in the model, and the space between the strands on the negatively stained wide fibril (containing the periodic substructure) would correspond with the light strip seen in cross and longitudinally sectioned fibrils. However, there is nothing in the negatively stained material suggestive of the asymmetry one would expect due to the cap seen in cross sections. Furthermore, the base of the cross sectioned fibrils often appears to be three-stranded rather than two. The differences seen between thin sectioned fibrils and negatively stained fibrils could be due to the different fixations and stains used in their preparation for electron microscopy.

The model proposed here thus accounts for much of the evidence from thin sectioned and negatively stained fibrils. Certain conclusions are inescapable. Fibrils are not simple tubules or solid rods but rather are formed of an arrangement of strands. Moreover, a definite periodicity is present.

Comparison of Fibrils with Other Prokaryotic and Eukaryotic Structures

Prokaryotic Structures

Prokaryotes contain a variety of nonmembrane-enclosed inclusion bodies, some of which are proteinaceous (97). There are, however,

only a few which bear any similarity to treponemal cytoplasmic fibrils. Ten nanometer fibrillar structures have been found in *Cytophaga columnaris* (85) and *Thiovulum majus* (24).

The fibrils found in the gliding bacterium, *Cytophaga columnaris*, are associated with the inner layer of the outer membrane (85). The fibrils run parallel to each other in wide bands which sometimes cross each other. The fibrils are about 10 nm wide and their center-to-center distance is about 16 nm. Triangular cross sections of these fibrils attached to the outer membrane look remarkably like the treponemal fibrils attached to the cytoplasmic membrane. In freeze-etched cells, these fibrils appear as linear arrays of particles (18), whereas treponemal fibrils are still fibrillar in freeze-etched cells (51). It has been suggested that these fibrils are the agents of gliding motility in Cytophaga (85). However, such fibrils have not been observed in *Myxococcus xanthus*, another gliding bacterium (18).

Thiovulum majus is a very large bacterium containing an "organite antapical" which was suspected by its discoverers to be the organ of motility (30). It is a polar body located between the inner and outer membranes and composed of a clump of about a hundred fibrils (10 nm wide) oriented perpendicularly to the cell surface. Since *Thiovulum* was later shown definitely to have typical bacterial flagella (24), the function of the fibrils remains obscure.

The fibrils found in *Cytophaga* and *Thiovulum* are similar to treponemal cytoplasmic fibrils in size but are located in the periplasmic space rather than in the cytoplasm. The only intracytoplasmic structures similar to treponemal fibrils in size are the components of a cytoplasmic membrane-associated organelle in *Halobacterium halobium* (20). The organelle is composed of a series of wavy striated fibrils, from 7.5 to 10 nm wide, which are quite different morphologically from treponemal fibrils.

Treponemal fibrils have been called microtubules (48), but are not the same as other bacterial "microtubules" (90,104), which are morphologically similar to the rhapidosomes found in various species of bacteria (113), including *Spirocheta litoralis* (59). Rhapidosomes are large tubules (20 to 30 nm in diameter) and normally have a definite length. They often appear only in degenerating cells and have no known biological activity (25,69).

Eukaryotic Structures

All eukaryotic movement, muscular, ciliar, flagellar or cytoplasmic, is apparently realized through the ATP-dependent sliding interaction of fibrillar proteins (1). Treponemal fibrils are not at all similar to eukaryotic microtubules. Even rhapidosomes, which are nearly the same size as microtubules, have only superficial structural similarities to them (25).

Actin and myosin are present in nonmuscle cells of widely separated eukaryotic phyla, including Protozoa, but have not been found in prokaryotes, with the possible exception of an actin-like protein in *E. coli* (74). Actins are essentially the same in all cells. The globular monomers, with a molecular weight of about 45,000, polymerize into double helical filaments about 6 nm wide. Myosins vary more than actins but are all made of heavy chains (180,000 to 240,000 molecular weight) and light chains (12,000 to 19,000 molecular

weight). Most myosins have a globular head and a rod-like tail. All myosins have similar properties of actin binding and ATP hydrolysis (89). Treponemal fibrils do not resemble actin, myosin or tubulin either in molecular weight or ultrastructure. It would be interesting, however, to know if fibrils are involved in a sliding filament motility interaction or have any other related properties, e.g., ATPase activity or ability to stimulate ATPase activity.

Function of Fibrils

Cytoplasmic fibrils appear to be unique to the genus *Treponema*. The question may be asked why treponemes should have fibrils while other spirochetes appear not to have them. Even though all spirochetes are obviously related and have peculiar characteristics in common, there are many differences among the species. Spirochetes are free-living, pathogenic or nonpathogenic host-associated and range in size from 0.1 to 0.75 μm thick and 2 to 250 μm long (15). Among other chemical and serological differences is the variation in peptidoglycan composition. *Treponema* and *Spirocheta* have peptidoglycan similar to that of gram-negative cells with the exception that ornithine is present rather than meso-diaminopimelic acid. Leptospires, on the other hand, do have meso-diaminopimelic acid (3).

The function of treponemal cytoplasmic fibrils is unknown, but it seems unlikely that they are nonfunctional. They are in specific relationships with other cell components (DNA, membrane) and are in a specific location relative to the shape of the cell. Fibrils are not transitory but are found in cells of all growth stages. Based on the location of the fibrils, two suggestions can be made as to their possible function: 1) shape maintenance and 2) DNA replication, segregation, or transcription.

Maintenance of Shape

Because isolated peptidoglycan often retains the shape of the cell, it is commonly cited as the shape maintaining component of the cell. But Henning has pointed out that it is not clear whether peptidoglycan is the only device for maintaining shape. Other cell components which may be involved in various bacteria are outside protein layers, the outer membrane or the cytoplasmic membrane (41). The shape-maintaining function must also be separated from the shape-specifying role since the information required to produce peptidoglycan of a specific shape could only involve either enzymes or a matrix onto which the peptidoglycan is laid down (42).

Treponemal fibrils are in a position to pull a rod into a helical shape, as was once hypothesized for axial filaments. Bradfield and Cater (14) wound an elastic band spirally around a piece of rubber tubing which had a metal rod inside and fastened the elastic to the tube very few inches. When the rod was removed, the tube was in the form of a spirochete. Tubing can also be held in a helical shape by an internal string (representing cytoplasmic fibrils). The string need only be passed through the tube and tied to the tube at both ends after pulling so that the string is shorter than the tube. If the tube is transparent it can be readily demonstrated that the string follows the inside of the curves and is helical, but with a smaller amplitude than that of the tubing.

Axial filaments were assumed not to be responsible for the helical shape once it was discovered that each filament is attached to the cell at only one point. There are also difficulties in ascribing the role of shape maintenance to the fibrils. For this model to be correct, it is necessary that there be only one band of fibrils attached at each end of the cell or that, if two bands are present and interdigitate, the fibrils be securely attached to the membrane. The nature of treponemal fibril attachment to the cytoplasmic membrane is not known and there appears not to be a specialized attachment apparatus at the end of the fibrils.

In any case, fibrils could not be the sole mechanism for shape maintenance since they do not completely surround the cell. They could only provide the tension to pull an already-formed cylinder into a helical shape.

Cell Division

The location of the nuclear area of treponemes next to the fibrils was consistently observed in the electron micrographs of thin sectioned *T. refringens*. Except for two vague references to a lighter area near the fibrils (48,83), this has not been previously reported. Most investigators have not used the Ryter-Kellenberger fixation which provides for the best preservation of the bacterial nuclear area (64). Even so, a few published pictures do allow the observation of the relationship between the nuclear area and the fibrils to be extended to other species of treponemes (44,57,101).

When cells were grown in ^{3}H-thymidine and then lysed and centrifuged on a gradient, the labeled DNA was distributed into several

areas of the gradient. This procedure failed to demonstrate the attachment of DNA to either fibrils or membrane components. The major difficulty in this approach is that the disruption procedure must release the fibrils from the membrane completely while allowing the DNA to remain attached to either fibrils or membrane. The only way in which fibril and membrane could be completely separated from one another in fibril isolation procedures was with the use of DNase.

The Kleinschmidt spreading procedure demonstrated DNA released from the cell while still attached to cell components. The resolution was not good enough, however, to demonstrate the attachment of DNA to fibrils rather than membrane. The lack of resolution in this procedure resulted from the necessity of using cytochrome c as a spreading agent and uranyl acetate as a stain in order to visualize the DNA. These are not good conditions for clear visualization of the fibrils.

The data, then, which best demonstrate the attachment of DNA to fibrils is from micrographs of thin sectioned cells. DNA was located near the fibrils in all cases and no evidence was seen for the attachment of DNA to the membrane. In thin sections of spheroplast-like cells, whose cytoplasm was disrupted, the strands of DNA could be seen directly attached to the cytoplasmic fibrils.

The attachment of DNA to the cell membrane of several bacteria has been established (71). Cytological studies demonstrated this attachment in micrographs of thin sectioned gram-negative and gram-positive cells (92) and of disrupted cells prepared by the Kleinschmidt spreading technique (32,40,103). Biochemical fractionation studies have also demonstrated this association (71).

This connection has been hypothesized to be necessary for DNA replication, segregation or transcription (54,71). Since the DNA in treponemes appears to be attached to fibrils rather than membrane, one or more of the roles usually ascribed to the membrane may actually be a function of cytoplasmic fibrils.

There is recent evidence that *E. coli* DNA may be attached to the membrane at a region where the cell wall closely adheres to the membrane. It has been suggested that association with the wall may be necessary if the site is to have sufficient physical strength for segregation of the chromosomes at cell division (78). In treponemes, perhaps fibrils are responsible for the segregation of DNA which is taken care of by the mitotic apparatus in eukaryotes and the membrane or membrane-wall in at least some of the bacteria.

APPENDIX

APPENDIX

ULTRASTRUCTURE OF *TREPONEMA HYODYSENTERIAE*

Introduction

Harris *et al.* (88) isolated two types of spirochetes from the colon of pigs infected with swine dysentery. Further work demonstrated that one of the spirochetes could produce the disease in healthy pigs and the name *T. hyodysenteriae* was proposed for the organism. Its inclusion in the genus *Treponema* was based on its requirement for anaerobiosis, structure, and location in the host (37). *Treponema hyodysenteriae* is a large, loosely coiled spirochete, measuring 0.3 to 0.4 μm in diameter and 5 to 8 μm in length. Seven to nine axial filaments originate from each end of the cell (33,37).

Ultrastructural studies on this organism were initiated in an attempt to determine if cytoplasmic fibrils were present and could be isolated with the same procedure used for *T. refringens*.

Materials and Methods

Treponema hyodysenteriae, obtained from J. M. Kinyon, Iowa State University, Ames, was grown in a prereduced anaerobically sterilized broth at 37 C as described by Kinyon and Harris (67).

Cells were disrupted with the CLBS procedure and centrifuged on a Renografin gradient as described earlier for *T. refringens*.

Several of the resulting bands were dialyzed against distilled water and used for electron microscopy.

Whole cells or cell fractions were negatively stained with 0.5% PTA, pH 7.5, on a carbon-Formvar coated grid and observed with a Philips 300 electron microscope.

Results

The outer envelope loosely enclosed the cytoplasmic cylinder and the axial filaments (Figure 90). Nine to 11 axial filaments were inserted subterminally at each end of the cell. The insertion points were at various distances from the end of the cell (Figure 91).

When *T. hyodysenteriae* was treated with the CLBS procedure used on *T. refringens*, the cells lysed. Electron microscopy revealed membrane, occasional striated tubules and many fragments of axial filaments, some with hooks. No fibrils were found.

The bands which formed after centrifugation in a Renografin gradient were not in the same pattern as that for *T. refringens*. Most of the membrane appeared in a band near the top of the gradient. In a band of approximately the same density as that of fibrils of *T. refringens*, a few bundles of 3 nm fibrous structures were seen (Figure 92).

Axial filaments, in pieces of various lengths, were found in several bands. The filaments were sheathed whereas their hooks, if present, were not sheathed (Figures 93 and 94). An electron dense line ran down the middle of many of the filaments. The filaments were broken jaggedly at many points and often the segments

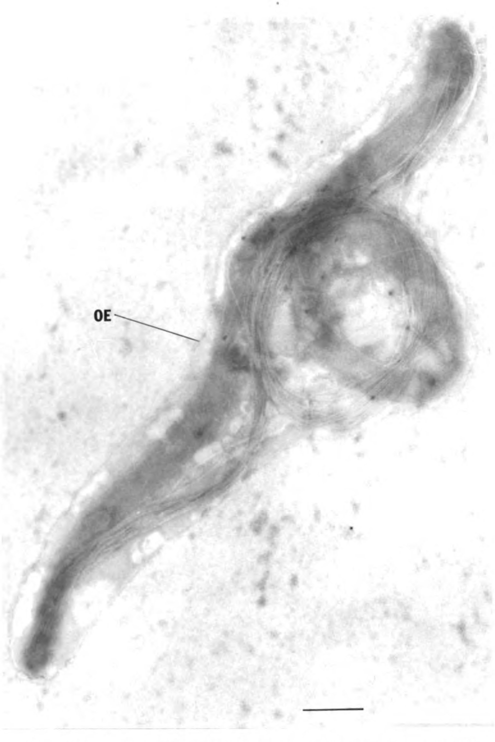

Figure 90. *T. hyodysenteriae* negatively stained with PTA. The cell has partially curled up inside the outer envelope (OE). Bar = 0.5 µm.

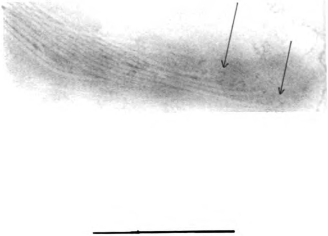

Figure 91. Enlargement of Figure 90. Points where axial filament basal bodies insert into the cell are visible (arrows). Bar = 0.5 µm.

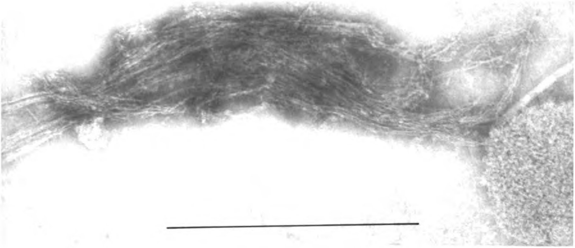

Figure 92. PTA-stained bundles of fibers from CLBS-disrupted *T. hyodysenteriae*. Bar = 0.5 µm.

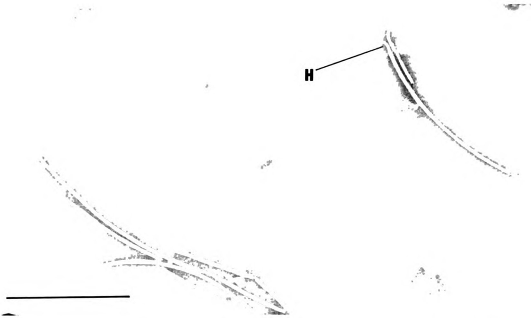

Figure 93. PTA-stained axial filament fragments from CLBS-disrupted *T. hyodysenteriae*. Hooks (H) are unsheathed. Bar = 0.5 µm.

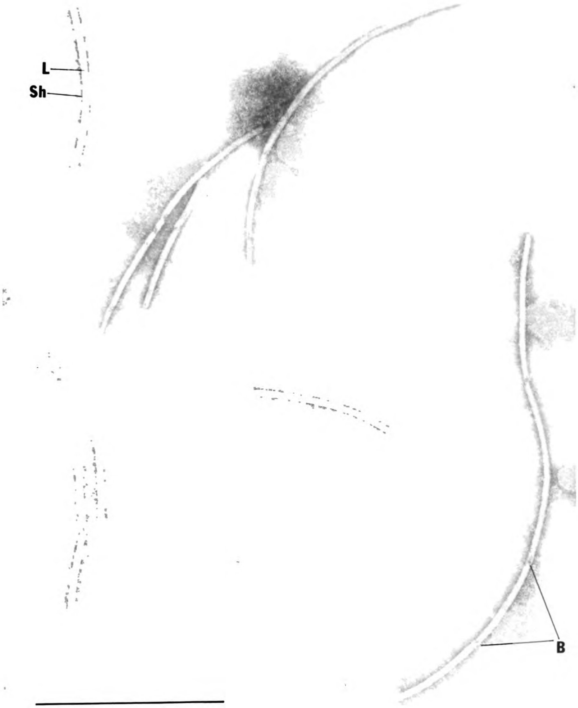

Figure 94. PTA-stained axial filament fragments from CLBS-disrupted *T. hyodysenteriae*. Sheath (Sh) is visible, as well as electron dense line running down the center of the filament (L). Axial filaments are broken (B) and still attached, apparently with the sheath. Bar = 0.5 μm.

were still attached to each other, presumably by the sheath (Figure 94). The breaks were often V-shaped and the filaments appeared to have polarity since filament on one side of each break was pointed and was indented on the other (Figure 94). It was determined that the distal end of the filament had the indentation by looking at filament segments which still had hooks attached (Figure 93).

Discussion

It is still unclear whether *T. hyodysenteriae* contains cytoplasmic fibrils of the type found in other treponemes. Fibrils were not seen in guinea pig serum-disrupted cells under the same conditions in which they are easily found in *T. refringens*. The fibrous structures found after centrifugation are narrower than cytoplasmic fibrils but are about the same size as the strands of which cytoplasmic fibrils are composed. Perhaps fibrils from various treponemal species differ in their fragility. The demonstration of fibrils next to the membrane of thin-sectioned *T. hyodysenteriae* cells would be required to determine if cytoplasmic fibrils were present.

Short fragments of bacterial flagella reportedly possess differently formed ends (13), but this has not yet been reported for spirochetal axial filaments. The indented, or incised, end of a bacterial flagellum is on the distal end as was reported above for *T. hyodysenteriae* axial filaments.

LITERATURE CITED

LITERATURE CITED

1. Alicea, H. A. and F. L. Renaud. 1975. Actin-tubulin homology revisited. Nature (London) 257:601-602.

2. Ashwell, G. 1957. Colorimetric analysis of sugars, p. 73-105. In S. P. Colowick and N. O. Kaplan (eds.), *Methods in Enzymology*, Vol. III. Academic Press, New York.

3. Azuma, I., T. Taniyama, Y. Yamamura, Y. Yanigihara, Y. Hattori, S. Yasuda, and I. Mifuchi. 1975. Chemical studies on the cell walls of *Leptospira biflexa* strain Urawa and *Treponema pallidum* strain Reiter. Jap. J. Microbiol. 19:45-51.

4. Babudieri, B. 1972. Discussions, p. 157-159. In B. Babudieri (ed.), *The Fine Morphology of Spirochaetas*. Leonarda Edizioni Scientificha, Rome.

5. Bertalanffy, L., F. Masin and M. Masin. 1956. Use of acridine-orange fluorescent technique in exfoliative cytology. Science 124:1024-1025.

6. Bharier, M. and D. Allis. 1974. Purification and characterization of axial filaments from *Treponema phagadenis* Biotype *reiterii* (the Reiter treponeme). J. Bacteriol. 120:1434-1442.

7. Bharier, M. A., F. A. Eiserling and S. C. Rittenberg. 1971. Electronmicroscopic observations on the structure of *Treponema zuelzerae* and its axial filaments. J. Bacteriol. 105:413-421.

8. Bharier, M. A. and S. C. Rittenberg. 1971. Chemistry of axial filaments of *Treponema zuelzerae*. J. Bacteriol. 105:422-429.

9. Bharier, M. A. and S. C. Rittenberg. 1971. Immobilization effects of anticell and antiaxial filament sera on *Treponema zuelzerae*. J. Bacteriol. 105:430-437.

10. Birch-Andersen, A., K. Hovind Hougen, and C. Borg-Petersen. 1973. Electron microscopy of *Leptospira*. I. *Leptospira* strain Pomona. Acta Path. Microbiol. Scand. sect. B 81:665-676.

11. Bladen, H. A. and E. G. Hampp. 1964. Ultrastructure of *Treponema microdentium* and *Borrelia vincentii*. J. Bacteriol. 87:1180-1191.

12. Blakemore, R. P. and E. Canale-Parola. 1973. Morphological and ecological characteristics of *Spirochaeta plicatilis*. Arch. Mikrobiol. 89:273-289.

13. Bode, W. 1973. The bacterial flagella and the flagellar protein flagellin. Angew. Chem. Int. Ed. 12:683-693.

14. Bradfield, J. R. G. and D. B. Cater. 1952. Electron-microscopic evidence on the structure of spirochaetes. Nature (London) 169:944-946.

15. Breznak, J. A. 1973. Biology of nonpathogenic, host-associated spirochetes. Crit. Rev. Microbiol. 2:457-489.

16. Buchanan, R. E. 1925. Classification of the genera and higher groups of bacteria. Historical, 1773-1922, p. 15-108. In *General Systematic Bacteriology*. Williams and Wilkins, Baltimore.

17. Bulloch, W. 1936. Classification of bacteria, p. 171-203. In *The History of Bacteriology*. Oxford University Press, London.

18. Burchard, R. P. and D. T. Brown. 1973. Surface structure of gliding bacteria after freeze-etching. J. Bacteriol. 114: 1351-1355.

19. Burrill, T. J. 1882. Classification of bacteria, p. 32-65. In *The Bacteria: An Account of Their Nature and Effects, Together With a Systematic Description of the Species*. H. W. Rokka, State Printer and Binder, Springfield, Illinois.

20. Cho, K. Y., C. H. Doy and E. H. Mercer. 1967. Ultrastructure of the obligate halophilic bacterium *Halobacterium halobium*. J. Bacteriol. 94:196-201.

21. Costerton, J. W., J. M. Ingram and K.-J. Chang. 1974. Structure and function of the cell envelope of gram-negative bacteria. Bacteriol. Rev. 38:87-110.

22. Cox, C. D. 1972. Shape of *Treponema pallidum*. J. Bacteriol. 109:943-944.

23. Davis, R. W., M. Simon and N. Davidson. 1971. Electronmicroscopic heteroduplex methods for mapping regions of base sequence homology in nucleic acids, p. 413-428. In L. Grossman and K. Modaves (eds.), *Methods in Enzymology*, Vol. 21. Academic Press, New York.

24. de Boer, W. E., J. W. M. LaRiviére and A. L. Houwink. 1961. Observations on the morphology of *Thiovulum majus* Hinze. Antonie van Leeuwenhoek J. of Microbiol. and Serol. 27:447-456.

25. Delk, A. S. and C. A. Dekker. 1972. Characterization of rhapidosomes of *Saprospira grandis*. J. Mol. Biol. 64:287-295.

26. De Pamphilis, M. L. and J. Adler. 1971. Attachment of flagellar basal bodies to the cell envelope: Specific attachment to the outer, lipopolysaccharide membrane and the cytoplasmic membrane. J. Bacteriol. 105:396-407.

27. Dobell, C. 1932. The first observations on entozoic protozoa and bacteria, p. 217-255. In *Antony van Leeuwenhoek and His "Little Animals"*. Harcourt, Brace and Co., New York.

28. Ellinghausen, H. C. 1959. Nephelometry and a nephelo-culture flask used in measuring growth of leptospires. Am. J. Vet. Res. 20:1072-1076.

29. Fairbanks, G., T. L. Steck, and D. F. H. Wallach. 1971. Electrophoretic analysis of the major polypeptides of the human erythrocyte membrane. Biochem. 10:2606-2617.

30. Faure-Fremiet, E. and Rouiller, C. 1958. Étude au microscope électronique d'une bacterie sulfureusa, *Thiovulum majus* Hinze. Exptl. Cell Res. 14:29-46.

31. Filip, C., G. Fletcher, J. L. Wulff and C. F. Earhart. 1973. Solubilization of the cytoplasmic membrane of *Escherichia coli* by the ionic detergent sodium-lauryl sarcosinate. J. Bacteriol. 115:717-722.

32. Ganesan, A. T. 1967. Particulate fractions in macromolecular synthesis and genetic transformation, p. 19-47. In Vogel, H. J. *et al.* (eds.), *Organizational Biosynthesis*. Academic Press, Inc., New York.

33. Glook, R. D., D. L. Harris, and J. P. Kluge. 1974. Localization of spirochetes with the structural characteristics of *Treponema hyodysenteriae* in the lesions of swine dysentery. Inf. Imm. 9:167-178.

34. Hardy, P. H., W. R. Fredericks and E. E. Nell. 1975. Isolation and antigenic characteristics of axial filaments from the Reiter treponeme. Inf. Imm. 11:380-386.

35. Hardy, P. H. and E. E. Nell. 1961. Influence of osmotic pressure on the morphology of the Reiter treponeme. J. Bacteriol. 82:967-978.

36. Hardy, P. H., E. E. Nell and W. R. Fredericks. 1975. Isolation and immunologic study of treponemal outer envelopes, p. 72. Am. Soc. of Microbiol. Proc.

37. Harris, D. L., Glock, R. D., C. R. Christensen, and J. M. Kinyon. 1972. Inoculation of pigs with *Treponema hyodysenteriae* (new species) and reproduction of the disease. Vet. Med./Small An. Clin. January, p. 61-64.

38. Harris, D. L., J. M. Kinyon, M. T. Mullin and R. D. Glock. 1972. Isolation and propagation of spirochetes from the colon of swine dysentery affected pigs. Can. J. Comp. Med. 36:74-76.

39. Haschemeyer, R. H. and R. J. Myers. 1972. Negative staining, p. 101-147. In M. A. Hayat (ed.), *Principles and Techniques of Electron Microscopy: Biological Applications,* Vol. 2. Van Nostrand Reinhold Co., New York.

40. Heidrich, H.-G. and W. L. Olsen. 1975. DNA-envelope complexes from *Escherichia coli*: A complex-specific protein and its possible function for the stability of the complex. J. Cell Biol. 67:444-460.

41. Henning, U. 1975. Determination of cell shape in bacteria. Annu. Rev. Microbiol. 29:45-60.

42. Henning, U. and U. Schwarz. 1973. Determinants of cell shape, p. 413-440. In L. Leive (ed.), *Bacterial Membranes and Walls.* Marcel Dekker, New York.

43. Holt, S. C. and E. Canale-Parola. 1968. Fine structure of *Spirochaeta stenostrepta,* a free-living anaerobic spirochete. J. Bacteriol. 96:822-835.

44. Hovind Hougen, K. 1974. The ultrastructure of cultivable treponemes. I. *Treponema phagadenis, Treponema vincentii, Treponema refringens.* Acta Path. Microbiol. Scand. sect. B 82:329-344.

45. Hovind Hougen, K. 1974. The ultrastructure of cultivable treponemes. II. *Treponema calligyrum, Treponema minutem, Treponema microdentiium.* Acta Path. Microbiol. Scand. sect. B 82:495-507.

46. Hovind Hougen, K. 1975. The ultrastructure of cultivable treponemes. III. *Treponema genitalis.* Acta Path. Microbiol. Scand. sect. B 83:91-99.

47. Hovind Hougen, K. 1972. Further observations on the ultrastructure of *Treponema pallidum* Nichols. Acta Path. Microbiol. Scand. sect. B 80:297-304.

48. Hovind Hougen, K. and A. Birch-Andersen. 1971. Electron microscopy of endoflagella and microtubules in *Treponema* Reiter. Acta Path. Microbiol. Scand. sect. B 79:37-50.

4

5

5

5

5

5

5

5

5

5

5

49. Hovind Hougen, K., A. Birch-Andersen, and H.-J. S. Jensen. 1973. Electron microscopy of *Treponema cuniculi*. Acta Path. Microbiol. Scand. sect. B. 81:15-26.

50. Jackson, S. W. 1969. The fine structure of *Treponema pallidum* Nichols strain. Thesis. Baylor University, Houston, Texas.

51. Jackson, S. and S. H. Black. 1971. Ultrastructure of *Treponema pallidum* Nichols following lysis by physical and chemical means. I. Envelope, wall, membrane and fibrils. Arch. Mikrobiol. 76:308-324.

52. Jackson, S. and S. H. Black. 1971. Ultrastructure of *Treponema pallidum* Nichols following lysis by physical and chemical means. II. Axial filaments. Arch. Mikrobiol. 76:325-340.

53. Jackson, S. W. and P. N. Zey. 1973. Ultrastructure of lipopolysaccharide isolated from *Treponema pallidum*. J. Bacteriol. 114:838-844.

54. Jacob, F., S. Brenner and F. Cuzin. 1963. On the regulation of DNA replication in bacteria. Cold Spring Harbor Symp. Quant. Biol. 28:329-348.

55. Jahn, T. L. and E. C. Bovee. 1965. Movement and locomotion of micro-organisms. Annu. Rev. Microbiol. 19:21-58.

56. Jepsen, O. B., K. Hovind Hougen and A. Birch-Andersen. 1968. Electron microscopy of *Treponema pallidum* Nichols. Acta Path. Microbiol. Scand. 74:241-258.

57. Johnson, R. C., M. S. Wachter and D. M. Ritzi. 1973. Treponeme outer cell envelope: Solubilization and reaggregation. Inf. and Imm. 7:249-258.

58. Jones, R. H., Z. Yoshii and O. J. Carver. 1970. Some morphologic features of axial fibers and body fibrils of treponemata, p. 110-111. In C. J. Arcenaux (ed.), *Proc. 28th Annu. Mtg. Elec. Micros. Soc. Am.* Claitor's Publishing Division, Baton Rouge.

59. Joseph, R. and E. Canale-Parola. 1972. Axial fibrils of anaerobic spirochetes: Ultrastructure and chemical characteristics. Arch. Mikrobiol. 81:146-168.

60. Joseph, R., S. C. Holt, and E. Canale-Parola. 1973. Peptidoglycan of free-living anaerobic spirochetes. J. Bacteriol. 115:426-435.

61. Kast, C. C. and J. A. Kolmer. 1933. One successful cultivation of *Spirocheta pallida* from syphilitic chancre of the rabbit. Amer. J. Syph. 17:533-538.

62. Kawata, T. 1961. Electron microscopy of fine structure of *Borrelia duttonii*. Jap. J. Microbiol. 5:203-209.

63. Kawata, T. and T. Inoue. 1964. Fine structure of the Reiter treponeme as revealed by electron microscopy using thin sectioning and negative staining techniques. Jap. J. Microbiol. 8:49-65.

64. Kellenberger, E. 1962. The study of natural and artificial DNA-plasms by thin sections, p. 233-249. In R. J. C. Harris (ed.), *The Interpretation of Ultrastructure,* Vol. 1. Academic Press, New York.

65. Kellenberger, E., A. Ryter and J. Séchaud. 1958. Electron microscope study of DNA-containing plasms. II. Vegetative and mature phage DNA as compared with normal bacterial nucleoids in different physiological states. J. Biophys. Biochem. Cytol. 4:671-676.

66. Khorvat, I. K. 1972. Structure and movement of a treponeme. Acta Microbiol. Acad. Sci. Hung. 19:121-124.

67. Kinyon, J. A. and D. L. Harris. 1974. Growth of *Treponema hyodysenteriae* in liquid medium. Vet. Rec. 95:219-220.

68. Klingmüller, G., Y. Ishibashi, K. Radke. 1968. Der elektronenmikroskopische Aufbau des *Treponema pallidum*. Arch. für Klin. u. Exp.Dermatol. 233:197-205.

69. Kuhrt, M. and J. L. Pate. 1973. Isolation and characterization of tubules and plasma membranes from *Cytophaga columnaris*. J. Bacteriol. 114:1309-1318.

70. Lataste-Dorolle, C. 1972. Structure and nature of the membrane of treponemas, p. 59-62. In B. Babudieri (ed.), *The Fine Morphology of Spirochaetas*. Leonardo Edizioni Scientifiche, Rome.

71. Leibowitz, R. J. and M. Schaechter. 1975. The attachment of the bacterial chromosome to the cell membrane. Int. Rev. Cytol. 41:1-28.

72. Listgarten, M. A. and S. S. Socransky. 1964. Electron microscopy of axial fibrils, outer envelope, and cell division of certain oral spirochetes. J. Bacteriol. 88:1087-1103.

73. Lowry, O. H., N. J. Rosebrough, A. L. Farr and R. J. Randall. 1951. Protein measurement with the folin phenol reagent. J. Biol. Chem. 193:265-275.

74. Minkoff, L. and R. Damadian. 1975. Actin-like proteins from *Escherichia coli*: Concept of cytotonus as the missing link between cell metabolism and the biological ion-exchange resin. J. Bacteriol. 125:353-365.

75. Murray, R. G. E. 1968. Bacterial cell wall anatomy in relation to the formation of spheroplasts and protoplasts, p. 1-18. In L. B. Guze (ed.), *Microbial Protoplasts and L-Forms*. Williams and Wilkins, Baltimore.

76. Nauman, R. K., S. C. Holt and C. D. Cox. 1969. Purification, ultrastructure, and composition of axial filaments from *Leptospira*. J. Bacteriol. 98:264-280.

77. Nevin, T. A. and W. J. Guest. 1967. Complement and lysozyme requirements for spirochetolysis in guinea pig serum. J. Bacteriol. 94:1388-1393.

78. Olsen, W. L., H.-G. Heidrich, K. Hannig and P. H. Hofschneider. 1974. DNA complexes isolated from *Escherichia coli* by free-flow electrophoresis: Biochemical and electron microscope characterization. J. Bacteriol. 118:646-653.

79. Ovčinnikov, N. M. and V. V. Delektorskij. 1972. The fibrils of *Treponema pallidum* (an electron-microscope investigation). WHO/VDT/RES/72.281. World Health Organization, Geneva.

80. Ovčinnikov, N. M. and V. V. Delektorskij. 1971. Current concepts of the morphology and biology of *Treponema pallidum* based on electron microscopy. Brit. J. Vener. Dis. 47:315-328.

81. Ovčinnikov, N. M. and V. V. Delektorskij. 1970. *Treponema pertenue* under the electron microscope. Brit. J. Vener. Dis. 46:349-379.

82. Ovčinnikov, N. M. and V. V. Delektorskij. 1969. Further material on the morphology of *Treponema pallidum* under the electron microscope. Brit. J. Vener. Dis. 45:87-116.

83. Ovčinnikov, N. M. and V. V. Delektorskij. 1968. Further study of ultrathin sections of *Treponema pallidum* under the electron microscope. Brit. J. Vener. Dis. 44:1-34.

84. Pate, J. L. and E. J. Ordal. 1967. The fine structure of *Chondrococcus columnaris*. I. Structure and formation of mesosomes. J. Cell Biol. 35:1-13.

85. Pate, J. L. and E. J. Ordal. 1967. The fine structure of *Chondrococcus columnaris*. III. The surface layers of *Chondrococcus columnaris*. J. Cell. Biol. 35:37-51.

86. Pillot, J. 1969. Analytical serology of Treponemataceae, p. 123-183. In J. B. G. Kwapinski (ed.), *Analytical Serology of Microorganisms*, Vol. 1. Interscience Publishers, New York.

87. Pillot, J. 1965. Contribution à l'étude du genre *Treponema*: Structures anatomique et antigenique. Thesis, L'Universite de Paris, Paris.

88. Pillot, J. and A. Ryter. 1965. Structure des spirochetes. I. Étude des genera *Treponema, Borrelia* et *Leptospira* au microscope électronique. Ann. Inst. Past. 108:791-804.

89. Pollard, T. D. and R. R. Weihing. 1974. Actin and myosin and cell movement. Crit. Rev. Biochem. 2:1-65.

90. Pope, L. M. and P. Jurtshuk. 1967. Microtubule in *Azotobacter vinelandii* strain O. J. Bacteriol. 94:2062-2064.

91. Ritchie, A. E. and H. C. Ellinghausen. 1965. Electron microscopy of leptospires. I. Anatomical features of *Leptospira pomona*. J. Bacteriol. 89:223-233.

92. Ryter, A. 1968. Association of the nucleus and the membrane of bacteria: A morphological study. Bacteriol. Rev. 32: 39-54.

93. Schaudinn, F. 1905. Zur Kenntis der *Spirochaete pallida*. Deutsche Med. Wochensch. 31:1665-1667.

94. Schaudinn, F. 1905. Korrespondenzen. Deutsche Med. Wochensch. 31:1728.

95. Schaudinn, F. and E. Hoffmann. 1905. Vorläufiger Bericht über das Vorkommen von Spirochaeten in syphilitischen Krankheitsprodukten u. bei Papillomen. Arb. Kaiserl. Gesundh. 22:528-534.

96. Sequira, P. J. L. 1956. The morphology of *Treponema pallidum*. Lancet 2:749.

97. Shively, J. M. 1974. Inclusion bodies of prokaryotes. Annu. Rev. Microbiol. 28:167-187.

98. Simpson, C. F. and F. H. White. 1961. Electron microscope studies and staining reactions of leptospires. J. Inf. Dis. 109:243-250.

99. Smibert, R. M. 1974. The spirochetes, p. 167-195. In R. E. Buchanan and N. E. Gibbons (eds.), *Bergey's Manual of Determinative Bacteriology*. The Williams and Wilkins Co., Baltimore.

100. Smibert, R. M. 1973. Spirochaetales, a review. Crit. Rev. Microbiol. 2:491-552.

101

102

103

104

105

106

107

10

10

11

11

11

1

101. Swain, R. H. A. and N. Anderson. 1972. The ultra-structure of species of treponemas and borreliae, p. 115-139. In B. Babudieri (ed.), *The Fine Morphology of Spirochaetas.* Leonardo Edizioni Scientifische, Rome.

102. Takashima, I and R. Yanagawa. 1975. Immunizing effects of structural components of *Leptospira icterohaemorrhagiae.* Zentrallbl. Bakt. Par. Inf. Hyg. 233:93-98.

103. Tremblay, G. Y., M. J. Daniels and M. Schaechter. 1969. Isolation of a cell membrane-DNA-nascent RNA complex from bacteria. J. Mol. Biol. 40:65-76.

104. van Iterson, W., J. F. M. Hoeniger and E. N. van Zanten. 1967. A "microtubule" in a bacterium. J. Cell Biol. 32:1-10.

105. Wang, C.-Y. and T. L. Jahn. 1972. A theory for the locomotion of spirochetes. J. Theor. Biol. 36:53-60.

106. Weber, K. and M. Osborn. 1969. The reliability of molecular weight determinations by dodecyl sulfate-polyacrylamide gel electrophoresis. J. Biol. Chem. 244:4406-4412.

107. Wiegand, S. E., P. L. Strobel and L. H. Glassman. 1972. Electron microscopic anatomy of pathogenic *Treponema pallidum.* J. Invest. Dermatol. 58:186-204.

108. Willcox, R. R. and T. Guthe. 1966. Culture of *T. pallidum in vitro*: II. The cultured strains, p. 54-60. In Treponema pallidum--*A Bibliographical Review of the Morphology, Culture and Survival of* T. pallidum *and Associated Organisms.* World Health Organization, Geneva.

109. Williams, C. A. and M. W. Chase. 1968. Carbohydrate analysis, p. 282-305. In C. A. Williams and M. W. Chase (eds.), *Methods in Immunology and Immunochemistry,* Vol. II. Academic Press, New York.

110. Williamson, D. L. 1974. Unusual fibrils from the spirochete-like sex ratio organism. J. Bacteriol. 117:904-906.

111. Winslow, C.-E.A., J. Bradhurst, R. E. Buchanan, C. Krumwede, L. A. Rogers and G. H. Smith. 1917. The families and genera of bacteria. J. Bacteriol. 2:205-566.

112. Winter, G. 1884. Classe, Schizomycetes, p. 33-67. In *Rabenhorst's Kryptogamen-Flora von Deutschland, Oesterreich u. der Schweiz.* Eduard Kummer, Leipzig.

113. Yamamoto, T. 1967. Presence of rhapidosomes in various species of bacteria and their morphological characteristics. J. Bacteriol. 94:1746-1756.

1

1

1

114. Yanagawa, R. and S. Faine. 1966. Morphological and serological analysis of leptospiral structure. Nature (London) 211:823-826.

115. Yanigihara, Y., Y. Hattori and I. Mifuchi. 1975. Purification of microfibers of spirochetes, p. 4. *Abstracts First Symposium on the Biology of the Parasitic Spirochetes*. Minneapolis.

116. Yanigihara, Y. and I. Mifuchi. 1968. Microfibers present in surface structures of *Leptospira*. J. Bacteriol. 95:2403-2406.